INVERSE DYNAMICS CONTROL OF PARALLEL MANIPULATORS AROUND SINGULAR CONFIGURATIONS

A THESIS SUBMITTED TO
THE GRADUATE SCHOOL OF NATURAL AND APPLIED SCIENCES
OF
MIDDLE EAST TECHNICAL UNIVERSITY

BY

MUSTAFA ÖZDEMİR

IN PARTIAL FULFILLMENT OF THE REQUIREMENTS
FOR
THE DEGREE OF MASTER OF SCIENCE
IN
MECHANICAL ENGINEERING

JANUARY 2008

Approval of the thesis:

INVERSE DYNAMICS CONTROL OF PARALLEL MANIPULATORS AROUND SINGULAR CONFIGURATIONS

submitted by **Mustafa Özdemir** in partial fulfillment of the requirements for the degree of **Master of Science in Mechanical Engineering Department, Middle East Technical University** by,

Prof. Dr. Canan Özgen _____
Dean, Graduate School of **Natural and Applied Sciences**

Prof. Dr. S. Kemal İder _____
Head of Department, **Mechanical Engineering**

Prof. Dr. S. Kemal İder _____
Supervisor, **Mechanical Engineering Dept., METU**

Examining Committee Members:

Prof. Dr. M. Kemal Özgören _____
Mechanical Engineering Dept., METU

Prof. Dr. S. Kemal İder _____
Mechanical Engineering Dept., METU

Prof. Dr. Reşit Soylu _____
Mechanical Engineering Dept., METU

Assist. Prof. Dr. Yiğit Yazıcıoğlu _____
Mechanical Engineering Dept., METU

Prof. Dr. Ozan Tekinalp _____
Aerospace Engineering Dept., METU

Date: 14.01.2008

I hereby declare that all information in this document has been obtained and presented in accordance with academic rules and ethical conduct. I also declare that, as required by these rules and conduct, I have fully cited and referenced all material and results that are not original to this work.

Name, Last name : Mustafa Özdemir

Signature :

ABSTRACT

INVERSE DYNAMICS CONTROL OF PARALLEL MANIPULATORS AROUND SINGULAR CONFIGURATIONS

Özdemir, Mustafa
M.S., Department of Mechanical Engineering
Supervisor: Prof. Dr. S. Kemal İder

January 2008, 98 pages

In this thesis, a technique for the motion of parallel manipulators through drive singularities is investigated. To remedy the problem of unbounded inverse dynamics solution in the neighborhood of drive singularities, an inverse dynamics controller which uses a conventional inverse dynamics control law outside the neighborhood of singularities and switches to the mode based on the formerly derived modified equations inside the neighborhood of singularities is proposed. As a result, good tracking performance is obtained while the actuator forces remain within the saturation limits of the actuators around singular configurations.

Keywords: Parallel Manipulator, Inverse Dynamics Control, Drive Singularity

ÖZ

PARALEL MANİPÜLATÖRLERİN TEKİL KONFİGÜRASYONLAR YAKININDA TERS DİNAMİK KONTROLÜ

Özdemir, Mustafa
Yüksek Lisans, Makine Mühendisliği Bölümü
Tez Yöneticisi: Prof. Dr. S. Kemal İder

Ocak 2008, 98 sayfa

Bu tezde paralel manipülatörlerin tahrik tekillikleri yakınındaki hareketi için bir yöntem üzerinde çalışılmıştır. Tahrik tekillikleri yakınında ters dinamik çözümün ıraksamasını önlemek için tekilliklerin uzağında konvansiyonel bir ters dinamik kontrol yöntemi kullanan ve tekilliklerin yakınında daha önceden türetilmiş modifiye denklemlere dayalı biçime değişen bir ters dinamik kontrolcü önerilmiştir. Sonuç olarak tekil konfigürasyonlar yakınında eyleyici kuvvetleri eyleyicilerin saturasyon limitleri içinde kalırken, iyi bir yörünge izleme performansı elde edilmiştir.

Anahtar Kelimeler: Paralel Manipülatör, Ters Dinamik Kontrol, Tahrik Tekilliği

To My Family

ACKNOWLEDGEMENTS

The author wishes to express his deepest gratitude to his supervisor Prof. Dr. S. Kemal İder for his guidance, advice, criticism, encouragements, and insight throughout the research.

The author would also like to thank to his family for their endless love and support throughout his life.

The author was supported by the Scientific and Technological Research Council of Turkey (TÜBİTAK) National Scholarship Program for M.Sc. Students.

TABLE OF CONTENTS

LIST OF TABLES

TABLES

LIST OF FIGURES

FIGURES

CHAPTER 1

INTRODUCTION

1.1 Literature Survey

Parallel manipulators are becoming more and more popular thanks to their higher load-carrying capacity, greater rigidity to weight ratio and more precise positioning capability of the end-effector compared to their conventional serial counterparts. Additionally, since all of the joints are not required to be actuated, it is possible to gather the actuators closer to the ground or on the ground itself resulting in lower weight and hence higher end-effector accelerations [1-3]. Merlet [4], Dasgupta and Mruthyunjaya [5] presented comprehensive reviews of the literature on the parallel manipulators. Despite the advantages, due to the closed loop structure, parallel manipulators suffer from drive singularities where the actuator forces become unboundedly large. Many researchers studied this type of singularity [6-21].

Gosselin and Angeles [6] showed that there are three types of singularities of parallel manipulators based on the two Jacobian matrices. The

rank deficiency of each Jacobian matrix corresponds to inverse kinematic singularities or drive singularities of the manipulator and the rank deficiency of both Jacobian matrices occurs if and only if the manipulator is at an architectural singularity. However, Daniali et al., [7] declared that the rank deficiency of both Jacobian matrices is not necessarily architecture-dependent.

Sefrioui and Gosselin [8] derived analytical expressions in quadratic form to describe the singularity loci of general three-degree-of-freedom planar parallel manipulators in terms of the roots of the determinant of the manipulator's Jacobian matrix. Additionally, a graphical representation of these loci superimposed on the manipulator's workspace is obtained. St-Onge and Gosselin [9] indicated that the singularity loci of the general Gough-Stewart platform should be a third-degree polynomial expression also by analyzing the Jacobian matrix.

Merlet [10] and Collins and Long [11] analyzed singularity of parallel manipulators using line geometry rather than the Jacobian matrix. Basu and Ghosal [12] proposed algebraic and geometric methods to determine the singularities of platform-type multi-loop spatial mechanisms containing spherical joints on the platform.

Earlier studies on the drive singularities typically focused on the determination of the locations of this type of singularity for avoiding them in the motion planning stage. At an inverse kinematic singularity the manipulator generally reaches a boundary of its workspace [6] and avoiding them does not limit its workspace in practice. Besides, architectural singularities can normally be eliminated by an appropriate selection of the kinematic parameters [6]. However, drive singularities characteristically arise within the workspace [6] and avoiding them restricts the practical workspace. For that reason, although parallel manipulators are uncontrollable at drive singularities [17], it is required to develop methods for moving parallel manipulators through those singular positions.

Özgören [18] studied the constrained motion control of a normally unconstrained mechanical system. As a part of his work, he considered drive singularities in a case where non-redundant number of actuators is used and developed a modification scheme by allowing a slight deviation from the desired trajectory only locally around the drive singularities.

Jui and Sun [19] devised a method to overcome the problem of unbounded actuator forces at drive singularity by relaxing the rigid constraint on timing due to trajectory parameterization with respect to time. Based upon the techniques of minimum time path tracking, they presented techniques for path verification and tracking and examined an inverse dynamics algorithm taking actuator bounds into consideration.

İder [20, 21] identified that if the trajectory is planned in such a way that certain conditions corresponding to the consistency of the dynamic equations are met, the manipulator can pass through the singular positions while the actuator forces remain bounded. Furthermore, he showed that the dynamic equations can be modified by using higher order derivative information to replace the linearly dependent equations in the neighborhood of the singularities. Analogous modifications were formerly used for kinematic singular positions of multibody systems by İder and Amirouche [22] and for drive singularities of redundant serial manipulators by İder [23].

1.2 Objective

The aim of this thesis is to propose an inverse dynamics controller for trajectory tracking control of parallel manipulators passing through drive singularities.

For this purpose, the controller uses the conventional inverse dynamics control law based on the regular inverse dynamics equations outside the neighborhood of drive singularities and switches to the mode based on the approximate dynamics obtained by İder [20, 21] inside the neighborhood of drive singularities where the modified equations are valid.

1.3 Scope of the Thesis

Chapter 1 presents the literature review on the singularity analysis of parallel manipulators and gives the objective of this thesis.

Chapter 2 is reserved to explain the inverse dynamics algorithm for parallel manipulators passing through drive singularities proposed in [20]. In this chapter, inverse dynamics problem and singular positions are defined and consistency conditions and modified equations are introduced as in [20].

Chapter 3 proposes a switching inverse dynamics controller for trajectory tracking control of parallel manipulators passing through drive singularities. In this chapter, the conventional inverse dynamics control law to be used outside the neighborhood of drive singularities is presented and the inverse dynamics control law to be switched inside the vicinity of drive singularities is derived.

In Chapter 4, the 2-RPR (revolute, prismatic, revolute joints) planar parallel manipulator with two legs is considered to test the performance of the proposed inverse dynamics controller. First, inverse dynamics problem and singular positions of this parallel manipulator are defined and the consistency condition and modified equation are given as done in [21]. Next, the conventional inverse dynamics controller to be used outside the neighborhood

of drive singularities is introduced and the inverse dynamics control law to be switched inside the neighborhood of drive singularities is derived using the method proposed in Chapter 3. Finally, the results of the numerical simulations carried out using the SIMULINK® model developed and the SIMULINK® model itself are presented.

Chapter 5 interprets the simulation results and recommends for future work on the trajectory tracking control of parallel manipulators in the presence of drive singularities.

CHAPTER 2

DYNAMIC MODEL

This chapter is reserved for a presentation of the work of İder [20, 21] on the inverse dynamics of parallel manipulators in the presence of drive singularities. His work provides the basic groundwork to this thesis.

Section 2.1 briefly reviews inverse dynamics and singular positions. Section 2.2 deals with consistency conditions and modified equations.

2.1 Inverse Dynamics and Singular Positions

Consider an n degree of freedom parallel robot. This system can be converted into an open-tree system by disconnecting a sufficient number of unactuated joints. Let the degree of freedom of the open-tree structure be m. Let $\mathbf{q} = \begin{bmatrix} q_1 & \cdots & q_m \end{bmatrix}^T$ denote the joint variables of the open-tree system. The $m-n$ loop closure equations to be satisfied in order to convert the open-tree structure into the closed-loop parallel manipulator can be written as

$$\boldsymbol{\varphi}(\mathbf{q}) = \mathbf{0} \tag{2.1}$$

where $\boldsymbol{\varphi}$ is a $(m-n)$-dimensional vector function. Equation (2.1) can be expressed at velocity level as

$$\boldsymbol{\Gamma}^G \dot{\mathbf{q}} = \mathbf{0} \tag{2.2}$$

where $\boldsymbol{\Gamma}^G = \boldsymbol{\Gamma}^G(\mathbf{q}) = \partial\boldsymbol{\varphi}/\partial\mathbf{q}$.

Let $\mathbf{x}(t) = \begin{bmatrix} x_1(t) & \cdots & x_n(t) \end{bmatrix}^T$ denote the prescribed Cartesian position and orientation coordinates of the end-effector. The n task equations which give the relation between the pose of the end-effector and the joint variables can be written as

$$\mathbf{f}(\mathbf{q}) = \mathbf{x} \tag{2.3}$$

where $\mathbf{f}$ is an n-dimensional vector function. Equation (2.3) can be expressed at velocity level as

$$\boldsymbol{\Gamma}^P \dot{\mathbf{q}} = \dot{\mathbf{x}} \tag{2.4}$$

where $\boldsymbol{\Gamma}^P = \boldsymbol{\Gamma}^P(\mathbf{q}) = \partial\mathbf{f}/\partial\mathbf{q}$.

Equations (2.2) and (2.4) can be combined to give

$$\boldsymbol{\Gamma}\dot{\mathbf{q}} = \mathbf{h} \tag{2.5}$$

where $\boldsymbol{\Gamma}^T = \begin{bmatrix} \boldsymbol{\Gamma}^{G^T} & \boldsymbol{\Gamma}^{P^T} \end{bmatrix}$ and $\mathbf{h}^T = \begin{bmatrix} \mathbf{0} & \dot{\mathbf{x}}^T \end{bmatrix}$. Differentiating Equation (2.5) with respect to time gives the acceleration level relations as follows:

$$\boldsymbol{\Gamma}\ddot{\mathbf{q}} = -\dot{\boldsymbol{\Gamma}}\dot{\mathbf{q}} + \dot{\mathbf{h}} \tag{2.6}$$

During the inverse kinematic solution, singularities arise when $|\boldsymbol{\Gamma}| = 0$. It is assumed that $\boldsymbol{\Gamma}$ never becomes singular so that an inverse kinematic singularity is not encountered.

If $\mathbf{q}$ is chosen for the generalized coordinates, the equations of motion of the parallel manipulator can be represented in the following matrix form obtained through the Lagrange's equations:

$$\mathbf{M}\ddot{\mathbf{q}} + \mathbf{B} = \mathbf{Z}^T\mathbf{T} + \boldsymbol{\Gamma}^{G^T}\boldsymbol{\lambda} \tag{2.7}$$

where $\mathbf{M} = \mathbf{M}(\mathbf{q})$ is the $m \times m$ generalized inertia matrix and $\mathbf{B} = \mathbf{B}(\mathbf{q}, \dot{\mathbf{q}})$ is the m-dimensional bias vector that includes the generalized Coriolis, centrifugal and gravity forces of the open-tree system, $\boldsymbol{\lambda}$ is the $(m-n)$-dimensional vector of Lagrange multipliers, $\mathbf{T}$ is the n-dimensional vector of the actuator forces, and each row of $\mathbf{Z}$ is the direction of one actuator force in the generalized space. If the variable of the joint which is actuated by the i^{th} actuator is q_k, then for the i^{th} row of $\mathbf{Z}$, $Z_{ik} = 1$ and $Z_{ij} = 0$ for $j = 1, 2, \cdots, m \ (j \neq k)$.

If the terms involving $\boldsymbol{\lambda}$ and $\mathbf{T}$ are combined, Equation (2.7) can be rewritten as follows:

$$\mathbf{A}^T\boldsymbol{\mu} = \mathbf{M}\ddot{\mathbf{q}} + \mathbf{B} \tag{2.8}$$

where $\mathbf{A}^T = \begin{bmatrix} \boldsymbol{\Gamma}^{G^T} & \mathbf{Z}^T \end{bmatrix}$ and $\boldsymbol{\mu}^T = \begin{bmatrix} \boldsymbol{\lambda}^T & \mathbf{T}^T \end{bmatrix}$.

In the inverse dynamics solution, singularities are encountered when $|\mathbf{A}| = 0$. This type of singularity is called drive singularity. At such singularities, the actuator forces take infinitely large values.

2.2 Consistency Conditions and Modified Equations

The rank deficiency of the $\mathbf{A}$ matrix results in drive singularities. At a drive singularity the rank r of $\mathbf{A}$ usually becomes $m-1$. The general case $r < m$ is considered though. Let rows s_k, $k = 1, \cdots, m-r$ of $\mathbf{A}^T$ can be

expressed as linear combinations of the other rows of $\mathbf{A}^T$ at the singular position, i.e.,

$$A^T_{s_k j} = \alpha_{kp} A^T_{pj} \tag{2.9}$$

for $p = 1, \cdots, m \ (p \neq s_k)$, $j = 1, \cdots, m$, $k = 1, \cdots, m-r$

where the linear combination coefficients α_{kp} may also depend on $\mathbf{q}$. Notice that in the equations, repeated subscript indices in a term imply summation over their corresponding ranges. Hence, the following relations must be at hand among the rows of the Equation (2.8).

$$A^T_{s_k j}\mu_j - \alpha_{kp} A^T_{pj}\mu_j = M_{s_k j}\ddot{q}_j + B_{s_k} - \alpha_{kp}\left(M_{pj}\ddot{q}_j + B_p\right) \tag{2.10}$$

for $k = 1, \cdots, m-r$

Putting Equations (2.9) into Equations (2.10) gives

$$M_{s_k j}\ddot{q}_j + B_{s_k} = \alpha_{kp}\left(M_{pj}\ddot{q}_j + B_p\right) \tag{2.11}$$

for $k = 1, \cdots, m-r$

Equations (2.11) signify the $m-r$ consistency conditions that $\ddot{\mathbf{q}}$ should satisfy at the singular position. Since $\ddot{\mathbf{q}}$ is related to $\ddot{\mathbf{x}}$ through Equation (2.6), the prescribed trajectory must satisfy Equations (2.11) at the drive singularity. Otherwise an inconsistent trajectory cannot be realized and the actuator forces grow without bounds as the drive singularity is approached.

Differentiating Equations (2.10) with respect to time yields

$$\begin{aligned}&\left(A^T_{s_k j} - \alpha_{kp} A^T_{pj}\right)\dot{\mu}_j + \left(\dot{A}^T_{s_k j} - \alpha_{kp}\dot{A}^T_{pj} - \dot{\alpha}_{kp} A^T_{pj}\right)\mu_j = \left(M_{s_k j} - \alpha_{kp} M_{pj}\right)\dddot{q}_j \\ &+\left(\dot{M}_{s_k j} - \alpha_{kp}\dot{M}_{pj} - \dot{\alpha}_{kp} M_{pj}\right)\ddot{q}_j + \dot{B}_{s_k} - \alpha_{kp}\dot{B}_p - \dot{\alpha}_{kp} B_p\end{aligned} \tag{2.12}$$

for $k = 1, \cdots, m-r$

Now, since Equations (2.9) are valid at the singular position, there exists a vicinity in which the first terms of Equations (2.12) are insignificant compared to the other terms. Therefore in that neighborhood these terms can be neglected to obtain

$$\begin{aligned}&\left(\dot{A}^T_{s_k j}-\alpha_{kp}\dot{A}^T_{pj}-\dot{\alpha}_{kp}A^T_{pj}\right)\mu_j=\left(M_{s_k j}-\alpha_{kp}M_{pj}\right)\ddot{q}_j\\&+\left(\dot{M}_{s_k j}-\alpha_{kp}\dot{M}_{pj}-\dot{\alpha}_{kp}M_{pj}\right)\ddot{q}_j+\dot{B}_{s_k}-\alpha_{kp}\dot{B}_p-\dot{\alpha}_{kp}B_p\end{aligned}\tag{2.13}$$

for $k=1,\ \cdots,\ m-r$

The $m-r$ Equations (2.13) are the modified equations that can be used to replace the s_k th rows, $k=1,\ \cdots,\ m-r$, of Equation (2.8).

Note that $\ddot{\mathbf{q}}$ which appears in the modified equations and the prescribed end-effector jerks $\dddot{\mathbf{x}}$ are related via the derivative of Equation (2.6),

$$\boldsymbol{\Gamma}\ddot{\mathbf{q}}=-2\dot{\boldsymbol{\Gamma}}\dot{\mathbf{q}}-\ddot{\boldsymbol{\Gamma}}\dot{\mathbf{q}}+\ddot{\mathbf{h}}\tag{2.14}$$

In addition, the coefficients of the forces in the modified Equations (2.13) depend on velocities. As a result, if at the singularity the system is in motion, the actuator forces in general affect the end-effector jerks instantaneously in the singular directions thanks to the modified equations.

When the modified equations replace the linearly dependent dynamic equations in Equation (2.8), Equation (2.8) takes the following form, which is applicable in the vicinity of the singular configurations.

$$\mathbf{D}^T\boldsymbol{\mu}=\mathbf{S}\tag{2.15}$$

where

$$D^T_{ij}=\begin{cases}A^T_{ij} & i\neq s_k\\ \dot{A}^T_{ij}-\alpha_{kp}\dot{A}^T_{pj}-\dot{\alpha}_{kp}A^T_{pj} & i=s_k\end{cases}\tag{2.16}$$

and

$$S_i=\begin{cases}M_{ij}\ddot{q}_j+B_i & i\neq s_k\\ \left(M_{ij}-\alpha_{kp}M_{pj}\right)\ddot{q}_j+\left(\dot{M}_{ij}-\alpha_{kp}\dot{M}_{pj}-\dot{\alpha}_{kp}M_{pj}\right)\ddot{q}_j & \\ +\dot{B}_i-\alpha_{kp}\dot{B}_p-\dot{\alpha}_{kp}B_p & i=s_k\end{cases}\tag{2.17}$$

for $k=1,\ \cdots,\ m-r$

Equation (2.15) is employed in the neighborhood of the drive singularities, i.e., $\left|g\left(\mathbf{q}\right)\right|<\varepsilon$ and Equation (2.8) is employed elsewhere, where $g\left(\mathbf{q}\right)=0$

represents the singularity condition and ε is a positive number which defines the size of the neighborhood. ε should be selected small enough to have the error in the modified equations in Equation (2.15) insignificant and also large enough to prevent the $\mathbf{A}$ matrix in Equation (2.8) from becoming ill-conditioned.

CHAPTER 3

INVERSE DYNAMICS CONTROL

This chapter proposes a switching inverse dynamics controller for trajectory tracking control of parallel manipulators in the presence of drive singularities. The controller uses the conventional inverse dynamics control law based on the regular inverse dynamics equations given by Equation (2.8) outside the neighborhood of drive singularities and switches to the mode based on the approximate dynamics given by Equation (2.15) inside the neighborhood of drive singularities where the modified equations are valid.

Section 3.1 presents the conventional inverse dynamics control law to be used outside the neighborhood of drive singularities. Section 3.2 derives the inverse dynamics control law to be switched inside the vicinity of drive singularities.

3.1 Inverse Dynamics Control outside the Neighborhood of Drive Singularities

The n elements of the m-dimensional generalized force vector $\mathbf{Z}^T\mathbf{T}$ in Equation (2.7) are the elements of the vector $\mathbf{T}$ and its remaining $m-n$ elements are zero. Accordingly, the rows of Equation (2.7) can be interchanged to have those $m-n$ zero elements at the bottom:

$$\bar{\mathbf{M}}\ddot{\mathbf{q}} + \bar{\mathbf{B}} = \begin{bmatrix} \mathbf{T} \\ \mathbf{0} \end{bmatrix} + \bar{\mathbf{\Gamma}}^{G^T}\boldsymbol{\lambda} \tag{3.1}$$

where $\bar{\mathbf{M}}$, $\bar{\mathbf{B}}$ and $\bar{\mathbf{\Gamma}}^{G^T}$ are obtained by interchanging the corresponding rows of $\mathbf{M}$, $\mathbf{B}$ and $\mathbf{\Gamma}^{G^T}$, respectively. This rearranged form suggests a partitioning process of $\bar{\mathbf{M}}$, $\bar{\mathbf{B}}$ and $\bar{\mathbf{\Gamma}}^{G^T}$ as follows:

$$\bar{\mathbf{M}} = \begin{bmatrix} \bar{\mathbf{M}}^a_{n\times m} \\ \bar{\mathbf{M}}^u_{(m-n)\times m} \end{bmatrix} \tag{3.2}$$

$$\bar{\mathbf{B}} = \begin{bmatrix} \bar{\mathbf{B}}^a_{n\times 1} \\ \bar{\mathbf{B}}^u_{(m-n)\times 1} \end{bmatrix} \tag{3.3}$$

$$\bar{\mathbf{\Gamma}}^{G^T} = \begin{bmatrix} \bar{\mathbf{\Gamma}}^{Ga^T}_{n\times(m-n)} \\ \bar{\mathbf{\Gamma}}^{Gu^T}_{(m-n)\times(m-n)} \end{bmatrix} \tag{3.4}$$

where superscripts a and u denote the partitions related to the actuated and unactuated joints, respectively. Thus, Equation (3.1) can be divided into the following two equations:

$$\mathbf{T} = \bar{\mathbf{M}}^a\ddot{\mathbf{q}} + \bar{\mathbf{B}}^a - \bar{\mathbf{\Gamma}}^{Ga^T}\boldsymbol{\lambda} \tag{3.5}$$

$$\bar{\mathbf{\Gamma}}^{Gu^T}\boldsymbol{\lambda} = \bar{\mathbf{M}}^u\ddot{\mathbf{q}} + \bar{\mathbf{B}}^u \tag{3.6}$$

Note that the drive singularity condition $\left|\bar{\mathbf{\Gamma}}^{Gu^T}\right| = 0$ is equivalent to $\left|\mathbf{A}\right| = 0$. As long as $\left|g\left(\mathbf{q}\right)\right| \geq \varepsilon$, $\mathbf{A}$ and hence $\bar{\mathbf{\Gamma}}^{Gu^T}$ are not ill-conditioned and the $\bar{\mathbf{\Gamma}}^{Gu^T}$ matrix is invertible outside the neighborhood of drive singularities. Hence, $\boldsymbol{\lambda}$ can be found using Equation (3.6) as follows:

$$\boldsymbol{\lambda} = \left(\bar{\mathbf{\Gamma}}^{Gu^T}\right)^{-1}\left(\bar{\mathbf{M}}^{u}\ddot{\mathbf{q}} + \bar{\mathbf{B}}^{u}\right) \tag{3.7}$$

Then, $\mathbf{T}$ can be determined substituting Equation (3.7) into Equation (3.5):

$$\mathbf{T} = \bar{\mathbf{M}}'\ddot{\mathbf{q}} + \bar{\mathbf{B}}' \tag{3.8}$$

where $n \times m$ matrix $\bar{\mathbf{M}}'$ is

$$\bar{\mathbf{M}}' = \bar{\mathbf{M}}^{a} - \bar{\mathbf{\Gamma}}^{Ga^T}\left(\bar{\mathbf{\Gamma}}^{Gu^T}\right)^{-1}\bar{\mathbf{M}}^{u} \tag{3.9}$$

and n-dimensional vector $\bar{\mathbf{B}}'$ is

$$\bar{\mathbf{B}}' = \bar{\mathbf{B}}^{a} - \bar{\mathbf{\Gamma}}^{Ga^T}\left(\bar{\mathbf{\Gamma}}^{Gu^T}\right)^{-1}\bar{\mathbf{B}}^{u} \tag{3.10}$$

Equation (2.6) can be rearranged as

$$\ddot{\mathbf{q}} = \mathbf{\Gamma}^{-1}\left(-\dot{\mathbf{\Gamma}}\dot{\mathbf{q}} + \dot{\mathbf{h}}\right) \tag{3.11}$$

Putting Equation (3.11) into Equation (3.8) yields

$$\mathbf{T} = \bar{\mathbf{M}}^{*}\dot{\mathbf{h}} + \bar{\mathbf{B}}^{*} \tag{3.12}$$

where $n \times m$ matrix $\bar{\mathbf{M}}^{*}$ is

$$\bar{\mathbf{M}}^{*} = \bar{\mathbf{M}}'\mathbf{\Gamma}^{-1} \tag{3.13}$$

and n-dimensional vector $\bar{\mathbf{B}}^{*}$ is

$$\bar{\mathbf{B}}^{*} = \bar{\mathbf{B}}' - \bar{\mathbf{M}}'\mathbf{\Gamma}^{-1}\dot{\mathbf{\Gamma}}\dot{\mathbf{q}} \tag{3.14}$$

In Equation (3.12), all of the elements in the first $m-n$ columns of the matrix $\bar{\mathbf{M}}^{*}$ are multiplied by the first $m-n$ zero elements in the vector $\dot{\mathbf{h}}$. This fact leads to a partitioning of the matrix $\bar{\mathbf{M}}^{*}$ as follows:

$$\bar{\mathbf{M}}^{*} = \begin{bmatrix} \bar{\mathbf{M}}^{*G}_{n\times(m-n)} & \bar{\mathbf{M}}^{*P}_{n\times n} \end{bmatrix} \tag{3.15}$$

Based on this partitioning, the relation between the input $\mathbf{T}$ and the output $\mathbf{x}$ can be obtained in the following form:

$$\mathbf{T} = \bar{\mathbf{M}}^{*P}\ddot{\mathbf{x}} + \bar{\mathbf{B}}^{*} \tag{3.16}$$

An inverse dynamics control law can then be formulated using Equation (3.16). In the control law, command accelerations $\mathbf{u}$ have to be specified. For example, using PD control, $\mathbf{u}$ can be generated as

$$\mathbf{u} = \ddot{\mathbf{x}}^{d} + \mathbf{C}_1\left(\dot{\mathbf{x}}^{d} - \dot{\mathbf{x}}\right) + \mathbf{C}_2\left(\mathbf{x}^{d} - \mathbf{x}\right) \tag{3.17}$$

where superscript d denotes desired values and $\mathbf{C}_1$ and $\mathbf{C}_2$ are constant feedback gain diagonal matrices.

Then, using Equation (3.16) the actuator forces $\mathbf{T}$ can be computed as

$$\mathbf{T} = \bar{\mathbf{M}}^{*P}\mathbf{u} + \bar{\mathbf{B}}^{*} \tag{3.18}$$

Since $\bar{\mathbf{M}}^{*P}$ is the $n \times n$ inertia matrix of the parallel manipulator expressed in the task space, the inverse of $\bar{\mathbf{M}}^{*P}$ exists because the inertia matrix should be positive definite for a proper system. Hence, in the absence of modeling error and disturbances, the application of the actuator forces given by Equation (3.18) results in actual accelerations which are equal to the command accelerations, i.e.,

$$\ddot{\mathbf{x}} = \mathbf{u} \tag{3.19}$$

As a result, Equations (3.17) and (3.19) lead to the following error equation:

$$\ddot{\mathbf{e}} + \mathbf{C}_1\dot{\mathbf{e}} + \mathbf{C}_2\mathbf{e} = \mathbf{0} \tag{3.20}$$

where $\mathbf{e} = \mathbf{x}^{d} - \mathbf{x}$.

Based on this error equation, the feedback gain matrices can be selected appropriately to ensure asymptotic stability.

3.2 Inverse Dynamics Control inside the Neighborhood of Drive Singularities

The rank deficiency of $\bar{\mathbf{\Gamma}}^{Gu^T}$ results in drive singularities. Combining the terms involving $\boldsymbol{\lambda}$ and $\mathbf{T}$ in Equation (3.1), Equation (2.8) can be rewritten as follows:

$$\bar{\mathbf{A}}^T\boldsymbol{\mu} = \bar{\mathbf{M}}\ddot{\mathbf{q}} + \bar{\mathbf{B}} \tag{3.21}$$

where $\bar{\mathbf{A}}^T = \begin{bmatrix} \bar{\mathbf{\Gamma}}^{G^T} & \bar{\mathbf{Z}}^T \end{bmatrix}$ and $\bar{\mathbf{Z}}^T = \begin{bmatrix} \mathbf{I}_n \\ \mathbf{0}_{(m-n)\times n} \end{bmatrix}$. Recall that $\mathbf{I}_n$ is an $n \times n$ identity matrix. This rearranged form suggests a partitioning process of $\bar{\mathbf{A}}^T$ as follows:

$$\bar{\mathbf{A}}^T = \begin{bmatrix} \bar{\mathbf{A}}^{a^T}_{n\times m} \\ \bar{\mathbf{A}}^{u^T}_{(m-n)\times m} \end{bmatrix} \tag{3.22}$$

where $\bar{\mathbf{A}}^{a^T} = \begin{bmatrix} \bar{\mathbf{\Gamma}}^{Ga^T} & \mathbf{I}_n \end{bmatrix}$ and $\bar{\mathbf{A}}^{u^T} = \begin{bmatrix} \bar{\mathbf{\Gamma}}^{Gu^T} & \mathbf{0}_{(m-n)\times n} \end{bmatrix}$. Thus, Equation (3.21) can be divided into the following two equations:

$$\bar{\mathbf{A}}^{a^T}\boldsymbol{\mu} = \bar{\mathbf{M}}^a\ddot{\mathbf{q}} + \bar{\mathbf{B}}^a \tag{3.23}$$

$$\bar{\mathbf{A}}^{u^T}\boldsymbol{\mu} = \bar{\mathbf{M}}^u\ddot{\mathbf{q}} + \bar{\mathbf{B}}^u \tag{3.24}$$

One should note that Equations (3.23) and (3.24) are just another way of writing Equations (3.5) and (3.6) respectively by combining the terms the terms involving $\boldsymbol{\lambda}$ and $\mathbf{T}$. By looking at $\bar{\mathbf{A}}^{a^T}$, one can claim that the rows of $\bar{\mathbf{A}}^{a^T}$ are always linearly independent due to $\mathbf{I}_n$. However, at a drive singularity, $\bar{\mathbf{\Gamma}}^{Gu^T}$, hence $\bar{\mathbf{A}}^{u^T}$ due to $\mathbf{0}$, become rank deficient. Therefore, Equation (2.9) gives essentially the relation among the linearly dependent rows of $\bar{\mathbf{A}}^{u^T}$, hence $\bar{\mathbf{\Gamma}}^{Gu^T}$, at a drive singularity. Then, at that drive singularity Equation (2.10) must give the relation between the linearly dependent rows of

Equation (3.24), hence Equation (3.6). Consequently, the linearly dependent equations in Equation (3.24), hence in Equation (3.6), can be replaced by the $m-r$ modified equations given by Equation (2.13). Noticing that Equation (2.10) does not include any of the actuator forces since Equation (3.6) does not, one can conclude that the modified equations also do not include any of the actuator forces. When, the $m-r$ modified equations replace the linearly dependent equations in Equation (3.6), the resulting system of equations can be written in matrix notation as follows:

$$\hat{\mathbf{\Gamma}}^{Gu^T}\boldsymbol{\lambda} = \hat{\mathbf{N}}^u\ddot{\mathbf{q}} + \hat{\mathbf{M}}^u\ddot{\mathbf{q}} + \hat{\mathbf{B}}^u \tag{3.25}$$

where the corresponding rows of the $(m-n)\times m$ matrix $\hat{\mathbf{N}}^u = \hat{\mathbf{N}}^u(\mathbf{q})$ consist of the coefficients of $\ddot{q}_j$'s $j=1, \cdots, m$ in the modified equations while its remaining $r-n$ rows are composed of zeros, $\hat{\mathbf{\Gamma}}^{Gu^T} = \hat{\mathbf{\Gamma}}^{Gu^T}(\mathbf{q}, \dot{\mathbf{q}})$ and $\hat{\mathbf{M}}^u = \hat{\mathbf{M}}^u(\mathbf{q}, \dot{\mathbf{q}})$ are obtained via replacing the corresponding rows of $\bar{\mathbf{\Gamma}}^{Gu^T}$ and $\bar{\mathbf{M}}^u$ by the rows consisting of the coefficients of λ_i's $i=1, \ldots, m-n$ and $\ddot{q}_j$'s in the modified equations, respectively and $\hat{\mathbf{B}}^u = \hat{\mathbf{B}}^u(\mathbf{q}, \dot{\mathbf{q}})$ is obtained via replacing the corresponding elements of $\bar{\mathbf{B}}^u$ by the remaining terms in the modified equations. Note that Equations (3.5) and (3.25) form together Equation (2.15).

$\boldsymbol{\lambda}$ can be found using Equation (3.25) as follows:

$$\boldsymbol{\lambda} = \left(\hat{\mathbf{\Gamma}}^{Gu^T}\right)^{-1}\left(\hat{\mathbf{N}}^u\ddot{\mathbf{q}} + \hat{\mathbf{M}}^u\ddot{\mathbf{q}} + \hat{\mathbf{B}}^u\right) \tag{3.26}$$

Then, $\mathbf{T}$ can be determined substituting Equation (3.26) into Equation (3.5):

$$\mathbf{T} = \hat{\mathbf{N}}'\ddot{\mathbf{q}} + \hat{\mathbf{M}}'\ddot{\mathbf{q}} + \hat{\mathbf{B}}' \tag{3.27}$$

where $n\times m$ matrices $\hat{\mathbf{N}}'$ and $\hat{\mathbf{M}}'$ are

$$\hat{\mathbf{N}}' = -\bar{\mathbf{\Gamma}}^{Ga^T}\left(\hat{\mathbf{\Gamma}}^{Gu^T}\right)^{-1}\hat{\mathbf{N}}^u \tag{3.28}$$

$$\hat{\mathbf{M}}' = \bar{\mathbf{M}}^a - \bar{\mathbf{\Gamma}}^{Ga^T}\left(\hat{\mathbf{\Gamma}}^{Gu^T}\right)^{-1}\hat{\mathbf{M}}^u \tag{3.29}$$

and n-dimensional vector $\hat{\mathbf{B}}'$ is

$$\hat{\mathbf{B}}' = \bar{\mathbf{B}}^a - \bar{\mathbf{\Gamma}}^{Ga^T}\left(\hat{\mathbf{\Gamma}}^{Gu^T}\right)^{-1}\hat{\mathbf{B}}^u \tag{3.30}$$

Equation (2.14) can be rearranged to obtain

$$\mathbf{\Gamma}\ddot{\mathbf{q}} = \mathbf{P}\ddot{\mathbf{q}} + \mathbf{R} + \ddot{\mathbf{h}} \tag{3.31}$$

where the $m \times m$ matrix $\mathbf{P} = \mathbf{P}\left(\mathbf{q}, \dot{\mathbf{q}}\right)$ and the m-dimensional vector $\mathbf{R} = \mathbf{R}\left(\mathbf{q}, \dot{\mathbf{q}}\right)$ includes the coefficients of $\ddot{q}_j$'s and the nonlinear terms in Equation (2.14), respectively. Solving Equation (3.31) for $\ddot{\mathbf{q}}$ gives

$$\ddot{\mathbf{q}} = \mathbf{\Gamma}^{-1}\left(\mathbf{P}\ddot{\mathbf{q}} + \mathbf{R} + \ddot{\mathbf{h}}\right) \tag{3.32}$$

On substituting Equation (3.11), Equation (3.32) becomes

$$\ddot{\mathbf{q}} = \mathbf{\Gamma}^{-1}\left[\mathbf{P}\mathbf{\Gamma}^{-1}\left(-\dot{\mathbf{\Gamma}}\dot{\mathbf{q}} + \dot{\mathbf{h}}\right) + \mathbf{R} + \ddot{\mathbf{h}}\right] \tag{3.33}$$

Putting Equations (3.11) and (3.33) into Equation (3.27) gives

$$\mathbf{T} = \hat{\mathbf{N}}^*\ddot{\mathbf{h}} + \hat{\mathbf{M}}^*\dot{\mathbf{h}} + \hat{\mathbf{B}}^* \tag{3.34}$$

where $n \times m$ matrices $\hat{\mathbf{N}}^*$ and $\hat{\mathbf{M}}^*$ are

$$\hat{\mathbf{N}}^* = \hat{\mathbf{N}}'\mathbf{\Gamma}^{-1} \tag{3.35}$$

$$\hat{\mathbf{M}}^* = \left(\hat{\mathbf{N}}'\mathbf{\Gamma}^{-1}\mathbf{P} + \hat{\mathbf{M}}'\right)\mathbf{\Gamma}^{-1} \tag{3.36}$$

and n-dimensional vector $\hat{\mathbf{B}}^*$ is

$$\hat{\mathbf{B}}^* = \hat{\mathbf{B}}' + \hat{\mathbf{N}}'\mathbf{\Gamma}^{-1}\left(\mathbf{R} - \mathbf{P}\mathbf{\Gamma}^{-1}\dot{\mathbf{\Gamma}}\dot{\mathbf{q}}\right) - \hat{\mathbf{M}}'\mathbf{\Gamma}^{-1}\dot{\mathbf{\Gamma}}\dot{\mathbf{q}} \tag{3.37}$$

In Equation (3.34), all of the elements in the first $m-n$ columns of the matrices $\hat{\mathbf{N}}^*$ and $\hat{\mathbf{M}}^*$ are multiplied by the first $m-n$ zero elements in the vectors $\ddot{\mathbf{h}}$ and $\dot{\mathbf{h}}$, respectively. This fact leads to a partitioning of the matrices $\hat{\mathbf{N}}^*$ and $\hat{\mathbf{M}}^*$ as follows:

$$\hat{\mathbf{N}}^* = \left[\hat{\mathbf{N}}^{*G}_{n\times(m-n)} \quad \hat{\mathbf{N}}^{*P}_{n\times n}\right] \tag{3.38}$$

$$\hat{\mathbf{M}}^{*} = \begin{bmatrix} \hat{\mathbf{M}}^{*G}_{n\times(m-n)} & \hat{\mathbf{M}}^{*P}_{n\times n} \end{bmatrix} \tag{3.39}$$

Based on this partitioning, the relation between the input $\mathbf{T}$ and the output $\mathbf{x}$ can be obtained in the following form:

$$\mathbf{T} = \hat{\mathbf{N}}^{*P}\ddot{\mathbf{x}} + \hat{\mathbf{M}}^{*P}\mathbf{x} + \hat{\mathbf{B}}^{*} \tag{3.40}$$

An inverse dynamics control law can then be formulated using Equation (3.40) provided that the desired trajectory is chosen to be consistent. It is then assumed that the trajectory tracking errors have become small at the onset of the neighborhood of drive singularities so that the actual trajectory almost satisfies the consistency conditions. This is possible if the initial positioning errors are handled for a sufficient time to settle down to small values by the inverse dynamics control law covered in Section 3.1.

The rank of $\hat{\mathbf{N}}^{*P}$ is $m-r$ which is indeed less than n. So, in the control law, both command accelerations $\mathbf{u}$ and command jerks $\dot{\mathbf{u}}$ have to be specified. Once $\mathbf{u}$ is generated as in Equation (3.17), the actuator forces $\mathbf{T}$ can be computed using Equation (3.40):

$$\mathbf{T} = \hat{\mathbf{N}}^{*P}\dot{\mathbf{u}} + \hat{\mathbf{M}}^{*P}\mathbf{u} + \hat{\mathbf{B}}^{*} \tag{3.41}$$

To show that the application of the computed forces from Equation (3.41) linearizes and decouples the system in the absence of modeling error and disturbances, substitution of Equation (3.41) into Equation (3.40) results in

$$\hat{\mathbf{N}}^{*P}\dot{\boldsymbol{\eta}} + \hat{\mathbf{M}}^{*P}\boldsymbol{\eta} = \mathbf{0} \tag{3.42}$$

where $\boldsymbol{\eta} = \mathbf{u} - \ddot{\mathbf{x}}$. Besides, since Equation (3.19) holds up to the onset of the neighborhood of drive singularities,

$$\boldsymbol{\eta}(\tau) = \mathbf{0} \tag{3.43}$$

where τ is the right end point of the closed time interval passed until the manipulator arrives at the onset of the neighborhood. Since the rank of the matrix $\hat{\mathbf{N}}^{*P}$ is less than n, namely $m-r$ as mentioned earlier, $n-m+r$ equations of Equation (3.42) can be converted to algebraic equations through

elementary row operations. Then, using those algebraic equations, $n-m+r$ of the η_j's can be obtained in terms of the others and those results can be used to reduce the system of Equation (3.42) by $n-m+r$ unknowns and $n-m+r$ equations. The reduced system is a linear first order system of $m-r$ differential equations in the $m-r$ unknowns $\kappa_1(t)$, …, $\kappa_{m-r}(t)$ and is in the form of

$$\begin{aligned} a_{11}\dot{\kappa}_1 + \ldots a_{1(m-r)}\dot{\kappa}_{m-r} + b_{11}\kappa_1 + \ldots b_{1(m-r)}\kappa_{m-r} &= 0 \\ &\vdots \\ a_{(m-r)1}\dot{\kappa}_1 + \ldots a_{(m-r)(m-r)}\dot{\kappa}_{m-r} + b_{(m-r)1}\kappa_1 + \ldots b_{(m-r)(m-r)}\kappa_{m-r} &= 0 \end{aligned} \tag{3.44}$$

subject to the initial conditions

$$\kappa_1(\tau) = 0,\ \kappa_2(\tau) = 0,\ \ldots,\ \kappa_{m-r}(\tau) = 0 \tag{3.45}$$

where $\kappa_1, \kappa_2, \ldots, \kappa_{m-r}$ denote the remaining η_j's in the reduced system and the coefficients $a_{11}(t), a_{12}(t), \cdots, a_{(m-r)(m-r)}(t)$ and $b_{11}(t), b_{12}(t), \cdots, b_{(m-r)(m-r)}(t)$ can be determined in terms of the elements of $\hat{\mathbf{N}}^{*P}$ and $\hat{\mathbf{M}}^{*P}$. Now, since the rank of the matrix $\begin{bmatrix} a_{11} & \ldots & a_{1(m-r)} \\ \vdots & \ddots & \vdots \\ a_{(m-r)1} & \cdots & a_{(m-r)(m-r)} \end{bmatrix}$ is $m-r$, Equation (3.44) can be written in the explicit form:

$$\begin{aligned} \dot{\kappa}_1 &= c_{11}\kappa_1 + c_{12}\kappa_2 + \ldots c_{1(m-r)}\kappa_{m-r}, \\ &\vdots \\ \dot{\kappa}_{m-r} &= c_{(m-r)1}\kappa_1 + c_{(m-r)2}\kappa_2 + \ldots c_{(m-r)(m-r)}\kappa_{m-r}, \end{aligned} \tag{3.46}$$

subject to the initial conditions (3.45). The Existence and Uniqueness Theorem for Linear First-Order Systems [24] states that if $\mathbf{\Lambda}(t)$ is a continuous matrix valued function of t and $\mathbf{\upsilon}(t)$ is a continuous vector valued function of t, each

on the closed time interval Υ, and if t_0 is a given point in Υ, then the initial value problem

$$\dot{\boldsymbol{\xi}}(t) = \boldsymbol{\Lambda}(t)\boldsymbol{\xi}(t) + \boldsymbol{\upsilon}(t) \tag{3.47}$$

$$\boldsymbol{\xi}(t_0) = \boldsymbol{\xi}_0 \tag{3.48}$$

has a unique solution $\boldsymbol{\xi}(t)$ on Υ. This theorem implies that, since the coefficients $c_{11}(t), c_{12}(t), \cdots, c_{(m-r)(m-r)}(t)$ are continuous on a closed time interval I including the time period passed inside the neighborhood of the singularity and the point τ as well, the system of Equation (3.46) subject to the initial conditions (3.45) has a unique solution on I. Consequently, the system represented by Equation (3.42) subject to initial conditions (3.43) has a unique solution on I, and obviously, it is the trivial solution, i.e., $\boldsymbol{\eta}(t) = \mathbf{0}$. Therefore, Equations (3.19) and (3.20) are still valid inside the neighborhood of drive singularities.

CHAPTER 4

CASE STUDY AND NUMERICAL SIMULATIONS

In this chapter, the 2-RPR (revolute, prismatic, revolute joints) planar parallel manipulator with two legs is considered to test the performance of the proposed inverse dynamics controller in the presence of drive singularities. Singularity robust inverse dynamics of this type of parallel manipulators was studied by İder [21].

Section 4.1 reviews inverse dynamics and singular positions of this parallel manipulator as dealt in [21]. Section 4.2 presents the consistency condition and modified equation as derived in [21]. Section 4.3 covers the conventional inverse dynamics controller to be used outside the neighborhood of drive singularities as depicted in Section 3.1. Section 4.4 derives the inverse dynamics control law to be switched inside the neighborhood of drive singularities using the findings of Section 3.2. Section 4.5 introduces the SIMULINK® model developed to carry out the numerical simulations. Section 4.6 presents the results of the simulations under different scenarios using the model depicted in Section 4.5. The numerical data and consistent and inconsistent reference trajectories used in these simulations are taken from the numerical example in [21].

4.1 Inverse Dynamics and Singular Positions

The 2-RPR planar parallel manipulator is shown in Figure 1. This parallel manipulator has 3 degrees of freedom $(n=3)$.

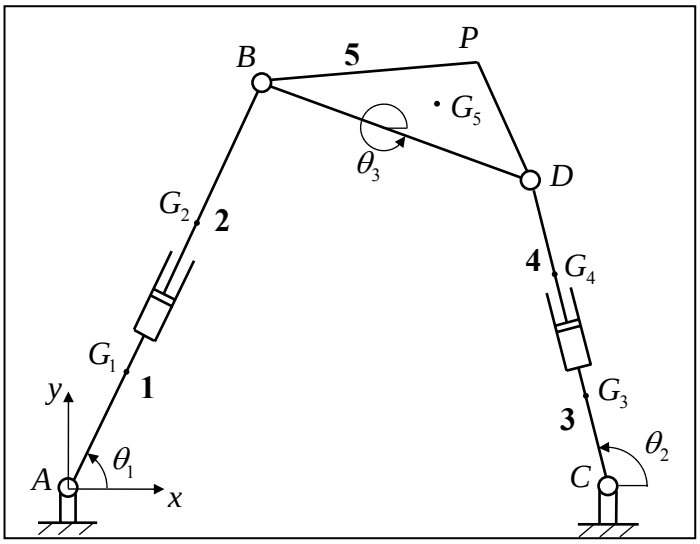

Figure 1 2-RPR planar parallel manipulator

This system can be converted into an open-tree system by disconnecting the revolute joint at D (Figure2). The degree of freedom of the open-tree structure is 5 $(m=5)$. $\mathbf{q}=[\theta_1 \quad \zeta_1 \quad \theta_2 \quad \zeta_2 \quad \theta_3]^T$ denotes the joint variables of the open-tree system, where $\zeta_1 = AB$ and $\zeta_2 = CD$. Let the joints whose variables

are θ_1, ζ_1 and ζ_2 be the actuated joints. The actuator force vector can be written as $\mathbf{T} = \begin{bmatrix} T_1 & F_1 & F_2 \end{bmatrix}^T$ where T_1 is the motor torque corresponding to θ_1, and F_1 and F_2 are the actuator forces corresponding to ζ_1 and ζ_2.

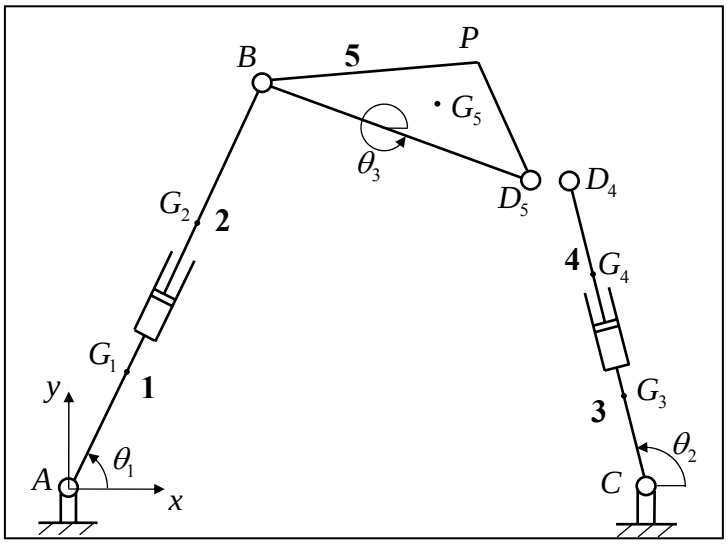

Figure 2 The open-tree system obtained by disconnecting the joint at D

Let the link dimensions of the manipulator be labeled as $a = AC$, $b = BD$, $c = BP$ and $\alpha = \angle PBD$. $\mathbf{x} = \begin{bmatrix} x_P & y_P & \theta_3 \end{bmatrix}^T$ denotes the position and orientation of the moving platform, where x_P, y_P are the coordinates of the end point P.

The position level loop closure constraint equations expressing the fact that D_4 and D_5 are always coincident can be written as

$$\phi_1 = \zeta_1 \cos\theta_1 + b\cos\theta_3 - a - \zeta_2 \cos\theta_2 = 0 \tag{4.1}$$

$$\phi_2 = \zeta_1 \sin\theta_1 + b\sin\theta_3 - \zeta_2 \sin\theta_2 = 0 \tag{4.2}$$

Equations (4.1) and (4.2) can be expressed at velocity level as

$$\mathbf{\Gamma}^G \dot{\mathbf{q}} = \mathbf{0} \tag{4.3}$$

where

$$\mathbf{\Gamma}^G = \begin{bmatrix} -\zeta_1 \sin\theta_1 & \cos\theta_1 & \zeta_2 \sin\theta_2 & -\cos\theta_2 & -b\sin\theta_3 \\ \zeta_1 \cos\theta_1 & \sin\theta_1 & -\zeta_2 \cos\theta_2 & -\sin\theta_2 & b\cos\theta_3 \end{bmatrix} \tag{4.4}$$

The position level task equations are

$$f_1 = \zeta_1 \cos\theta_1 + c\cos(\theta_3 + \alpha) = x_P \tag{4.5}$$

$$f_2 = \zeta_1 \sin\theta_1 + c\sin(\theta_3 + \alpha) = y_P \tag{4.6}$$

$$f_3 = \theta_3 = \theta_3 \tag{4.7}$$

Equations (4.5)-(4.7) can be expressed at velocity level as

$$\mathbf{\Gamma}^P \dot{\mathbf{q}} = \dot{\mathbf{x}} \tag{4.8}$$

where

$$\mathbf{\Gamma}^P = \begin{bmatrix} -\zeta_1 \sin\theta_1 & \cos\theta_1 & 0 & 0 & -c\sin(\theta_3 + \alpha) \\ \zeta_1 \cos\theta_1 & \sin\theta_1 & 0 & 0 & c\cos(\theta_3 + \alpha) \\ 0 & 0 & 0 & 0 & 1 \end{bmatrix} \tag{4.9}$$

Equations (4.3) and (4.8) can be combined to give

$$\mathbf{\Gamma}\dot{\mathbf{q}} = \mathbf{h} \tag{4.10}$$

where

$$\mathbf{\Gamma} = \begin{bmatrix} -\zeta_1 \sin\theta_1 & \cos\theta_1 & \zeta_2 \sin\theta_2 & -\cos\theta_2 & -b\sin\theta_3 \\ \zeta_1 \cos\theta_1 & \sin\theta_1 & -\zeta_2 \cos\theta_2 & -\sin\theta_2 & b\cos\theta_3 \\ -\zeta_1 \sin\theta_1 & \cos\theta_1 & 0 & 0 & -c\sin(\theta_3 + \alpha) \\ \zeta_1 \cos\theta_1 & \sin\theta_1 & 0 & 0 & c\cos(\theta_3 + \alpha) \\ 0 & 0 & 0 & 0 & 1 \end{bmatrix} \tag{4.11}$$

Differentiating Equation (4.10) with respect to time gives the acceleration level relations as follows:

$$\boldsymbol{\Gamma}\ddot{\mathbf{q}} = -\dot{\boldsymbol{\Gamma}}\dot{\mathbf{q}} + \dot{\mathbf{h}} \tag{4.12}$$

where

$$\dot{\boldsymbol{\Gamma}} = \begin{bmatrix} \dot{\Gamma}_{11} & \dot{\Gamma}_{12} & \dot{\Gamma}_{13} & \dot{\Gamma}_{14} & \dot{\Gamma}_{15} \\ \dot{\Gamma}_{21} & \dot{\Gamma}_{22} & \dot{\Gamma}_{23} & \dot{\Gamma}_{24} & \dot{\Gamma}_{25} \\ \dot{\Gamma}_{31} & \dot{\Gamma}_{32} & 0 & 0 & \dot{\Gamma}_{35} \\ \dot{\Gamma}_{41} & \dot{\Gamma}_{42} & 0 & 0 & \dot{\Gamma}_{45} \\ 0 & 0 & 0 & 0 & 0 \end{bmatrix} \tag{4.13}$$

The time derivatives are

$$\dot{\Gamma}_{11} = -\dot{\zeta}_1 \sin\theta_1 - \zeta_1\dot{\theta}_1 \cos\theta_1 \tag{4.14}$$

$$\dot{\Gamma}_{12} = -\dot{\theta}_1 \sin\theta_1 \tag{4.15}$$

$$\dot{\Gamma}_{13} = \dot{\zeta}_2 \sin\theta_2 + \zeta_2\dot{\theta}_2 \cos\theta_2 \tag{4.16}$$

$$\dot{\Gamma}_{14} = \dot{\theta}_2 \sin\theta_2 \tag{4.17}$$

$$\dot{\Gamma}_{15} = -b\dot{\theta}_3 \cos\theta_3 \tag{4.18}$$

$$\dot{\Gamma}_{21} = \dot{\zeta}_1 \cos\theta_1 - \zeta_1\dot{\theta}_1 \sin\theta_1 \tag{4.19}$$

$$\dot{\Gamma}_{22} = \dot{\theta}_1 \cos\theta_1 \tag{4.20}$$

$$\dot{\Gamma}_{23} = -\dot{\zeta}_2 \cos\theta_2 + \zeta_2\dot{\theta}_2 \sin\theta_2 \tag{4.21}$$

$$\dot{\Gamma}_{24} = -\dot{\theta}_2 \cos\theta_2 \tag{4.22}$$

$$\dot{\Gamma}_{25} = -b\dot{\theta}_3 \sin\theta_3 \tag{4.23}$$

$$\dot{\Gamma}_{31} = -\dot{\zeta}_1 \sin\theta_1 - \zeta_1\dot{\theta}_1 \cos\theta_1 \tag{4.24}$$

$$\dot{\Gamma}_{32} = -\dot{\theta}_1 \sin\theta_1 \tag{4.25}$$

$$\dot{\Gamma}_{35} = -c\dot{\theta}_3 \cos\left(\theta_3 + \alpha\right) \tag{4.26}$$

$$\dot{\Gamma}_{41} = \dot{\zeta}_1 \cos\theta_1 - \zeta_1\dot{\theta}_1 \sin\theta_1 \tag{4.27}$$

$$\dot{\Gamma}_{42} = \dot{\theta}_1 \cos\theta_1 \tag{4.28}$$

$$\dot{\Gamma}_{45} = -c\dot{\theta}_3 \sin\left(\theta_3 + \alpha\right) \tag{4.29}$$

During the inverse kinematic solution, singularities arise when $|\mathbf{\Gamma}| = 0$. Since $|\mathbf{\Gamma}| = \zeta_1 \zeta_2$, the kinematic singular positions are the positions where $\zeta_1 = 0$ or $\zeta_2 = 0$. These positions are not accessible in practice because of the legs' finite lengths, i.e., an inverse kinematic singularity is not encountered in practice.

Once $\mathbf{q}$ is chosen for the generalized coordinates, the dynamic behavior of the open-chain system can be obtained through the Lagrange's equations. The Lagrangian of the open-chain system is the difference between its kinetic energy and potential energy

$$L = K - U \tag{4.30}$$

Use of Lagrange's equations yields the 5 differential equations for the open-chain system

$$\frac{d}{dt}\left(\frac{\partial L}{\partial \dot{q}_i}\right) - \frac{\partial L}{\partial q_i} = Q_i \quad i = 1, \cdots, 5 \tag{4.31}$$

where Q_i's are the generalized forces.

The kinetic energy of each link is

$$K_i = \frac{1}{2} m_i v_i^2 + \frac{1}{2} I_i \omega_i^2 \quad i = 1, \cdots, 5 \tag{4.32}$$

where m_i, $i = 1, \cdots, 5$ are the masses of the links, v_i, $i = 1, \cdots, 5$ are the velocities of the mass centers of the links, I_i, $i = 1, \cdots, 5$ are the centroidal moments of inertia of the links and ω_i, $i = 1, \cdots, 5$ are the angular velocities of the links. The velocities of the mass centers of the links are

$$\mathbf{v}_i = \frac{d\mathbf{r}_i}{dt} \quad i = 1, \cdots, 5 \tag{4.33}$$

where $\mathbf{r}_i$, $i = 1, \cdots, 5$ are the position vectors of the mass centers of the links. The position vectors of the mass centers of the links are given in the exponential form as:

$$\mathbf{r}_1 = g_1 e^{j\theta_1} \tag{4.34}$$

$$\mathbf{r}_2 = \left(\zeta_1 - g_2\right) e^{j\theta_1} \tag{4.35}$$

$$\mathbf{r}_3 = g_3 e^{j\theta_2} \tag{4.36}$$

$$\mathbf{r}_4 = \left(\zeta_2 - g_4\right) e^{j\theta_2} \tag{4.37}$$

$$\mathbf{r}_5 = \zeta_1 e^{j\theta_1} + g_5 e^{j(\theta_3+\beta)} \tag{4.38}$$

where j is the unit imaginary number and the locations of the mass centers G_i, $i = 1, \cdots, 5$ are indicated by $g_1 = AG_1$, $g_2 = BG_2$, $g_3 = CG_3$, $g_4 = DG_4$, $g_5 = BG_5$ and $\beta = \angle G_5 BD$.

Differentiating, one obtains:

$$\mathbf{v}_1 = j g_1 \dot{\theta}_1 e^{j\theta_1} \tag{4.39}$$

$$\mathbf{v}_2 = \dot{\zeta}_1 e^{j\theta_1} + j\dot{\theta}_1 \left(\zeta_1 - g_2\right) e^{j\theta_1} \tag{4.40}$$

$$\mathbf{v}_3 = j g_3 \dot{\theta}_2 e^{j\theta_2} \tag{4.41}$$

$$\mathbf{v}_4 = \dot{\zeta}_2 e^{j\theta_2} + j\dot{\theta}_2 \left(\zeta_2 - g_4\right) e^{j\theta_2} \tag{4.42}$$

$$\mathbf{v}_5 = \dot{\zeta}_1 e^{j\theta_1} + j\zeta_1 \dot{\theta}_1 e^{j\theta_1} + j\dot{\theta}_3 g_5 e^{j(\theta_3+\beta)} \tag{4.43}$$

or in terms of their Cartesian x and y components:

$$\mathbf{v}_1 = \begin{bmatrix} -g_1 \dot{\theta}_1 \sin\theta_1 \\ g_1 \dot{\theta}_1 \cos\theta_1 \end{bmatrix} \tag{4.44}$$

$$\mathbf{v}_2 = \begin{bmatrix} \dot{\zeta}_1 \cos\theta_1 - \dot{\theta}_1 \left(\zeta_1 - g_2\right) \sin\theta_1 \\ \dot{\zeta}_1 \sin\theta_1 + \dot{\theta}_1 \left(\zeta_1 - g_2\right) \cos\theta_1 \end{bmatrix} \tag{4.45}$$

$$\mathbf{v}_3 = \begin{bmatrix} -g_3 \dot{\theta}_2 \sin\theta_2 \\ g_3 \dot{\theta}_2 \cos\theta_2 \end{bmatrix} \tag{4.46}$$

$$\mathbf{v}_4 = \begin{bmatrix} \dot{\zeta}_2 \cos\theta_2 - \dot{\theta}_2 \left(\zeta_2 - g_4\right) \sin\theta_2 \\ \dot{\zeta}_2 \sin\theta_2 + \dot{\theta}_2 \left(\zeta_2 - g_4\right) \cos\theta_2 \end{bmatrix} \tag{4.47}$$

$$\mathbf{v}_5 = \begin{bmatrix} \dot{\zeta}_1 \cos\theta_1 - \zeta_1\dot{\theta}_1 \sin\theta_1 - \dot{\theta}_3 g_5 \sin(\theta_3+\beta) \\ \dot{\zeta}_1 \sin\theta_1 + \zeta_1\dot{\theta}_1 \cos\theta_1 + \dot{\theta}_3 g_5 \cos(\theta_3+\beta) \end{bmatrix} \tag{4.48}$$

Then, the kinetic energy of each link will be given by:

$$\begin{aligned} K_1 &= \frac{1}{2} m_1 \left[\left(-g_1\dot{\theta}_1 \sin\theta_1\right)^2 + \left(g_1\dot{\theta}_1 \cos\theta_1\right)^2 \right] + \frac{1}{2} I_1 \dot{\theta}_1^2 \\ &= \frac{1}{2} m_1 g_1^2 \dot{\theta}_1^2 + \frac{1}{2} I_1 \dot{\theta}_1^2 \end{aligned} \tag{4.49}$$

$$\begin{aligned} K_2 &= \frac{1}{2} m_2 \left\{ \left[\dot{\zeta}_1 \cos\theta_1 - \dot{\theta}_1 (\zeta_1 - g_2) \sin\theta_1 \right]^2 \right. \\ &\quad \left. + \left[\dot{\zeta}_1 \sin\theta_1 + \dot{\theta}_1 (\zeta_1 - g_2) \cos\theta_1 \right]^2 \right\} + \frac{1}{2} I_2 \dot{\theta}_1^2 \\ &= \frac{1}{2} m_2 \left[\dot{\zeta}_1^2 + (\zeta_1 - g_2)^2 \dot{\theta}_1^2 \right] + \frac{1}{2} I_2 \dot{\theta}_1^2 \end{aligned} \tag{4.50}$$

$$\begin{aligned} K_3 &= \frac{1}{2} m_3 \left[\left(-g_3\dot{\theta}_2 \sin\theta_2\right)^2 + \left(g_3\dot{\theta}_2 \cos\theta_2\right)^2 \right] + \frac{1}{2} I_3 \dot{\theta}_2^2 \\ &= \frac{1}{2} m_3 g_3^2 \dot{\theta}_2^2 + \frac{1}{2} I_3 \dot{\theta}_2^2 \end{aligned} \tag{4.51}$$

$$\begin{aligned} K_4 &= \frac{1}{2} m_4 \left\{ \left[\dot{\zeta}_2 \cos\theta_2 - \dot{\theta}_2 (\zeta_2 - g_4) \sin\theta_2 \right]^2 \right. \\ &\quad \left. + \left[\dot{\zeta}_2 \sin\theta_2 + \dot{\theta}_2 (\zeta_2 - g_4) \cos\theta_2 \right]^2 \right\} + \frac{1}{2} I_4 \dot{\theta}_2^2 \\ &= \frac{1}{2} m_4 \left[\dot{\zeta}_2^2 + (\zeta_2 - g_4)^2 \dot{\theta}_2^2 \right] + \frac{1}{2} I_4 \dot{\theta}_2^2 \end{aligned} \tag{4.52}$$

$$\begin{aligned} K_5 &= \frac{1}{2} m_5 \left\{ \left[\dot{\zeta}_1 \cos\theta_1 - \zeta_1\dot{\theta}_1 \sin\theta_1 - \dot{\theta}_3 g_5 \sin(\theta_3+\beta) \right]^2 \right. \\ &\quad \left. + \left[\dot{\zeta}_1 \sin\theta_1 + \zeta_1\dot{\theta}_1 \cos\theta_1 + \dot{\theta}_3 g_5 \cos(\theta_3+\beta) \right]^2 \right\} + \frac{1}{2} I_5 \dot{\theta}_3^2 \\ &= \frac{1}{2} m_5 \left[\dot{\zeta}_1^2 + \zeta_1^2\dot{\theta}_1^2 + g_5^2\dot{\theta}_3^2 + 2g_5\dot{\zeta}_1\dot{\theta}_3 \sin(\theta_1 - \theta_3 - \beta) \right. \\ &\quad \left. + 2\zeta_1 g_5 \dot{\theta}_1\dot{\theta}_3 \cos(\theta_1 - \theta_3 - \beta) \right] + \frac{1}{2} I_5 \dot{\theta}_3^2 \end{aligned} \tag{4.53}$$

The kinetic energy of the open chain system is the sum of the kinetic energies of each link:

$$
\begin{aligned}
K = {} & \frac{1}{2} m_1 g_1^2 \dot{\theta}_1^2 + \frac{1}{2} I_1 \dot{\theta}_1^2 + \frac{1}{2} m_2 \left[\dot{\zeta}_1^2 + \left(\zeta_1 - g_2 \right)^2 \dot{\theta}_1^2 \right] + \frac{1}{2} I_2 \dot{\theta}_1^2 \\
& + \frac{1}{2} m_3 g_3^2 \dot{\theta}_2^2 + \frac{1}{2} I_3 \dot{\theta}_2^2 + \frac{1}{2} m_4 \left[\dot{\zeta}_2^2 + \left(\zeta_2 - g_4 \right)^2 \dot{\theta}_2^2 \right] + \frac{1}{2} I_4 \dot{\theta}_2^2 \\
& + \frac{1}{2} m_5 \left[\dot{\zeta}_1^2 + \zeta_1^2 \dot{\theta}_1^2 + g_5^2 \dot{\theta}_3^2 + 2 g_5 \dot{\zeta}_1 \dot{\theta}_3 \sin\left(\theta_1 - \theta_3 - \beta \right) \right. \\
& \left. + 2 \zeta_1 g_5 \dot{\theta}_1 \dot{\theta}_3 \cos\left(\theta_1 - \theta_3 - \beta \right) \right] + \frac{1}{2} I_5 \dot{\theta}_3^2
\end{aligned}
\tag{4.54}
$$

The potential energy of each link is

$$U_i = m_i g h_i \quad i = 1, \cdots, 5 \tag{4.55}$$

where g is the gravitational acceleration and h_i, $i = 1, \cdots, 5$ are the distances from the datum to the mass centers of the links. Choosing the joint at A as the datum, the potential energy of each link will be given by:

$$U_1 = m_1 g g_1 \sin\theta_1 \tag{4.56}$$

$$U_2 = m_2 g \left(\zeta_1 - g_2 \right) \sin\theta_1 \tag{4.57}$$

$$U_3 = m_3 g g_3 \sin\theta_2 \tag{4.58}$$

$$U_4 = m_4 g \left(\zeta_2 - g_4 \right) \sin\theta_2 \tag{4.59}$$

$$U_5 = m_5 g \left[\zeta_1 \sin\theta_1 + g_5 \sin\left(\theta_3 + \beta \right) \right] \tag{4.60}$$

The potential energy of the open chain system is the sum of the potential energies of each link:

$$
\begin{aligned}
U = {} & m_1 g g_1 \sin\theta_1 + m_2 g \left(\zeta_1 - g_2 \right) \sin\theta_1 + m_3 g g_3 \sin\theta_2 + m_4 g \left(\zeta_2 - g_4 \right) \sin\theta_2 \\
& + m_5 g \left[\zeta_1 \sin\theta_1 + g_5 \sin\left(\theta_3 + \beta \right) \right]
\end{aligned}
\tag{4.61}
$$

Substituting Equations (4.54) and (4.61) into Equation (4.30), the Lagrangian of the open-chain system is

$$
\begin{aligned}
L = {} & \frac{1}{2} m_1 g_1^2 \dot{\theta}_1^2 + \frac{1}{2} I_1 \dot{\theta}_1^2 + \frac{1}{2} m_2 \left[\dot{\zeta}_1^2 + \left(\zeta_1 - g_2 \right)^2 \dot{\theta}_1^2 \right] + \frac{1}{2} I_2 \dot{\theta}_1^2 \\
& + \frac{1}{2} m_3 g_3^2 \dot{\theta}_2^2 + \frac{1}{2} I_3 \dot{\theta}_2^2 + \frac{1}{2} m_4 \left[\dot{\zeta}_2^2 + \left(\zeta_2 - g_4 \right)^2 \dot{\theta}_2^2 \right] + \frac{1}{2} I_4 \dot{\theta}_2^2 \\
& + \frac{1}{2} m_5 \left[\dot{\zeta}_1^2 + \zeta_1^2 \dot{\theta}_1^2 + g_5^2 \dot{\theta}_3^2 + 2 g_5 \dot{\zeta}_1 \dot{\theta}_3 \sin\left(\theta_1 - \theta_3 - \beta \right) \right. \\
& \left. + 2 \zeta_1 g_5 \dot{\theta}_1 \dot{\theta}_3 \cos\left(\theta_1 - \theta_3 - \beta \right) \right] + \frac{1}{2} I_5 \dot{\theta}_3^2 \\
& - m_1 g g_1 \sin\theta_1 - m_2 g \left(\zeta_1 - g_2 \right) \sin\theta_1 - m_3 g g_3 \sin\theta_2 - m_4 g \left(\zeta_2 - g_4 \right) \sin\theta_2 \\
& - m_5 g \left[\zeta_1 \sin\theta_1 + g_5 \sin\left(\theta_3 + \beta \right) \right]
\end{aligned}
\tag{4.62}
$$

The partial derivatives are

$$
\begin{aligned}
\frac{\partial L}{\partial \dot{\theta}_1} = {} & \left[m_1 g_1^2 + I_1 + I_2 + m_2 \left(\zeta_1 - g_2 \right)^2 + m_5 \zeta_1^2 \right] \dot{\theta}_1 \\
& + m_5 \zeta_1 g_5 \dot{\theta}_3 \cos\left(\theta_1 - \theta_3 - \beta \right)
\end{aligned}
\tag{4.63}
$$

$$
\frac{\partial L}{\partial \dot{\zeta}_1} = \left(m_2 + m_5 \right) \dot{\zeta}_1 + m_5 g_5 \dot{\theta}_3 \sin\left(\theta_1 - \theta_3 - \beta \right) \tag{4.64}
$$

$$
\frac{\partial L}{\partial \dot{\theta}_2} = \left[m_3 g_3^2 + I_3 + I_4 + m_4 \left(\zeta_2 - g_4 \right)^2 \right] \dot{\theta}_2 \tag{4.65}
$$

$$
\frac{\partial L}{\partial \dot{\zeta}_2} = m_4 \dot{\zeta}_2 \tag{4.66}
$$

$$
\frac{\partial L}{\partial \dot{\theta}_3} = m_5 \zeta_1 g_5 \dot{\theta}_1 \cos\left(\theta_1 - \theta_3 - \beta \right) + m_5 g_5 \dot{\zeta}_1 \sin\left(\theta_1 - \theta_3 - \beta \right) + \left(m_5 g_5^2 + I_5 \right) \dot{\theta}_3 \tag{4.67}
$$

$$
\begin{aligned}
\frac{\partial L}{\partial \theta_1} = {} & m_5 g_5 \dot{\theta}_3 \left[\dot{\zeta}_1 \cos\left(\theta_1 - \theta_3 - \beta \right) - \zeta_1 \dot{\theta}_1 \sin\left(\theta_1 - \theta_3 - \beta \right) \right] \\
& - \left[m_1 g_1 + m_2 \left(\zeta_1 - g_2 \right) + m_5 \zeta_1 \right] g \cos\theta_1
\end{aligned}
\tag{4.68}
$$

$$
\begin{aligned}
\frac{\partial L}{\partial \zeta_1} = {} & m_2 \left(\zeta_1 - g_2 \right) \dot{\theta}_1^2 + m_5 \dot{\theta}_1 \left[\zeta_1 \dot{\theta}_1 + g_5 \dot{\theta}_3 \cos\left(\theta_1 - \theta_3 - \beta \right) \right] \\
& - \left(m_2 + m_5 \right) g \sin\theta_1
\end{aligned}
\tag{4.69}
$$

$$
\frac{\partial L}{\partial \theta_2} = - \left[m_3 g_3 + m_4 \left(\zeta_2 - g_4 \right) \right] g \cos\theta_2 \tag{4.70}
$$

$$\frac{\partial L}{\partial \zeta_2} = m_4\left[\left(\zeta_2 - g_4\right)\dot{\theta}_2^2 - g\sin\theta_2\right] \tag{4.71}$$

$$\begin{aligned}\frac{\partial L}{\partial \theta_3} = -m_5 g_5 \Big\{&\dot{\theta}_3\left[\dot{\zeta}_1\cos\left(\theta_1-\theta_3-\beta\right) - \zeta_1\dot{\theta}_1\sin\left(\theta_1-\theta_3-\beta\right)\right] \\ &+ g\cos\left(\theta_3+\beta\right)\Big\}\end{aligned} \tag{4.72}$$

The time derivatives of the first group of terms are

$$\begin{aligned}\frac{d}{dt}\left(\frac{\partial L}{\partial \dot{\theta}_1}\right) = &\left[m_1 g_1^2 + I_1 + I_2 + m_2\left(\zeta_1 - g_2\right)^2 + m_5\zeta_1^2\right]\ddot{\theta}_1 \\ &+ m_5\zeta_1 g_5\ddot{\theta}_3\cos\left(\theta_1-\theta_3-\beta\right) \\ &+ 2\left[m_2\left(\zeta_1 - g_2\right) + m_5\zeta_1\right]\dot{\theta}_1\dot{\zeta}_1 + m_5 g_5\dot{\zeta}_1\dot{\theta}_3\cos\left(\theta_1-\theta_3-\beta\right) \\ &- \left(m_5\zeta_1 g_5\dot{\theta}_1\dot{\theta}_3 - m_5\zeta_1 g_5\dot{\theta}_3^2\right)\sin\left(\theta_1-\theta_3-\beta\right)\end{aligned} \tag{4.73}$$

$$\begin{aligned}\frac{d}{dt}\left(\frac{\partial L}{\partial \dot{\zeta}_1}\right) = &\left(m_2 + m_5\right)\ddot{\zeta}_1 + m_5 g_5\ddot{\theta}_3\sin\left(\theta_1-\theta_3-\beta\right) \\ &+ \left(m_5 g_5\dot{\theta}_1\dot{\theta}_3 - m_5 g_5\dot{\theta}_3^2\right)\cos\left(\theta_1-\theta_3-\beta\right)\end{aligned} \tag{4.74}$$

$$\frac{d}{dt}\left(\frac{\partial L}{\partial \dot{\theta}_2}\right) = \left[m_3 g_3^2 + I_3 + I_4 + m_4\left(\zeta_2 - g_4\right)^2\right]\ddot{\theta}_2 + 2m_4\left(\zeta_2 - g_4\right)\dot{\theta}_2\dot{\zeta}_2 \tag{4.75}$$

$$\frac{d}{dt}\left(\frac{\partial L}{\partial \dot{\zeta}_2}\right) = m_4\ddot{\zeta}_2 \tag{4.76}$$

$$\begin{aligned}\frac{d}{dt}\left(\frac{\partial L}{\partial \dot{\theta}_3}\right) = &\, m_5\zeta_1 g_5\ddot{\theta}_1\cos\left(\theta_1-\theta_3-\beta\right) + m_5 g_5\ddot{\zeta}_1\sin\left(\theta_1-\theta_3-\beta\right) \\ &+ \left(m_5 g_5^2 + I_5\right)\ddot{\theta}_3 - \left(m_5\zeta_1 g_5\dot{\theta}_1^2 - m_5\zeta_1 g_5\dot{\theta}_1\dot{\theta}_3\right)\sin\left(\theta_1-\theta_3-\beta\right) \\ &+ \left(2m_5 g_5\dot{\zeta}_1\dot{\theta}_1 - m_5 g_5\dot{\zeta}_1\dot{\theta}_3\right)\cos\left(\theta_1-\theta_3-\beta\right)\end{aligned} \tag{4.77}$$

The corresponding set of Lagrange's equations of the open-chain system is then

$$
\begin{aligned}
T_1 &= \frac{d}{dt}\left(\frac{\partial L}{\partial \dot{\theta}_1}\right) - \frac{\partial L}{\partial \theta_1} \\
&= \left[m_1 g_1^2 + I_1 + I_2 + m_2 \left(\zeta_1 - g_2\right)^2 + m_5 \zeta_1^2 \right] \ddot{\theta}_1 + m_5 \zeta_1 g_5 \ddot{\theta}_3 \cos\left(\theta_1 - \theta_3 - \beta\right) \\
&\quad + 2\left[m_2 \left(\zeta_1 - g_2\right) + m_5 \zeta_1 \right] \dot{\theta}_1 \dot{\zeta}_1 + m_5 \zeta_1 g_5 \dot{\theta}_3^2 \sin\left(\theta_1 - \theta_3 - \beta\right) \\
&\quad + \left[m_1 g_1 + m_2 \left(\zeta_1 - g_2\right) + m_5 \zeta_1 \right] g \cos\theta_1
\end{aligned} \tag{4.78}
$$

$$
\begin{aligned}
F_1 &= \frac{d}{dt}\left(\frac{\partial L}{\partial \dot{\zeta}_1}\right) - \frac{\partial L}{\partial \zeta_1} \\
&= \left(m_2 + m_5\right) \ddot{\zeta}_1 + m_5 g_5 \ddot{\theta}_3 \sin\left(\theta_1 - \theta_3 - \beta\right) - \left[m_2 \left(\zeta_1 - g_2\right) + m_5 \zeta_1 \right] \dot{\theta}_1^2 \\
&\quad - m_5 g_5 \dot{\theta}_3^2 \cos\left(\theta_1 - \theta_3 - \beta\right) + \left(m_2 + m_5\right) g \sin\theta_1
\end{aligned} \tag{4.79}
$$

$$
\begin{aligned}
0 &= \frac{d}{dt}\left(\frac{\partial L}{\partial \dot{\theta}_2}\right) - \frac{\partial L}{\partial \theta_2} \\
&= \left[m_3 g_3^2 + I_3 + I_4 + m_4 \left(\zeta_2 - g_4\right)^2 \right] \ddot{\theta}_2 + 2 m_4 \left(\zeta_2 - g_4\right) \dot{\theta}_2 \dot{\zeta}_2 \\
&\quad + \left[m_3 g_3 + m_4 \left(\zeta_2 - g_4\right) \right] g \cos\theta_2
\end{aligned} \tag{4.80}
$$

$$
\begin{aligned}
F_2 &= \frac{d}{dt}\left(\frac{\partial L}{\partial \dot{\zeta}_2}\right) - \frac{\partial L}{\partial \zeta_2} \\
&= m_4 \ddot{\zeta}_2 - m_4 \left[\left(\zeta_2 - g_4\right) \dot{\theta}_2^2 - g \sin\theta_2 \right]
\end{aligned} \tag{4.81}
$$

$$
\begin{aligned}
0 &= \frac{d}{dt}\left(\frac{\partial L}{\partial \dot{\theta}_3}\right) - \frac{\partial L}{\partial \theta_3} \\
&= m_5 \zeta_1 g_5 \ddot{\theta}_1 \cos\left(\theta_1 - \theta_3 - \beta\right) + m_5 g_5 \ddot{\zeta}_1 \sin\left(\theta_1 - \theta_3 - \beta\right) + \left(m_5 g_5^2 + I_5\right) \ddot{\theta}_3 \\
&\quad + m_5 g_5 \left[-\zeta_1 \dot{\theta}_1^2 \sin\left(\theta_1 - \theta_3 - \beta\right) + 2 \dot{\zeta}_1 \dot{\theta}_1 \cos\left(\theta_1 - \theta_3 - \beta\right) + g \cos\left(\theta_3 + \beta\right) \right]
\end{aligned} \tag{4.82}
$$

Equations (4.78)-(4.82) can be expressed in matrix form as follows:

$$
\mathbf{M}\ddot{\mathbf{q}} + \mathbf{B} = \mathbf{Z}^T \mathbf{T} \tag{4.83}
$$

where $\mathbf{M}$, $\mathbf{B}$ and $\mathbf{Z}^T$ are

$$\mathbf{M} = \begin{bmatrix} M_{11} & 0 & 0 & 0 & M_{15} \\ 0 & M_{22} & 0 & 0 & M_{25} \\ 0 & 0 & M_{33} & 0 & 0 \\ 0 & 0 & 0 & M_{44} & 0 \\ M_{51} & M_{52} & 0 & 0 & M_{55} \end{bmatrix} \tag{4.84}$$

$$\mathbf{B} = \begin{bmatrix} B_1 \\ B_2 \\ B_3 \\ B_4 \\ B_5 \end{bmatrix} \tag{4.85}$$

$$\mathbf{Z}^T = \begin{bmatrix} 1 & 0 & 0 \\ 0 & 1 & 0 \\ 0 & 0 & 0 \\ 0 & 0 & 1 \\ 0 & 0 & 0 \end{bmatrix} \tag{4.86}$$

and the elements of $\mathbf{M}$ and $\mathbf{B}$ are given below:

$$M_{11} = m_1 g_1^2 + I_1 + I_2 + m_2 \left(\zeta_1 - g_2\right)^2 + m_5 \zeta_1^2 \tag{4.87}$$

$$M_{15} = m_5 \zeta_1 g_5 \cos\left(\theta_1 - \theta_3 - \beta\right) \tag{4.88}$$

$$M_{22} = m_2 + m_5 \tag{4.89}$$

$$M_{25} = m_5 g_5 \sin\left(\theta_1 - \theta_3 - \beta\right) \tag{4.90}$$

$$M_{33} = m_3 g_3^2 + I_3 + I_4 + m_4 \left(\zeta_2 - g_4\right)^2 \tag{4.91}$$

$$M_{44} = m_4 \tag{4.92}$$

$$M_{51} = m_5 \zeta_1 g_5 \cos\left(\theta_1 - \theta_3 - \beta\right) \tag{4.93}$$

$$M_{52} = m_5 g_5 \sin\left(\theta_1 - \theta_3 - \beta\right) \tag{4.94}$$

$$M_{55} = m_5 g_5^2 + I_5 \tag{4.95}$$

$$\begin{aligned} B_1 = {} & 2\left[m_2\left(\zeta_1 - g_2\right) + m_5 \zeta_1\right]\dot{\theta}_1 \dot{\zeta}_1 + m_5 \zeta_1 g_5 \dot{\theta}_3^2 \sin\left(\theta_1 - \theta_3 - \beta\right) \\ & + \left[m_1 g_1 + m_2\left(\zeta_1 - g_2\right) + m_5 \zeta_1\right] g \cos\theta_1 \end{aligned} \tag{4.96}$$

$$B_2 = -\left[m_2 \left(\zeta_1 - g_2 \right) + m_5 \zeta_1 \right] \dot{\theta}_1^2 - m_5 g_5 \dot{\theta}_3^2 \cos\left(\theta_1 - \theta_3 - \beta \right) + \left(m_2 + m_5 \right) g \sin\theta_1 \tag{4.97}$$

$$B_3 = 2m_4 \left(\zeta_2 - g_4 \right) \dot{\theta}_2 \dot{\zeta}_2 + \left[m_3 g_3 + m_4 \left(\zeta_2 - g_4 \right) \right] g \cos\theta_2 \tag{4.98}$$

$$B_4 = -m_4 \left[\left(\zeta_2 - g_4 \right) \dot{\theta}_2^2 - g \sin\theta_2 \right] \tag{4.99}$$

$$B_5 = m_5 g_5 \left[-\zeta_1 \dot{\theta}_1^2 \sin\left(\theta_1 - \theta_3 - \beta \right) + 2\dot{\zeta}_1 \dot{\theta}_1 \cos\left(\theta_1 - \theta_3 - \beta \right) + g \cos\left(\theta_3 + \beta \right) \right] \tag{4.100}$$

Then, imposing the constraint equations on Equation (4.83), the dynamic behavior of the parallel manipulator can be expressed by the following matrix equation:

$$\mathbf{M}\ddot{\mathbf{q}} + \mathbf{B} = \mathbf{Z}^T \mathbf{T} + \mathbf{\Gamma}^{G^T} \boldsymbol{\lambda} \tag{4.101}$$

where $\boldsymbol{\lambda} = \left[\lambda_1 \quad \lambda_2 \right]^T$.

Combining the terms involving $\boldsymbol{\lambda}$ and $\mathbf{T}$, Equation (4.101) can be written again as

$$\mathbf{A}^T \boldsymbol{\mu} = \mathbf{M}\ddot{\mathbf{q}} + \mathbf{B} \tag{4.102}$$

where

$$\boldsymbol{\mu}^T = \left[\boldsymbol{\lambda}^T \quad \mathbf{T}^T \right] \tag{4.103}$$

and

$$\mathbf{A}^T = \begin{bmatrix} -\zeta_1 \sin\theta_1 & \zeta_1 \cos\theta_1 & 1 & 0 & 0 \\ \cos\theta_1 & \sin\theta_1 & 0 & 1 & 0 \\ \zeta_2 \sin\theta_2 & -\zeta_2 \cos\theta_2 & 0 & 0 & 0 \\ -\cos\theta_2 & -\sin\theta_2 & 0 & 0 & 1 \\ -b\sin\theta_3 & b\cos\theta_3 & 0 & 0 & 0 \end{bmatrix} \tag{4.104}$$

Since $\left| \mathbf{A} \right| = b\zeta_2 \sin\left(\theta_3 - \theta_2 \right)$, drive singularities arise when $\zeta_2 = 0$ or $\theta_3 - \theta_2 = \pm n\pi$, $\left(n = 0, 1, 2, \ldots \right)$. Noting that ζ_2 cannot become zero in practice, the drive singular positions are those positions where the points B, D and C happen to be collinear.

4.2 Consistency Conditions and Modified Equations

At a singular position, the third and fifth rows of $\mathbf{A}^T$ become linearly independent as

$$A_{3j}^T + \sigma \frac{\zeta_2}{b} A_{5j}^T = 0 \quad j = 1, \ldots, 5 \tag{4.105}$$

where $\sigma = 1$ if $\theta_2 = \theta_3$ and $\sigma = -1$ if $\theta_3 - \theta_2 = \pi$. The same relation must be present among the third and fifth rows of Equation (4.102).

$$\begin{aligned} &\left(A_{31}^T + \sigma \frac{\zeta_2}{b} A_{51}^T \right) \lambda_1 + \left(A_{32}^T + \sigma \frac{\zeta_2}{b} A_{52}^T \right) \lambda_2 = M_{33} \ddot{\theta}_2 \\ &+ \sigma \frac{\zeta_2}{b} \left(M_{51} \ddot{\theta}_1 + M_{52} \ddot{\zeta}_1 + M_{55} \ddot{\theta}_3 \right) + B_3 + \sigma \frac{\zeta_2}{b} B_5 \end{aligned} \tag{4.106}$$

On substituting Equation (4.105), Equation (4.106) becomes

$$M_{33} \ddot{\theta}_2 + \sigma \frac{\zeta_2}{b} \left(M_{51} \ddot{\theta}_1 + M_{52} \ddot{\zeta}_1 + M_{55} \ddot{\theta}_3 \right) + B_3 + \sigma \frac{\zeta_2}{b} B_5 = 0 \tag{4.107}$$

Equation (4.107) is the consistency condition that $\ddot{\mathbf{q}}$ should satisfy at the singular position.

Differentiating Equation (4.106) with respect to time, one obtains

$$\begin{aligned} &\left(A_{31}^T + \sigma \frac{\zeta_2}{b} A_{51}^T \right) \dot{\lambda}_1 + \left(A_{32}^T + \sigma \frac{\zeta_2}{b} A_{52}^T \right) \dot{\lambda}_2 + \left(\dot{A}_{31}^T + \sigma \frac{\zeta_2}{b} \dot{A}_{51}^T + \sigma \frac{\dot{\zeta}_2}{b} A_{51}^T \right) \lambda_1 \\ &+ \left(\dot{A}_{32}^T + \sigma \frac{\zeta_2}{b} \dot{A}_{52}^T + \sigma \frac{\dot{\zeta}_2}{b} A_{52}^T \right) \lambda_2 = M_{33} \dddot{\theta}_2 + \sigma \frac{\zeta_2}{b} \left(M_{51} \dddot{\theta}_1 + M_{52} \dddot{\zeta}_1 + M_{55} \dddot{\theta}_3 \right) \\ &+ \dot{M}_{33} \ddot{\theta}_2 + \sigma \frac{\zeta_2}{b} \left(\dot{M}_{51} \ddot{\theta}_1 + \dot{M}_{52} \ddot{\zeta}_1 + \dot{M}_{55} \ddot{\theta}_3 \right) + \sigma \frac{\dot{\zeta}_2}{b} \left(M_{51} \ddot{\theta}_1 + M_{52} \ddot{\zeta}_1 + M_{55} \ddot{\theta}_3 \right) \\ &+ \dot{B}_3 + \sigma \frac{\zeta_2}{b} \dot{B}_5 + \sigma \frac{\dot{\zeta}_2}{b} B_5 \end{aligned} \tag{4.108}$$

In view of the fact that the coefficients of $\dot{\lambda}_1$ and $\dot{\lambda}_2$ vanish thanks to Equation (4.105) at the singular position, there is a neighborhood in which the terms

containing $\dot{\lambda}_1$ and $\dot{\lambda}_2$ are negligible. Therefore in that neighborhood they can be dropped to yield

$$H_1\lambda_1 + H_2\lambda_2 = \Psi \tag{4.109}$$

where

$$H_1 = \dot{A}_{31}^T + \sigma\frac{\zeta_2}{b}\dot{A}_{51}^T + \sigma\frac{\dot{\zeta}_2}{b}A_{51}^T \tag{4.110}$$

$$H_2 = \dot{A}_{32}^T + \sigma\frac{\zeta_2}{b}\dot{A}_{52}^T + \sigma\frac{\dot{\zeta}_2}{b}A_{52}^T \tag{4.111}$$

$$\begin{aligned}\Psi = {} & M_{33}\ddot{\theta}_2 + \sigma\frac{\zeta_2}{b}\left(M_{51}\ddot{\theta}_1 + M_{52}\ddot{\zeta}_1 + M_{55}\ddot{\theta}_3\right) \\ & + \dot{M}_{33}\ddot{\theta}_2 + \sigma\frac{\zeta_2}{b}\left(\dot{M}_{51}\ddot{\theta}_1 + \dot{M}_{52}\ddot{\zeta}_1 + \dot{M}_{55}\ddot{\theta}_3\right) \\ & + \sigma\frac{\dot{\zeta}_2}{b}\left(M_{51}\ddot{\theta}_1 + M_{52}\ddot{\zeta}_1 + M_{55}\ddot{\theta}_3\right) + \dot{B}_3 + \sigma\frac{\zeta_2}{b}\dot{B}_5 + \sigma\frac{\dot{\zeta}_2}{b}B_5\end{aligned} \tag{4.112}$$

The time derivatives that appear in Equation (4.109) are

$$\dot{A}_{31}^T = \dot{\zeta}_2\sin\theta_2 + \zeta_2\dot{\theta}_2\cos\theta_2 \tag{4.113}$$

$$\dot{A}_{32}^T = -\dot{\zeta}_2\cos\theta_2 + \zeta_2\dot{\theta}_2\sin\theta_2 \tag{4.114}$$

$$\dot{A}_{51}^T = -b\dot{\theta}_3\cos\theta_3 \tag{4.115}$$

$$\dot{A}_{52}^T = -b\dot{\theta}_3\sin\theta_3 \tag{4.116}$$

$$\dot{M}_{33} = 2m_4\dot{\zeta}_2\left(\zeta_2 - g_4\right) \tag{4.117}$$

$$\dot{M}_{51} = m_5\dot{\zeta}_1 g_5\cos\left(\theta_1 - \theta_3 - \beta\right) - m_5\zeta_1 g_5\left(\dot{\theta}_1 - \dot{\theta}_3\right)\sin\left(\theta_1 - \theta_3 - \beta\right) \tag{4.118}$$

$$\dot{M}_{52} = m_5 g_5\left(\dot{\theta}_1 - \dot{\theta}_3\right)\cos\left(\theta_1 - \theta_3 - \beta\right) \tag{4.119}$$

$$\dot{M}_{55} = 0 \tag{4.120}$$

$$\begin{aligned}\dot{B}_3 = {} & 2m_4\left(\zeta_2 - g_4\right)\dot{\zeta}_2\ddot{\theta}_2 + 2m_4\left(\zeta_2 - g_4\right)\dot{\theta}_2\ddot{\zeta}_2 + 2m_4\dot{\theta}_2\dot{\zeta}_2^2 \\ & + m_4 g\dot{\zeta}_2\cos\theta_2 - \left[m_3 g_3 + m_4\left(\zeta_2 - g_4\right)\right]g\dot{\theta}_2\sin\theta_2\end{aligned} \tag{4.121}$$

$$\begin{aligned}\dot{B}_5 = m_5 g_5 \Big\{ & \Big[-2\zeta_1 \dot{\theta}_1 \sin\left(\theta_1 - \theta_3 - \beta\right) + 2\dot{\zeta}_1 \cos\left(\theta_1 - \theta_3 - \beta\right) \Big] \ddot{\theta}_1 \\ & + 2\dot{\theta}_1 \ddot{\zeta}_1 \cos\left(\theta_1 - \theta_3 - \beta\right) - \dot{\zeta}_1 \dot{\theta}_1^2 \sin\left(\theta_1 - \theta_3 - \beta\right) \\ & - \zeta_1 \dot{\theta}_1^2 \left(\dot{\theta}_1 - \dot{\theta}_3\right) \cos\left(\theta_1 - \theta_3 - \beta\right) \\ & - 2\dot{\zeta}_1 \dot{\theta}_1 \left(\dot{\theta}_1 - \dot{\theta}_3\right) \sin\left(\theta_1 - \theta_3 - \beta\right) - g\dot{\theta}_3 \sin\left(\theta_3 + \beta\right) \Big\}\end{aligned} \tag{4.122}$$

Equation (4.109) is the modified equation that can be used to replace the third or fifth equation of Equation (4.102).

Note that $\ddot{\mathbf{q}}$ which appears in the modified equation and the prescribed end-effector jerks $\dddot{\mathbf{x}}$ are related via the derivative of Equation (4.12),

$$\boldsymbol{\Gamma}\ddot{\mathbf{q}} = -2\dot{\boldsymbol{\Gamma}}\dot{\mathbf{q}} - \ddot{\boldsymbol{\Gamma}}\mathbf{q} + \ddot{\mathbf{h}} \tag{4.123}$$

where

$$\ddot{\boldsymbol{\Gamma}} = \begin{bmatrix} \ddot{\Gamma}_{11} & \ddot{\Gamma}_{12} & \ddot{\Gamma}_{13} & \ddot{\Gamma}_{14} & \ddot{\Gamma}_{15} \\ \ddot{\Gamma}_{21} & \ddot{\Gamma}_{22} & \ddot{\Gamma}_{23} & \ddot{\Gamma}_{24} & \ddot{\Gamma}_{25} \\ \ddot{\Gamma}_{31} & \ddot{\Gamma}_{32} & 0 & 0 & \ddot{\Gamma}_{35} \\ \ddot{\Gamma}_{41} & \ddot{\Gamma}_{42} & 0 & 0 & \ddot{\Gamma}_{45} \\ 0 & 0 & 0 & 0 & 0 \end{bmatrix} \tag{4.124}$$

with

$$\ddot{\Gamma}_{11} = -\zeta_1 \ddot{\theta}_1 \cos\theta_1 - \ddot{\zeta}_1 \sin\theta_1 - 2\dot{\theta}_1 \dot{\zeta}_1 \cos\theta_1 + \zeta_1 \dot{\theta}_1^2 \sin\theta_1 \tag{4.125}$$

$$\ddot{\Gamma}_{12} = -\ddot{\theta}_1 \sin\theta_1 - \dot{\theta}_1^2 \cos\theta_1 \tag{4.126}$$

$$\ddot{\Gamma}_{13} = \zeta_2 \ddot{\theta}_2 \cos\theta_2 + \ddot{\zeta}_2 \sin\theta_2 + 2\dot{\zeta}_2 \dot{\theta}_2 \cos\theta_2 - \zeta_2 \dot{\theta}_2^2 \sin\theta_2 \tag{4.127}$$

$$\ddot{\Gamma}_{14} = \ddot{\theta}_2 \sin\theta_2 + \dot{\theta}_2^2 \cos\theta_2 \tag{4.128}$$

$$\ddot{\Gamma}_{15} = -b\ddot{\theta}_3 \cos\theta_3 + b\dot{\theta}_3^2 \sin\theta_3 \tag{4.129}$$

$$\ddot{\Gamma}_{21} = -\zeta_1 \ddot{\theta}_1 \sin\theta_1 + \ddot{\zeta}_1 \cos\theta_1 - 2\dot{\theta}_1 \dot{\zeta}_1 \sin\theta_1 - \zeta_1 \dot{\theta}_1^2 \cos\theta_1 \tag{4.130}$$

$$\ddot{\Gamma}_{22} = \ddot{\theta}_1 \cos\theta_1 - \dot{\theta}_1^2 \sin\theta_1 \tag{4.131}$$

$$\ddot{\Gamma}_{23} = \zeta_2 \ddot{\theta}_2 \sin\theta_2 - \ddot{\zeta}_2 \cos\theta_2 + 2\dot{\theta}_2 \dot{\zeta}_2 \sin\theta_2 + \zeta_2 \dot{\theta}_2^2 \cos\theta_2 \tag{4.132}$$

$$\ddot{\Gamma}_{24} = -\ddot{\theta}_2 \cos\theta_2 + \dot{\theta}_2^2 \sin\theta_2 \tag{4.133}$$

$$\ddot{\Gamma}_{25} = -b\ddot{\theta}_3 \sin\theta_3 - b\dot{\theta}_3^2 \cos\theta_3 \tag{4.134}$$

$$\ddot{\Gamma}_{31} = -\zeta_1\ddot{\theta}_1 \cos\theta_1 - \ddot{\zeta}_1 \sin\theta_1 - 2\dot{\theta}_1\dot{\zeta}_1 \cos\theta_1 + \zeta_1\dot{\theta}_1^2 \sin\theta_1 \tag{4.135}$$

$$\ddot{\Gamma}_{32} = -\ddot{\theta}_1 \sin\theta_1 - \dot{\theta}_1^2 \cos\theta_1 \tag{4.136}$$

$$\ddot{\Gamma}_{35} = -c\ddot{\theta}_3 \cos(\theta_3 + \alpha) + c\dot{\theta}_3^2 \sin(\theta_3 + \alpha) \tag{4.137}$$

$$\ddot{\Gamma}_{41} = -\zeta_1\ddot{\theta}_1 \sin\theta_1 + \ddot{\zeta}_1 \cos\theta_1 - 2\dot{\theta}_1\dot{\zeta}_1 \sin\theta_1 - \zeta_1\dot{\theta}_1^2 \cos\theta_1 \tag{4.138}$$

$$\ddot{\Gamma}_{42} = \ddot{\theta}_1 \cos\theta_1 - \dot{\theta}_1^2 \sin\theta_1 \tag{4.139}$$

$$\ddot{\Gamma}_{45} = -c\ddot{\theta}_3 \sin(\theta_3 + \alpha) - c\dot{\theta}_3^2 \cos(\theta_3 + \alpha) \tag{4.140}$$

When the modified equation replaces the third equation in Equation (4.102), Equation (4.102) takes the following form by which one can find $\boldsymbol{\mu}$ (and hence $\mathbf{T}$) in the neighborhood of the drive singularities,

$$\mathbf{D}^T\boldsymbol{\mu} = \mathbf{S} \tag{4.141}$$

where

$$D_{ij}^T = \begin{cases} A_{ij}^T & i = 1,\ 2,\ 4,\ 5; \quad j = 1,\ \ldots,\ 5 \\ H_j & i = 3; \qquad j = 1,\ 2 \\ 0 & i = 3; \qquad j = 3,\ 4,\ 5 \end{cases} \tag{4.142}$$

and

$$S_i = \begin{cases} M_{ij}\ddot{q}_j + B_i & i = 1,\ 2,\ 4,\ 5 \\ \Psi & i = 3 \end{cases} \tag{4.143}$$

Equation (4.141) is utilized in the neighborhood of the drive singularities, i.e., $|\theta_3 - \theta_2 \pm n\pi| < \varepsilon \quad (n = 0,\ 1,\ 2,\ \ldots)$ and Equation (4.102) is used elsewhere, where ε is a positive number which defines the size of the neighborhood. ε should be selected small enough to have the error in the modified equation in Equation (4.141) insignificant and also large enough to prevent the $\mathbf{A}$ matrix in Equation (4.102) from becoming ill-conditioned.

4.3 Inverse Dynamics Control outside the Neighborhood of Drive Singularities

The first, second and fourth elements of the generalized force vector $\mathbf{Z}^T\mathbf{T}$ in Equation (4.101) are the elements of the vector $\mathbf{T}$ and its third and fifth elements are zero. Accordingly, the third and fourth rows of Equation (4.101) can be interchanged to have those two zero elements at the bottom:

$$\bar{\mathbf{M}}\ddot{\mathbf{q}} + \bar{\mathbf{B}} = \begin{bmatrix} \mathbf{T} \\ \mathbf{0} \end{bmatrix} + \bar{\mathbf{\Gamma}}^{G^T}\boldsymbol{\lambda} \tag{4.144}$$

where $\bar{\mathbf{M}}$, $\bar{\mathbf{B}}$ and $\bar{\mathbf{\Gamma}}^{G^T}$ are obtained by interchanging the third and fourth rows of $\mathbf{M}$, $\mathbf{B}$ and $\mathbf{\Gamma}^{G^T}$, respectively as follows:

$$\bar{\mathbf{M}} = \begin{bmatrix} M_{11} & 0 & 0 & 0 & M_{15} \\ 0 & M_{22} & 0 & 0 & M_{25} \\ 0 & 0 & 0 & M_{44} & 0 \\ 0 & 0 & M_{33} & 0 & 0 \\ M_{51} & M_{52} & 0 & 0 & M_{55} \end{bmatrix} \tag{4.145}$$

$$\bar{\mathbf{B}} = \begin{bmatrix} B_1 \\ B_2 \\ B_4 \\ B_3 \\ B_5 \end{bmatrix} \tag{4.146}$$

$$\bar{\mathbf{\Gamma}}^{G^T} = \begin{bmatrix} -\zeta_1 \sin\theta_1 & \zeta_1 \cos\theta_1 \\ \cos\theta_1 & \sin\theta_1 \\ -\cos\theta_2 & -\sin\theta_2 \\ \zeta_2 \sin\theta_2 & -\zeta_2 \cos\theta_2 \\ -b\sin\theta_3 & b\cos\theta_3 \end{bmatrix} \tag{4.147}$$

This rearranged form suggests a partitioning process of $\bar{\mathbf{M}}$, $\bar{\mathbf{B}}$ and $\bar{\mathbf{\Gamma}}^{G^T}$ as follows:

$$\bar{\mathbf{M}} = \begin{bmatrix} \bar{\mathbf{M}}^a_{3\times 5} \\ \bar{\mathbf{M}}^u_{2\times 5} \end{bmatrix} \tag{4.148}$$

$$\bar{\mathbf{B}} = \begin{bmatrix} \bar{\mathbf{B}}^a_{3\times 1} \\ \bar{\mathbf{B}}^u_{2\times 1} \end{bmatrix} \tag{4.149}$$

$$\bar{\mathbf{\Gamma}}^{G^T} = \begin{bmatrix} \bar{\mathbf{\Gamma}}^{Ga^T}_{3\times 2} \\ \bar{\mathbf{\Gamma}}^{Gu^T}_{2\times 2} \end{bmatrix} \tag{4.150}$$

where

$$\bar{\mathbf{M}}^a = \begin{bmatrix} M_{11} & 0 & 0 & 0 & M_{15} \\ 0 & M_{22} & 0 & 0 & M_{25} \\ 0 & 0 & 0 & M_{44} & 0 \end{bmatrix} \tag{4.151}$$

$$\bar{\mathbf{M}}^u = \begin{bmatrix} 0 & 0 & M_{33} & 0 & 0 \\ M_{51} & M_{52} & 0 & 0 & M_{55} \end{bmatrix} \tag{4.152}$$

$$\bar{\mathbf{B}}^a = \begin{bmatrix} B_1 \\ B_2 \\ B_4 \end{bmatrix} \tag{4.153}$$

$$\bar{\mathbf{B}}^u = \begin{bmatrix} B_3 \\ B_5 \end{bmatrix} \tag{4.154}$$

$$\bar{\mathbf{\Gamma}}^{Ga^T} = \begin{bmatrix} -\zeta_1 \sin\theta_1 & \zeta_1 \cos\theta_1 \\ \cos\theta_1 & \sin\theta_1 \\ -\cos\theta_2 & -\sin\theta_2 \end{bmatrix} \tag{4.155}$$

$$\bar{\mathbf{\Gamma}}^{Gu^T} = \begin{bmatrix} \zeta_2 \sin\theta_2 & -\zeta_2 \cos\theta_2 \\ -b\sin\theta_3 & b\cos\theta_3 \end{bmatrix} \tag{4.156}$$

Thus, Equation (4.144) can be divided into the following two equations:

$$\mathbf{T} = \bar{\mathbf{M}}^a \ddot{\mathbf{q}} + \bar{\mathbf{B}}^a - \bar{\mathbf{\Gamma}}^{Ga^T} \boldsymbol{\lambda} \tag{4.157}$$

$$\bar{\mathbf{\Gamma}}^{Gu^T} \boldsymbol{\lambda} = \bar{\mathbf{M}}^u \ddot{\mathbf{q}} + \bar{\mathbf{B}}^u \tag{4.158}$$

As $\left|\bar{\mathbf{\Gamma}}^{Gu^T}\right| = -b\zeta_2 \sin\left(\theta_3 - \theta_2\right)$, the drive singularity condition $\left|\bar{\mathbf{\Gamma}}^{Gu^T}\right| = 0$ is equivalent to $\left|\mathbf{A}\right| = 0$. As long as $\left|\theta_3 - \theta_2 \pm n\pi\right| \geq \varepsilon \ \ (n = 0, 1, 2, \ldots)$, $\mathbf{A}$ and hence $\bar{\mathbf{\Gamma}}^{Gu^T}$ are not ill-conditioned and the $\bar{\mathbf{\Gamma}}^{Gu^T}$ matrix is invertible outside the neighborhood of drive singularities. Hence, $\boldsymbol{\lambda}$ can be found using Equation (4.158) as follows:

$$\boldsymbol{\lambda} = \left(\bar{\mathbf{\Gamma}}^{Gu^T}\right)^{-1}\left(\bar{\mathbf{M}}^{u}\ddot{\mathbf{q}} + \bar{\mathbf{B}}^{u}\right) \tag{4.159}$$

Then, $\mathbf{T}$ can be determined substituting Equation (4.159) into Equation (4.157):

$$\mathbf{T} = \bar{\mathbf{M}}'\ddot{\mathbf{q}} + \bar{\mathbf{B}}' \tag{4.160}$$

where 3×5 matrix $\bar{\mathbf{M}}'$ is

$$\bar{\mathbf{M}}' = \bar{\mathbf{M}}^{a} - \bar{\mathbf{\Gamma}}^{Ga^T}\left(\bar{\mathbf{\Gamma}}^{Gu^T}\right)^{-1}\bar{\mathbf{M}}^{u} \tag{4.161}$$

and 3-dimensional vector $\bar{\mathbf{B}}'$ is

$$\bar{\mathbf{B}}' = \bar{\mathbf{B}}^{a} - \bar{\mathbf{\Gamma}}^{Ga^T}\left(\bar{\mathbf{\Gamma}}^{Gu^T}\right)^{-1}\bar{\mathbf{B}}^{u} \tag{4.162}$$

Equation (4.12) can be rearranged as

$$\ddot{\mathbf{q}} = \mathbf{\Gamma}^{-1}\left(-\dot{\mathbf{\Gamma}}\dot{\mathbf{q}} + \dot{\mathbf{h}}\right) \tag{4.163}$$

Putting Equation (4.163) into Equation (4.160) yields

$$\mathbf{T} = \bar{\mathbf{M}}^{*}\dot{\mathbf{h}} + \bar{\mathbf{B}}^{*} \tag{4.164}$$

where 3×5 matrix $\bar{\mathbf{M}}^{*}$ is

$$\bar{\mathbf{M}}^{*} = \bar{\mathbf{M}}'\mathbf{\Gamma}^{-1} \tag{4.165}$$

and 3-dimensional vector $\bar{\mathbf{B}}^{*}$ is

$$\bar{\mathbf{B}}^{*} = \bar{\mathbf{B}}' - \bar{\mathbf{M}}'\mathbf{\Gamma}^{-1}\dot{\mathbf{\Gamma}}\dot{\mathbf{q}} \tag{4.166}$$

In Equation (4.164), all of the elements in the first two columns of the matrix $\bar{\mathbf{M}}^{*}$ are multiplied by the first two zero elements in the vector $\dot{\mathbf{h}}$. This fact leads to a partitioning of the matrix $\bar{\mathbf{M}}^{*}$ as follows:

$$\bar{\mathbf{M}}^{*} = \begin{bmatrix} \bar{\mathbf{M}}^{*G}_{3\times 2} & \bar{\mathbf{M}}^{*P}_{3\times 3} \end{bmatrix} \tag{4.167}$$

where

$$\bar{\mathbf{M}}^{*G} = \begin{bmatrix} \bar{M}^{*}_{11} & \bar{M}^{*}_{12} \\ \bar{M}^{*}_{21} & \bar{M}^{*}_{22} \\ \bar{M}^{*}_{31} & \bar{M}^{*}_{32} \end{bmatrix} \tag{4.168}$$

and

$$\bar{\mathbf{M}}^{*P} = \begin{bmatrix} \bar{M}^{*}_{13} & \bar{M}^{*}_{14} & \bar{M}^{*}_{15} \\ \bar{M}^{*}_{23} & \bar{M}^{*}_{24} & \bar{M}^{*}_{25} \\ \bar{M}^{*}_{33} & \bar{M}^{*}_{34} & \bar{M}^{*}_{35} \end{bmatrix} \tag{4.169}$$

Then, the relation between the input $\mathbf{T}$ and the output $\mathbf{x}$ can be obtained in the following form:

$$\mathbf{T} = \bar{\mathbf{M}}^{*P}\ddot{\mathbf{x}} + \bar{\mathbf{B}}^{*} \tag{4.170}$$

An inverse dynamics control law can then be formulated using Equation (4.170). Once $\mathbf{u}$ is generated by the command acceleration generator, the actuator forces $\mathbf{T}$ can be computed as

$$\mathbf{T} = \bar{\mathbf{M}}^{*P}\mathbf{u} + \bar{\mathbf{B}}^{*} \tag{4.171}$$

4.4 Inverse Dynamics Control inside the Neighborhood of Drive Singularities

The rank deficiency of $\bar{\mathbf{\Gamma}}^{GuT}$ results in drive singularities. When the modified equation replaces the linearly dependent dynamic equation in Equation (4.158) and the terms involving $\ddot{q}_j$'s and $\ddot{q}_j$'s are factored, the resulting system of equations can be written in matrix notation as follows:

$$\hat{\boldsymbol{\Gamma}}^{Gu^T}\boldsymbol{\lambda} = \hat{\mathbf{N}}^u\ddot{\mathbf{q}} + \hat{\mathbf{M}}^u\ddot{\mathbf{q}} + \hat{\mathbf{B}}^u \tag{4.172}$$

$\hat{\mathbf{N}}^u = \hat{\mathbf{N}}^u(\mathbf{q})$, $\hat{\mathbf{M}}^u = \hat{\mathbf{M}}^u(\mathbf{q},\dot{\mathbf{q}})$, $\hat{\mathbf{B}}^u = \hat{\mathbf{B}}^u(\mathbf{q},\dot{\mathbf{q}})$ and $\hat{\boldsymbol{\Gamma}}^{Gu^T} = \hat{\boldsymbol{\Gamma}}^{Gu^T}(\mathbf{q},\dot{\mathbf{q}})$ will have the following expressions:

$$\hat{\mathbf{N}}^u = \begin{bmatrix} \sigma\frac{\zeta_2}{b}M_{51} & \sigma\frac{\zeta_2}{b}M_{52} & M_{33} & 0 & \sigma\frac{\zeta_2}{b}M_{55} \\ 0 & 0 & 0 & 0 & 0 \end{bmatrix} \tag{4.173}$$

$$\hat{\mathbf{M}}^u = \begin{bmatrix} \hat{M}_{31} & \hat{M}_{32} & \hat{M}_{33} & \hat{M}_{34} & \hat{M}_{35} \\ M_{51} & M_{52} & 0 & 0 & M_{55} \end{bmatrix} \tag{4.174}$$

$$\hat{\mathbf{B}}^u = \begin{bmatrix} \hat{B}_3 \\ B_5 \end{bmatrix} \tag{4.175}$$

$$\hat{\boldsymbol{\Gamma}}^{Gu^T} = \begin{bmatrix} H_1 & H_2 \\ -b\sin\theta_3 & b\cos\theta_3 \end{bmatrix} \tag{4.176}$$

where

$$\begin{aligned} \hat{M}_{31} &= \sigma\frac{\zeta_2}{b}\dot{M}_{51} + \sigma\frac{\dot{\zeta}_2}{b}M_{51} \\ &\quad + \sigma\frac{\zeta_2}{b}m_5 g_5\left[-2\zeta_1\dot{\theta}_1\sin(\theta_1-\theta_3-\beta) + 2\dot{\zeta}_1\cos(\theta_1-\theta_3-\beta)\right] \end{aligned} \tag{4.177}$$

$$\hat{M}_{32} = \sigma\frac{\zeta_2}{b}\dot{M}_{52} + \sigma\frac{\dot{\zeta}_2}{b}M_{52} + 2\sigma\frac{\zeta_2}{b}m_5 g_5\dot{\theta}_1\cos(\theta_1-\theta_3-\beta) \tag{4.178}$$

$$\hat{M}_{33} = \dot{M}_{33} + 2m_4(\zeta_2 - g_4)\dot{\zeta}_2 \tag{4.179}$$

$$\hat{M}_{34} = 2m_4(\zeta_2 - g_4)\dot{\theta}_2 \tag{4.180}$$

$$\hat{M}_{35} = \sigma\frac{\zeta_2}{b}\dot{M}_{55} + \sigma\frac{\dot{\zeta}_2}{b}M_{55} \tag{4.181}$$

$$\begin{aligned}\hat{B}_3 &= 2m_4\dot{\theta}_2\dot{\zeta}_2^2 + m_4 g\dot{\zeta}_2\cos\theta_2 - \left[m_3 g_3 + m_4\left(\zeta_2 - g_4\right)\right] g\dot{\theta}_2\sin\theta_2 \\ &+\sigma\frac{\zeta_2}{b}\left\{m_5 g_5\left[-\dot{\zeta}_1\dot{\theta}_1^2\sin\left(\theta_1-\theta_3-\beta\right) - \zeta_1\dot{\theta}_1^2\left(\dot{\theta}_1-\dot{\theta}_3\right)\cos\left(\theta_1-\theta_3-\beta\right)\right.\right. \\ &\left.\left.-2\dot{\zeta}_1\dot{\theta}_1\left(\dot{\theta}_1-\dot{\theta}_3\right)\sin\left(\theta_1-\theta_3-\beta\right) - g\dot{\theta}_3\sin\left(\theta_3+\beta\right)\right]\right\} \\ &+\sigma\frac{\dot{\zeta}_2}{b}B_5\end{aligned} \tag{4.182}$$

Note that Equations (4.157) and (4.172) form together Equation (4.141).

$\boldsymbol{\lambda}$ can be found using Equation (4.172) as follows:

$$\boldsymbol{\lambda} = \left(\hat{\boldsymbol{\Gamma}}^{Gu^T}\right)^{-1}\left(\hat{\mathbf{N}}^u\ddot{\mathbf{q}} + \hat{\mathbf{M}}^u\ddot{\mathbf{q}} + \hat{\mathbf{B}}^u\right) \tag{4.183}$$

Then, $\mathbf{T}$ can be determined substituting Equation (4.183) into Equation (4.157):

$$\mathbf{T} = \hat{\mathbf{N}}'\ddot{\mathbf{q}} + \hat{\mathbf{M}}'\ddot{\mathbf{q}} + \hat{\mathbf{B}}' \tag{4.184}$$

where 3×5 matrices $\hat{\mathbf{N}}'$ and $\hat{\mathbf{M}}'$ are

$$\hat{\mathbf{N}}' = -\bar{\boldsymbol{\Gamma}}^{Ga^T}\left(\hat{\boldsymbol{\Gamma}}^{Gu^T}\right)^{-1}\hat{\mathbf{N}}^u \tag{4.185}$$

$$\hat{\mathbf{M}}' = \bar{\mathbf{M}}^a - \bar{\boldsymbol{\Gamma}}^{Ga^T}\left(\hat{\boldsymbol{\Gamma}}^{Gu^T}\right)^{-1}\hat{\mathbf{M}}^u \tag{4.186}$$

and 3-dimensional vector $\hat{\mathbf{B}}'$ is

$$\hat{\mathbf{B}}' = \bar{\mathbf{B}}^a - \bar{\boldsymbol{\Gamma}}^{Ga^T}\left(\hat{\boldsymbol{\Gamma}}^{Gu^T}\right)^{-1}\hat{\mathbf{B}}^u \tag{4.187}$$

The terms in Equation (4.123) involving $\ddot{q}_j$'s can be factored to yield

$$\boldsymbol{\Gamma}\ddot{\mathbf{q}} = \mathbf{P}\ddot{\mathbf{q}} + \mathbf{R} + \ddot{\mathbf{h}} \tag{4.188}$$

where 5×5 matrix $\mathbf{P} = \mathbf{P}\left(\mathbf{q},\dot{\mathbf{q}}\right)$ and 5-dimensional vector $\mathbf{R} = \mathbf{R}\left(\mathbf{q},\dot{\mathbf{q}}\right)$ are

$$\mathbf{P} = \begin{bmatrix} P_{11} & P_{12} & P_{13} & P_{14} & P_{15} \\ P_{21} & P_{22} & P_{23} & P_{24} & P_{25} \\ P_{31} & P_{32} & 0 & 0 & P_{35} \\ P_{41} & P_{42} & 0 & 0 & P_{45} \\ 0 & 0 & 0 & 0 & 0 \end{bmatrix} \tag{4.189}$$

and

$$\mathbf{R} = \begin{bmatrix} R_1 \\ R_2 \\ R_3 \\ R_4 \\ 0 \end{bmatrix} \tag{4.190}$$

with

$$P_{11} = 3\left(\dot{\zeta}_1 \sin\theta_1 + \zeta_1\dot{\theta}_1 \cos\theta_1\right) \tag{4.191}$$

$$P_{12} = 3\dot{\theta}_1 \sin\theta_1 \tag{4.192}$$

$$P_{13} = -3\left(\dot{\zeta}_2 \sin\theta_2 + \zeta_2\dot{\theta}_2 \cos\theta_2\right) \tag{4.193}$$

$$P_{14} = -3\dot{\theta}_2 \sin\theta_2 \tag{4.194}$$

$$P_{15} = 3b\dot{\theta}_3 \cos\theta_3 \tag{4.195}$$

$$P_{21} = 3\left(\zeta_1\dot{\theta}_1 \sin\theta_1 - \dot{\zeta}_1 \cos\theta_1\right) \tag{4.196}$$

$$P_{22} = -3\dot{\theta}_1 \cos\theta_1 \tag{4.197}$$

$$P_{23} = 3\left(\dot{\zeta}_2 \cos\theta_2 - \zeta_2\dot{\theta}_2 \sin\theta_2\right) \tag{4.198}$$

$$P_{24} = 3\dot{\theta}_2 \cos\theta_2 \tag{4.199}$$

$$P_{25} = 3b\dot{\theta}_3 \sin\theta_3 \tag{4.200}$$

$$P_{31} = 3\left(\dot{\zeta}_1 \sin\theta_1 + \zeta_1\dot{\theta}_1 \cos\theta_1\right) \tag{4.201}$$

$$P_{32} = 3\dot{\theta}_1 \sin\theta_1 \tag{4.202}$$

$$P_{35} = 3c\dot{\theta}_3 \cos\left(\theta_3 + \alpha\right) \tag{4.203}$$

$$P_{41} = 3\left(\zeta_1\dot{\theta}_1 \sin\theta_1 - \dot{\zeta}_1 \cos\theta_1\right) \tag{4.204}$$

$$P_{42} = -3\dot{\theta}_1 \cos\theta_1 \tag{4.205}$$

$$P_{45} = 3c\dot{\theta}_3 \sin\left(\theta_3 + \alpha\right) \tag{4.206}$$

$$R_1 = 3\dot{\theta}_1^2\dot{\zeta}_1 \cos\theta_1 - \zeta_1\dot{\theta}_1^3 \sin\theta_1 - 3\dot{\zeta}_2\dot{\theta}_2^2 \cos\theta_2 + \zeta_2\dot{\theta}_2^3 \sin\theta_2 - b\dot{\theta}_3^3 \sin\theta_3 \tag{4.207}$$

$$R_2 = 3\dot{\theta}_1^2\dot{\zeta}_1 \sin\theta_1 + \zeta_1\dot{\theta}_1^3 \cos\theta_1 - 3\dot{\theta}_2^2\dot{\zeta}_2 \sin\theta_2 - \zeta_2\dot{\theta}_2^3 \cos\theta_2 + b\dot{\theta}_3^3 \cos\theta_3 \tag{4.208}$$

$$R_3 = 3\dot{\theta}_1^2\dot{\zeta}_1 \cos\theta_1 - \zeta_1\dot{\theta}_1^3 \sin\theta_1 - c\dot{\theta}_3^3 \sin(\theta_3 + \alpha) \tag{4.209}$$

$$R_4 = 3\dot{\theta}_1^2\dot{\zeta}_1 \sin\theta_1 + \zeta_1\dot{\theta}_1^3 \cos\theta_1 + c\dot{\theta}_3^3 \cos(\theta_3 + \alpha) \tag{4.210}$$

Solving Equation (4.188) for $\ddot{\mathbf{q}}$ gives

$$\ddot{\mathbf{q}} = \boldsymbol{\Gamma}^{-1}\left(\mathbf{P}\ddot{\mathbf{q}} + \mathbf{R} + \ddot{\mathbf{h}}\right) \tag{4.211}$$

On substituting Equation (4.163), Equation (4.211) becomes

$$\ddot{\mathbf{q}} = \boldsymbol{\Gamma}^{-1}\left[\mathbf{P}\boldsymbol{\Gamma}^{-1}\left(-\dot{\boldsymbol{\Gamma}}\dot{\mathbf{q}} + \dot{\mathbf{h}}\right) + \mathbf{R} + \ddot{\mathbf{h}}\right] \tag{4.212}$$

Putting Equations (4.163) and (4.212) into Equation (4.184) gives

$$\mathbf{T} = \hat{\mathbf{N}}^*\ddot{\mathbf{h}} + \hat{\mathbf{M}}^*\dot{\mathbf{h}} + \hat{\mathbf{B}}^* \tag{4.213}$$

where 3×5 matrices $\hat{\mathbf{N}}^*$ and $\hat{\mathbf{M}}^*$ are

$$\hat{\mathbf{N}}^* = \hat{\mathbf{N}}'\boldsymbol{\Gamma}^{-1} \tag{4.214}$$

$$\hat{\mathbf{M}}^* = \left(\hat{\mathbf{N}}'\boldsymbol{\Gamma}^{-1}\mathbf{P} + \hat{\mathbf{M}}'\right)\boldsymbol{\Gamma}^{-1} \tag{4.215}$$

and 3-dimensional vector $\hat{\mathbf{B}}^*$ is

$$\hat{\mathbf{B}}^* = \hat{\mathbf{B}}' + \hat{\mathbf{N}}'\boldsymbol{\Gamma}^{-1}\left(\mathbf{R} - \mathbf{P}\boldsymbol{\Gamma}^{-1}\dot{\boldsymbol{\Gamma}}\dot{\mathbf{q}}\right) - \hat{\mathbf{M}}'\boldsymbol{\Gamma}^{-1}\dot{\boldsymbol{\Gamma}}\dot{\mathbf{q}} \tag{4.216}$$

In Equation (4.213), all of the elements in the first two columns of the matrices $\hat{\mathbf{N}}^*$ and $\hat{\mathbf{M}}^*$ are multiplied by the first two zero elements in the vectors $\ddot{\mathbf{h}}$ and $\dot{\mathbf{h}}$, respectively. This fact leads to a partitioning of the matrices $\hat{\mathbf{N}}^*$ and $\hat{\mathbf{M}}^*$ as follows:

$$\hat{\mathbf{N}}^* = \begin{bmatrix} \hat{\mathbf{N}}^{*G}_{3\times 2} & \hat{\mathbf{N}}^{*P}_{3\times 3} \end{bmatrix} \tag{4.217}$$

$$\hat{\mathbf{M}}^* = \begin{bmatrix} \hat{\mathbf{M}}^{*G}_{3\times 2} & \hat{\mathbf{M}}^{*P}_{3\times 3} \end{bmatrix} \tag{4.218}$$

where

$$\hat{\mathbf{N}}^{*G} = \begin{bmatrix} \hat{N}^*_{11} & \hat{N}^*_{12} \\ \hat{N}^*_{21} & \hat{N}^*_{22} \\ \hat{N}^*_{31} & \hat{N}^*_{32} \end{bmatrix} \tag{4.219}$$

$$\hat{\mathbf{N}}^{*P} = \begin{bmatrix} \hat{N}^*_{13} & \hat{N}^*_{14} & \hat{N}^*_{15} \\ \hat{N}^*_{23} & \hat{N}^*_{24} & \hat{N}^*_{25} \\ \hat{N}^*_{33} & \hat{N}^*_{34} & \hat{N}^*_{35} \end{bmatrix} \tag{4.220}$$

$$\hat{\mathbf{M}}^{*G} = \begin{bmatrix} \hat{M}^*_{11} & \hat{M}^*_{12} \\ \hat{M}^*_{21} & \hat{M}^*_{22} \\ \hat{M}^*_{31} & \hat{M}^*_{32} \end{bmatrix} \tag{4.221}$$

$$\hat{\mathbf{M}}^{*P} = \begin{bmatrix} \hat{M}^*_{13} & \hat{M}^*_{14} & \hat{M}^*_{15} \\ \hat{M}^*_{23} & \hat{M}^*_{24} & \hat{M}^*_{25} \\ \hat{M}^*_{33} & \hat{M}^*_{34} & \hat{M}^*_{35} \end{bmatrix} \tag{4.222}$$

Then, the relation between the input $\mathbf{T}$ and the output $\mathbf{x}$ can be obtained in the following form:

$$\mathbf{T} = \hat{\mathbf{N}}^{*P}\ddot{\mathbf{x}} + \hat{\mathbf{M}}^{*P}\ddot{\mathbf{x}} + \hat{\mathbf{B}}^* \tag{4.223}$$

An inverse dynamics control law can then be formulated using Equation (4.223). The rank of $\hat{\mathbf{N}}^{*P}$ is 1. So, in the control law, both command accelerations $\mathbf{u}$ and command jerks $\dot{\mathbf{u}}$ have to be specified. Using $\mathbf{u}$ generated by the command acceleration generator as done outside the neighborhood of drive singularities and the time derivative of it, i.e., command jerks $\dot{\mathbf{u}}$, the actuator forces $\mathbf{T}$ can be computed using Equation (4.223):

$$\mathbf{T} = \hat{\mathbf{N}}^{*P}\dot{\mathbf{u}} + \hat{\mathbf{M}}^{*P}\mathbf{u} + \hat{\mathbf{B}}^* \tag{4.224}$$

4.5 SIMULINK® Model

The SIMULINK® model developed to perform the simulation of the proposed control system is shown in Figure 3. The clock generates the

simulation time and at each simulation step the Embedded MATLAB® Function called Desired Motion outputs the prescribed pose, velocity and acceleration of the end-effector. The desired and actual end-effector states are passed to the Embedded MATLAB® Function called Errors in the End-Effector States to yield the errors in the end-effector states. Taking the desired accelerations and the errors in the end-effector states as inputs, the Embedded MATLAB® Function called Command Accelerations generates the command accelerations according to a chosen control strategy.

The Embedded MATLAB® Functions called Control Torque and Forces outside the Neighborhood of the Drive Singularity and Control Torque and Forces inside the Neighborhood of the Drive Singularity use Equations (4.171) and (4.224), respectively to evaluate the required motor torque T_1 and the actuator forces F_1 and F_2. The switch allows the 1st input to pass through when the 2nd input is greater than or equal to the specified threshold, namely ε. If not the 3rd input is allowed to pass through. Note that the inputs are numbered from top to bottom, i.e., the 1st and 3rd inputs are the outputs of the Embedded MATLAB® Functions called Control Torque and Forces outside the Neighborhood of the Drive Singularity and Control Torque and Forces inside the Neighborhood of the Drive Singularity, respectively whereas the 2nd input is the output of the Embedded MATLAB® Function called Switching Criterion which evaluates $g(\mathbf{q})$.

Application of the control torque and forces to the parallel manipulator is executed in the subsystem called 2-RPR Planar Parallel Manipulator which is shown in Figure 4. The Embedded MATLAB® Function called Direct Dynamics solves Equation (4.101) and the loop closure constraint equations at acceleration level for actual joint accelerations and Lagrange multipliers but outputs only the actual joint accelerations to be integrated twice for obtaining the actual joint velocities and displacements.

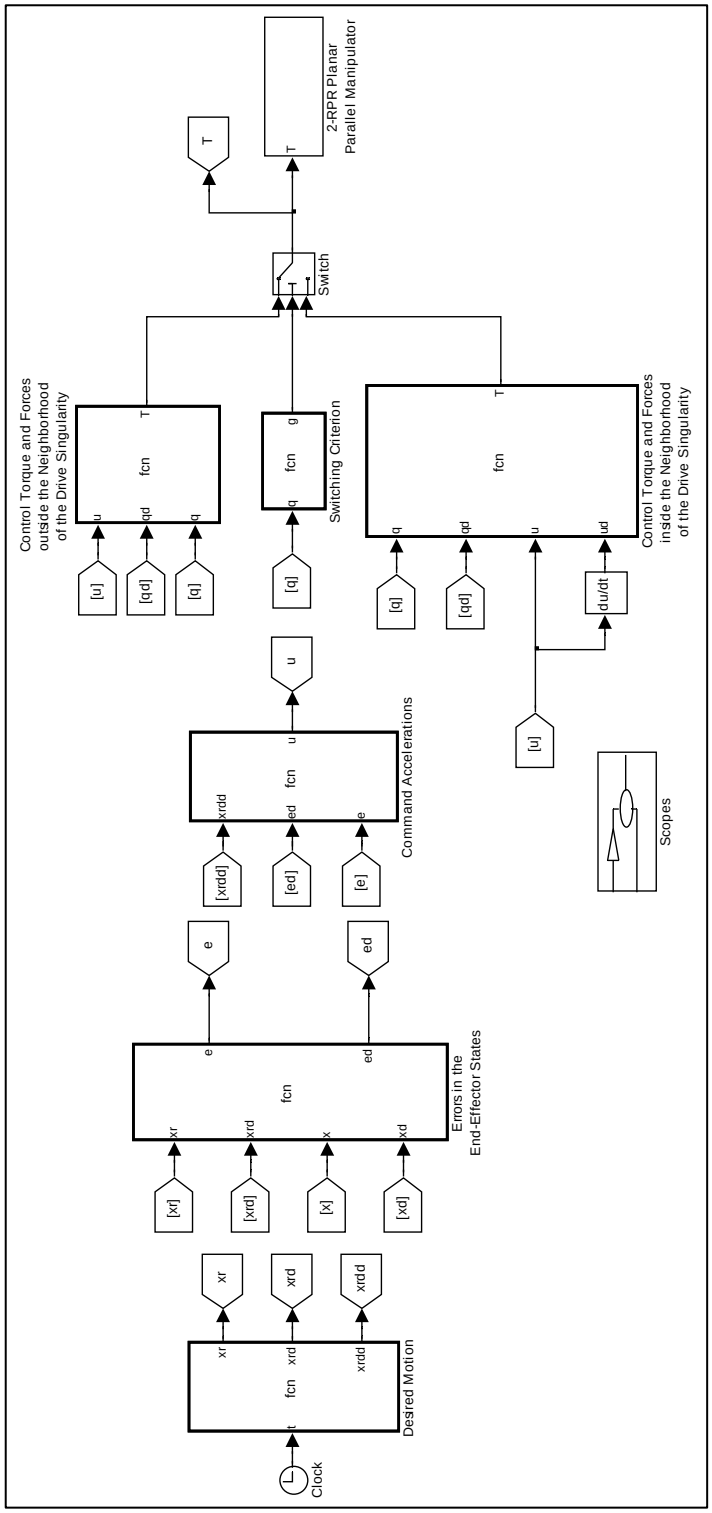

Figure 3 SIMULINK® model

Once the actual joint velocities and displacements are found, the actual end-effector states are determined using task equations at position and velocity levels by the Embedded MATLAB® Function called Direct Kinematics to be fed back for calculating the errors in the end-effector states at the next time step.

Scopes are used to display the computed motor torque and actuator forces and the errors in the end-effector states. For brevity, those scopes are banded together in the subsystem called Scopes which is shown in Figure 5.

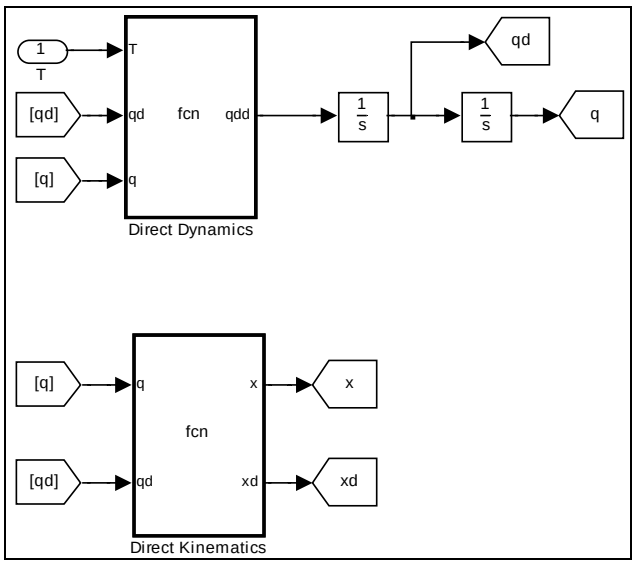

Figure 4 The subsystem called 2-RPR Planar Parallel Manipulator

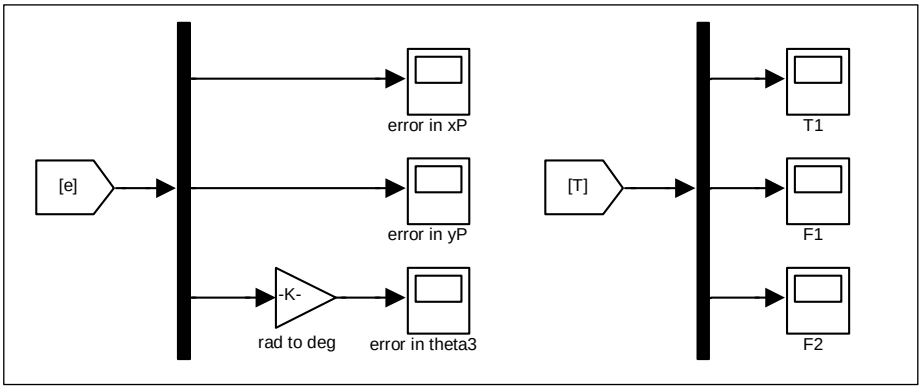

Figure 5 The subsystem called Scopes

4.6 Numerical Example

The data used are as follows: The link lengths are $a = 1$ m, $b = 0.4$ m, $c = 0.2$ m, $\alpha = 0$. The masses and the centroidal moments of inertia are $m_1 = 2$ kg, $m_2 = 1.5$ kg, $m_3 = 2$ kg, $m_4 = 1.5$ kg, $m_5 = 1$ kg, $I_1 = 0.05$ kg.m^2, $I_2 = 0.03$ kg.m^2, $I_3 = 0.05$ kg.m^2, $I_4 = 0.03$ kg.m^2 and $I_5 = 0.02$ kg.m^2. The mass center locations are $g_1 = 0.15$ m, $g_2 = 0.15$ m, $g_3 = 0.15$ m, $g_4 = 0.15$ m, $g_5 = 0.15$ m and $\beta = 0$.

Consider a deployment motion where the platform is desired to move with a constant orientation given as $\theta_3 = 320^\circ$ and with point P having a trajectory $s(t)$ along a straight line whose angle with x-axis is given as

$\gamma = 200^\circ$, starting from the initial position $x_{P_0} = 0.800$ m, $y_{P_0} = 0.916$ m (Figure 6). Here, to recall later, one can easily conclude that

$$s(0) = 0 \tag{4.225}$$

The distance between the initial and final positions is determined to be $L = 1.5$ m and this distance is desired to be taken in $T = 1$ s, i.e.,

$$s(T) = L \tag{4.226}$$

Hence the desired Cartesian motion of the platform can be written as

$$\mathbf{x} = \begin{bmatrix} x_{P_0} + s(t)\cos\gamma \\ y_{P_0} + s(t)\sin\gamma \\ 320^\circ \end{bmatrix} \tag{4.227}$$

In addition, it is desired that the system has zero initial and final velocities, i.e.,

$$\dot{s}(0) = 0 \tag{4.228}$$

$$\dot{s}(T) = 0 \tag{4.229}$$

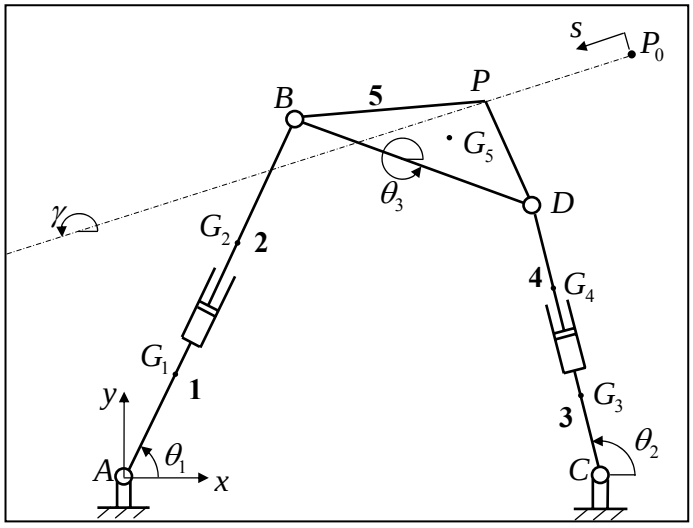

Figure 6 Desired motion of the parallel manipulator

When point P comes to $s = L_d = 0.6618$ m, a drive singularity is encountered since θ_2 becomes equal to $\theta_3 - \pi$ and the other joint variables at that instance can be found as $\theta_1 = 1.5404$ rad, $\zeta_1 = 0.8186$ m and $\zeta_2 = 0.8729$ m. This singular configuration is shown in Figure 7. By the way, it is convenient to note down the following equation to revisit later:

$$s(T_d) = L_d \tag{4.230}$$

where T_d denotes the time when the singularity happens. The consistency condition is given by (4.107) with $\sigma = -1$. The desired trajectory should be planned via an appropriate choice of $s(t)$ to satisfy the consistency condition.

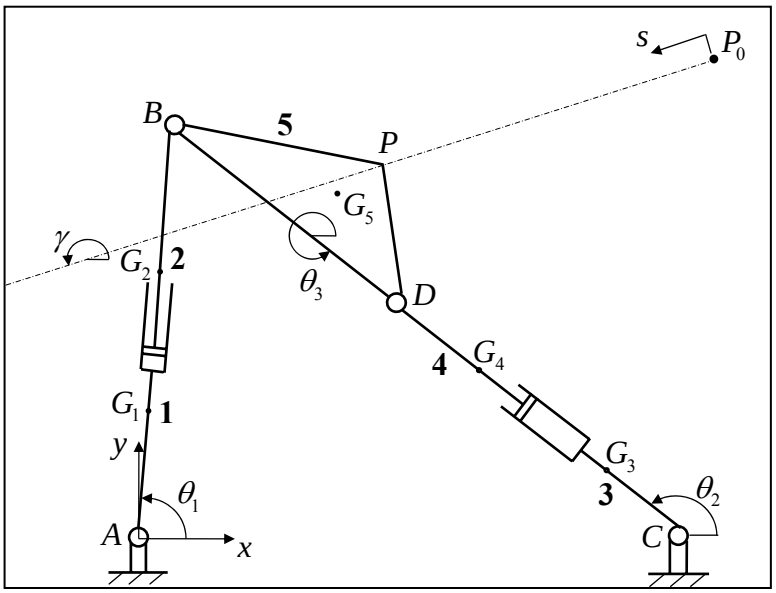

Figure 7 Singular configuration of the parallel manipulator

An arbitrary inconsistent trajectory cannot be realized by the actuators of the manipulator. This fact is illustrated by considering an arbitrary third order polynomial for $s(t)$ having zero initial and final velocities, i.e., $s(t) = \frac{3L}{T^2}t^2 - \frac{2L}{T^3}t^3$ (Figure 8).

In such a case, the conventional inverse dynamics control law is applicable only. A PD controller is decided to be used. Therefore, the command accelerations are generated as in Equation (3.17). The constant feedback gain diagonal matrices are chosen to be in binomial form, i.e., $\mathbf{C}_1 = 2\omega_0\mathbf{I}_3$ and $\mathbf{C}_2 = \omega_0^2\mathbf{I}_3$ where ω_0 is a positive constant and selected as $\omega_0 = 30$ rad/s.

Besides, it is assumed that initially the parallel manipulator is at rest with $\theta_1 = 1.0439$ rad, $\zeta_1 = 1.1960$ m, $\theta_2 = 1.7023$ rad, $\zeta_2 = 0.7729$ m and $\theta_3 = 5.5501$ rad. The corresponding end-effector pose is $x_{P_0} = 0.795$ m, $y_{P_0} = 0.900$ m and $\theta_{3_0} = 318^\circ$. Hence the parallel manipulator is assumed to be initially mispositioned.

The closed loop system is simulated using the fourth-order Runge-Kutta solver with a fixed step size of 0.001 s and assuming no modeling error. The motor torque and actuator forces are shown in Figures 9 and 10. (In the figures the torque and forces are out of range around the singular position.) The singular position is reached when $t = 0.461$ s. The motor torque and actuator forces grow without bounds as the singularity is approached and take infinitely large values at the singular position.

However, in a real application the output powers of the actuators are limited. Hence, the maximum torque and forces exerted by the actuators are limited and, as a result, the actuators unavoidably saturate as the singularity is approached. To take actuator bounds into account, the closed loop system is

simulated again by setting the actuator limits as $\pm 250\ \mathrm{N \cdot m}$ for the motor torque T_1 and $\pm 300\ \mathrm{N}$ for the actuator forces F_1 and F_2. For this case the errors in the end-effector states, the motor torque and actuator forces are shown in Figures 11 through 14. It can be seen that tracking would be very poor and unacceptable and the manipulator could not perform the desired task in an application where an arbitrary inconsistent trajectory is chosen for the prescribed motion which passes through the drive singular position.

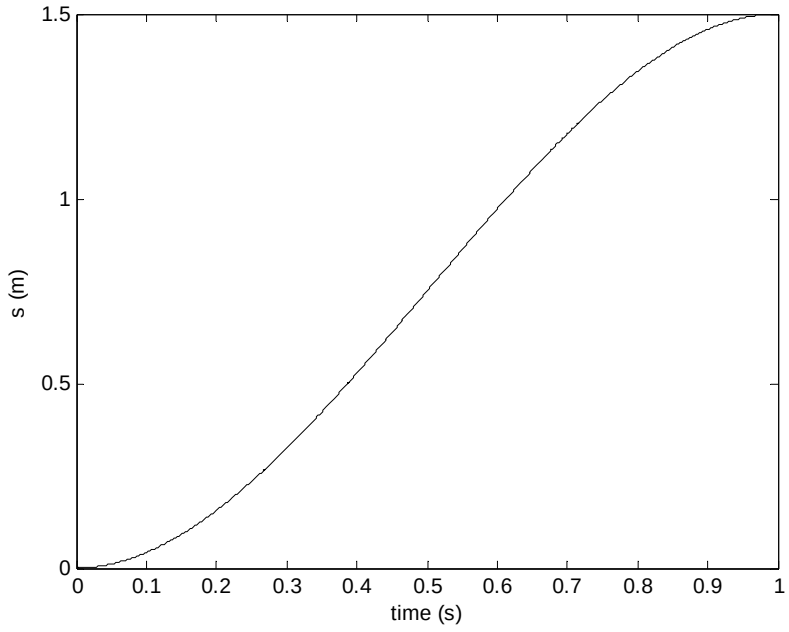

Figure 8 A time function that does not satisfy the consistency condition

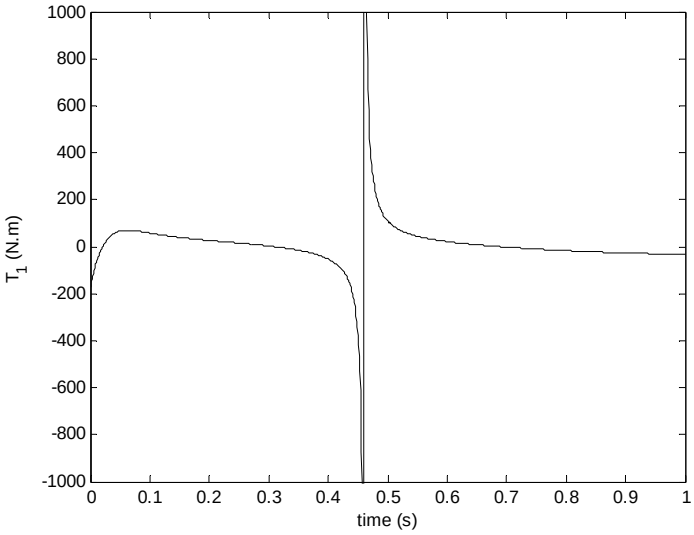

Figure 9 Motor torque T_1 for the inconsistent trajectory

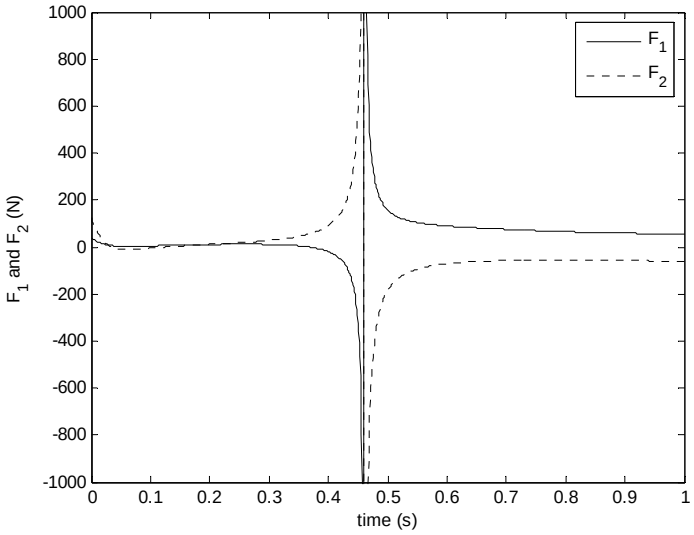

Figure 10 Actuator forces F_1 and F_2 for the inconsistent trajectory

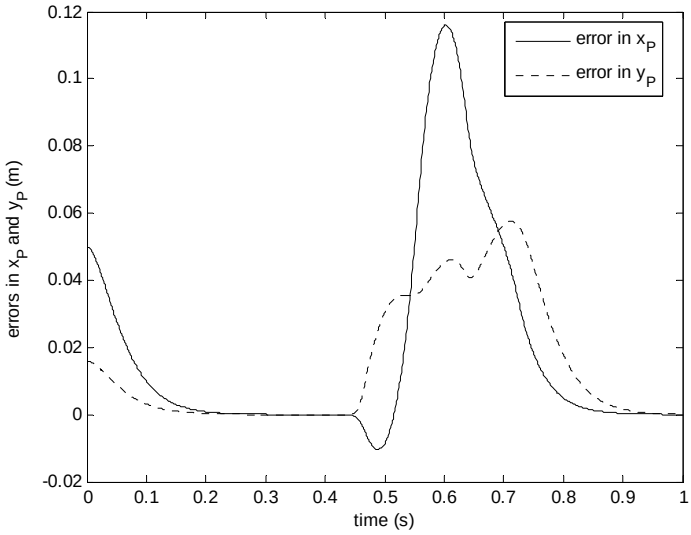

Figure 11 Errors in x_P and y_P for the inconsistent trajectory considering actuator limits

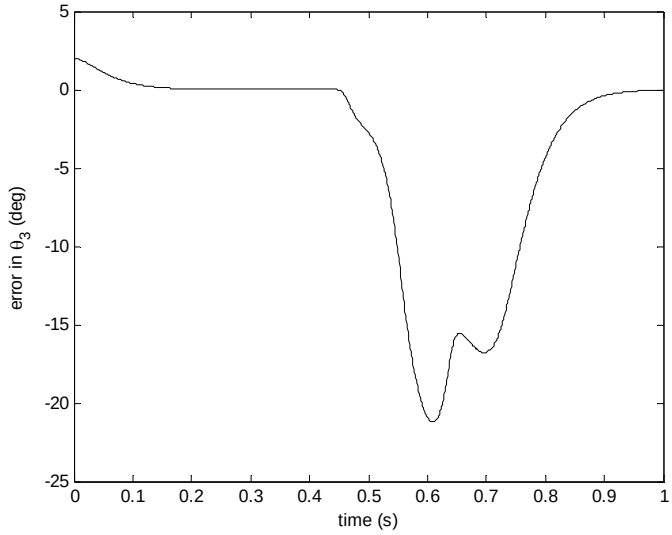

Figure 12 Error in θ_3 for the inconsistent trajectory considering actuator limits

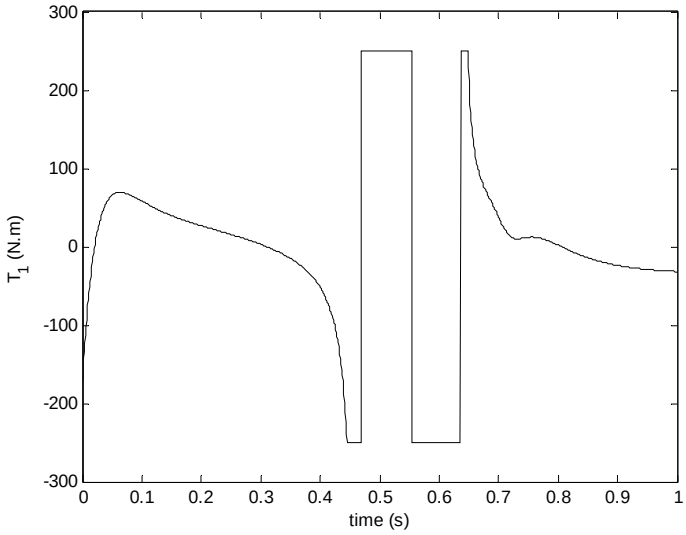

Figure 13 Motor torque T_1 for the inconsistent trajectory considering actuator limits

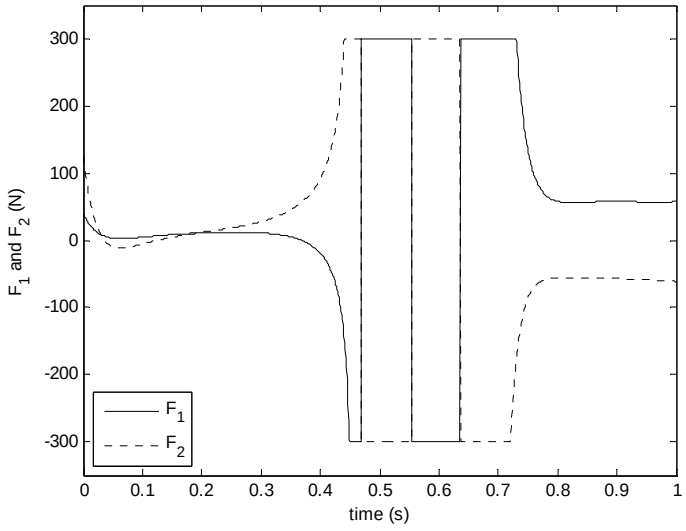

Figure 14 Actuator forces F_1 and F_2 for the inconsistent trajectory considering actuator limits

As it is obvious from the above results, for the time function $s(t)$ a polynomial is required to be chosen which satisfies the consistency condition at the drive singularity in addition to having zero initial and final velocities. For this purpose, one can specify the time T_d and the velocity of the end point at the singular configuration, $v_P(T_d)$. Let T_d and $v_P(T_d)$ be chosen as 0.62 s and 1.7 m/s, respectively. Incidentally, one can establish that

$$\dot{s}(T_d) = v_P(T_d) \tag{4.231}$$

Using Equation (4.231), $\dot{\mathbf{x}}$ and $\ddot{\mathbf{x}}$ at T_d can be written as

$$\dot{\mathbf{x}}(T_d) = \begin{bmatrix} v_P(T_d)\cos\gamma \\ v_P(T_d)\sin\gamma \\ 0 \end{bmatrix} \tag{4.232}$$

$$\ddot{\mathbf{x}}(T_d) = \begin{bmatrix} a_P(T_d)\cos\gamma \\ a_P(T_d)\sin\gamma \\ 0 \end{bmatrix} \tag{4.233}$$

where

$$\ddot{s}(T_d) = a_P(T_d) \tag{4.234}$$

Substituting the numerical values of $\mathbf{q}(T_d)$ found above into Equation (4.10) where $\dot{\mathbf{x}}(T_d)$ is given by (4.232) yields $\dot{\mathbf{q}}$ at T_d as follows: $\dot{\theta}_1 = 1.9290$ rad/s, $\dot{\zeta}_1 = -0.6298$ m/s, $\dot{\theta}_2 = 1.6866$ rad/s, $\dot{\zeta}_2 = 0.8500$ m/s and $\dot{\theta}_3 = 0$ rad/s. Having the numerical values of $\mathbf{q}(T_d)$ and $\dot{\mathbf{q}}(T_d)$ now, Equation (4.12) where $\ddot{\mathbf{x}}(T_d)$ is given by (4.233) and the consistency condition constitute together the six equations required to solve for the six unknowns $\ddot{\mathbf{q}}$ at T_d and $a_P(T_d)$ as follows: $\ddot{\theta}_1 = 14.9871$ rad/s^2, $\ddot{\zeta}_1 = -0.8778$ m/s^2, $\ddot{\theta}_2 = 7.2240$ rad/s^2, $\ddot{\zeta}_2 = 7.7792$ m/s^2, $\ddot{\theta}_3 = 0$ rad/s^2 and $a_P(T_d) = 10.5922$ m/s^2. Consequently, the sixth order polynomial satisfying all of the Equations (4.225), (4.226), (4.228),

(4.229), (4.230), (4.231) and (4.234) together is shown in Figure 15 and given below:

$$s(t) = 20.7303t^2 - 87.8009t^3 + 146.5637t^4 - 103.6459t^5 + 25.6528t^6 \qquad (4.235)$$

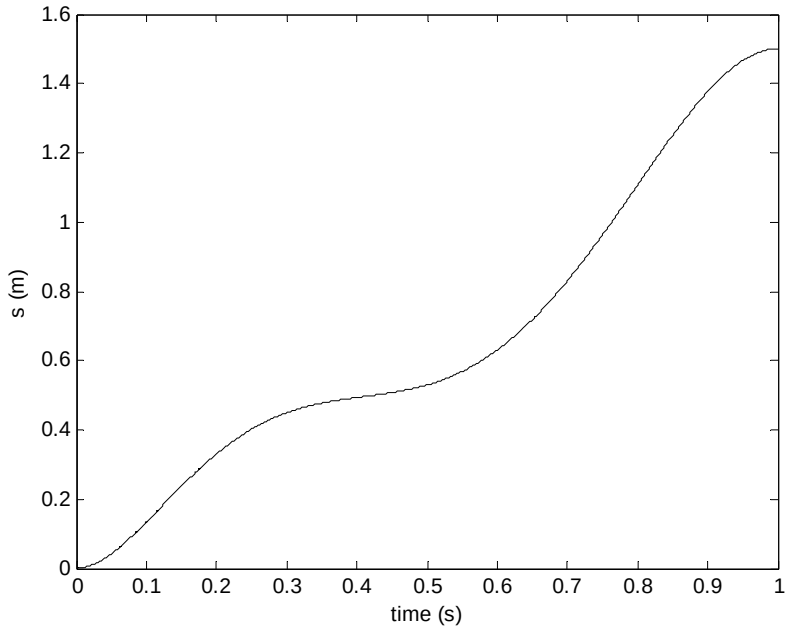

Figure 15 A time function that satisfies the consistency condition

Once the trajectory is chosen to be consistent, to test the proposed switching inverse dynamics controller, the model is run twelve times under different scenarios. These scenarios are presented in Table 1. The solver type and the step size used in these twelve simulations are the same with the ones used in the previous two simulations carried out for the inconsistent trajectory.

In addition, it is assumed in these simulations that the manipulator is at the same initial configuration so that the initial position error is the same with those previous two simulations.

In the first four scenarios, the closed loop control system is simulated using a PD controller in the absence of modeling error. The constant feedback gain diagonal matrices are chosen to be in binomial form as in the previous two simulations carried out for the inconsistent trajectory, and so that a critically damped response is achieved.

In the second four scenarios, the closed loop control system is simulated using 5 % smaller values for the mass and inertia values in the model to see the effects of modeling error. But the controller type in use is still PD.

Table 1 The scenarios simulated

Scenarios	Modeling Error	Controller Type	ω_0 (rad/s)	ε (deg)
1	No	PD	30	0.5
2	No	PD	50	0.5
3	No	PD	30	1
4	No	PD	50	1
5	Yes	PD	30	0.5
6	Yes	PD	50	0.5
7	Yes	PD	30	1
8	Yes	PD	50	1
9	Yes	PID	30	0.5
10	Yes	PID	50	0.5
11	Yes	PID	30	1
12	Yes	PID	50	1

In the last four scenarios, an integral control action is added to the closed loop control system to see the effects of the PID controller on the closed loop response considering the same modeling error as in the second four scenarios. When a PID controller is used, command accelerations are generated as

$$\mathbf{u} = \ddot{\mathbf{x}}^d + \mathbf{C}_1\left(\dot{\mathbf{x}}^d - \dot{\mathbf{x}}\right) + \mathbf{C}_2\left(\mathbf{x}^d - \mathbf{x}\right) + \mathbf{C}_3\int\left(\mathbf{x}^d - \mathbf{x}\right)dt \tag{4.236}$$

where the constant feedback gain diagonal matrices are again chosen to be in binomial form, i.e., $\mathbf{C}_1 = 3\omega_0\mathbf{I}_3$, $\mathbf{C}_2 = 3\omega_0^2\mathbf{I}_3$ and $\mathbf{C}_3 = \omega_0^3\mathbf{I}_3$.

Furthermore, in each quartet ω_0 and ε are altered to understand the effects of the selected positive constant ω_0 and the specified size of the neighborhood of the drive singularity on the closed loop response, respectively.

For each scenario four different graphs are plotted to present the simulation results: errors in x_P and y_P, error in θ_3, motor torque T_1 and actuator forces F_1 and F_2 (Figures 16-63). The key points in the results, namely, steady-state errors before the neighborhood of the singularity, maximum errors in the neighborhood of the singularity, maximum errors after the neighborhood of the singularity, steady-state errors after the neighborhood of the singularity, maximum control torque and forces, jumps in the control torque and forces at the onset of the neighborhood of the singularity, jumps in the control torque and forces at the exit of the neighborhood of the singularity, and control torque and forces at the singularity are also tabulated in Tables 2-9 for ease of interpretation. The results are as follows:

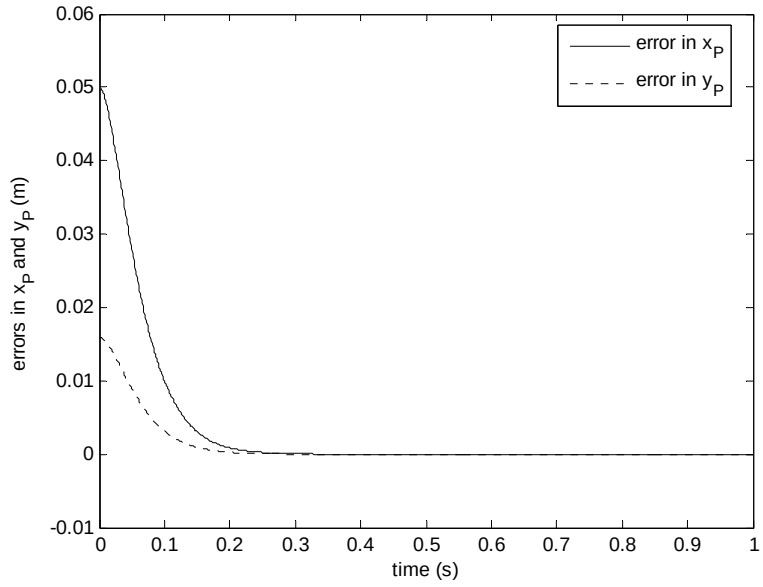

Figure 16 1st Scenario – errors in x_P and y_P

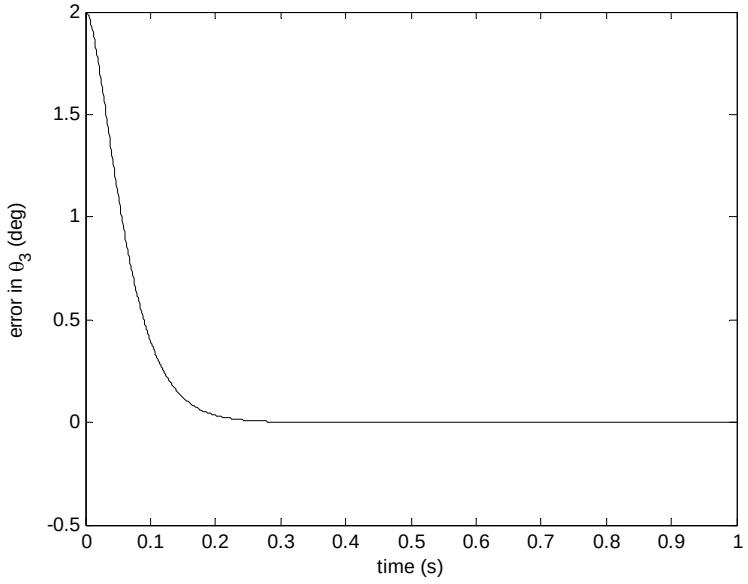

Figure 17 1st Scenario – error in θ_3

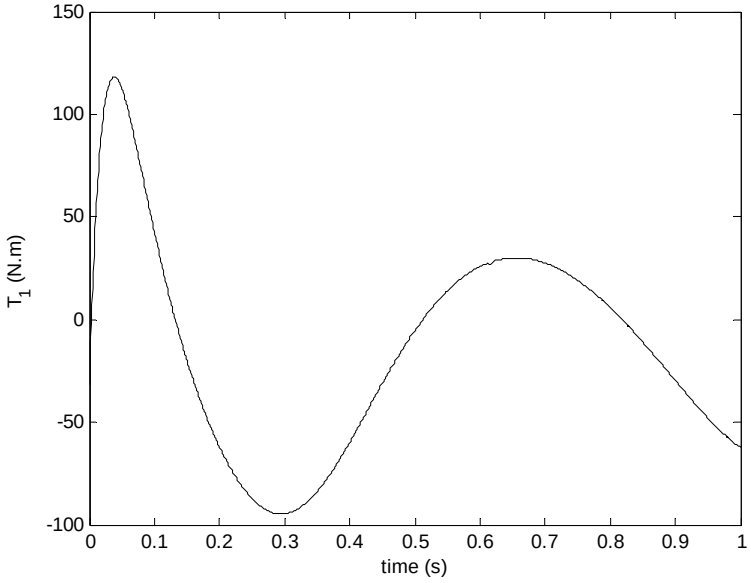

Figure 18 1st Scenario – Motor torque T_1

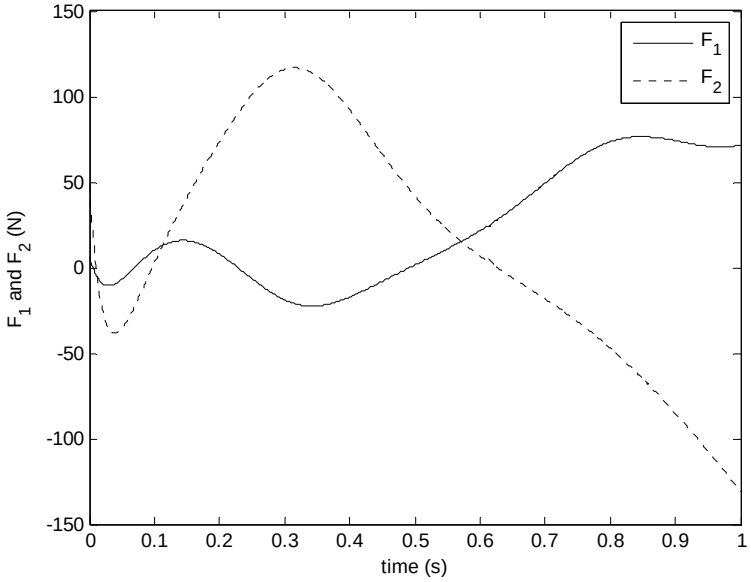

Figure 19 1st Scenario – Actuator forces F_1 and F_2

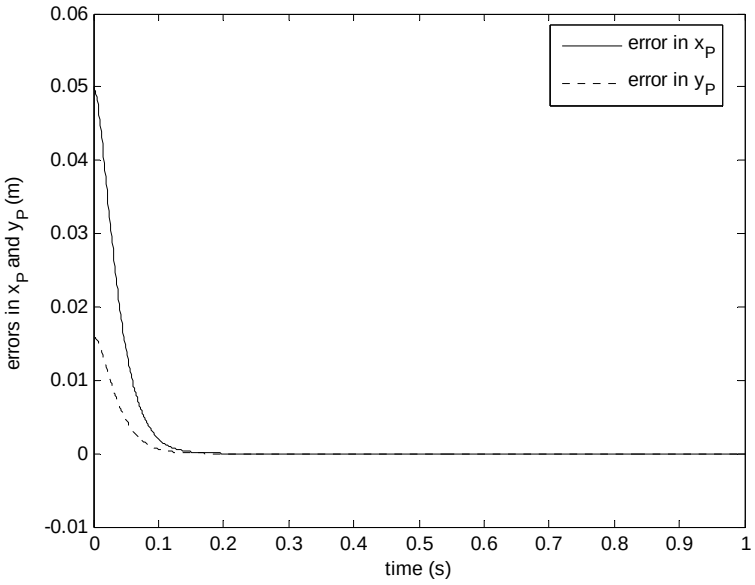

Figure 20 2nd Scenario – errors in x_P and y_P

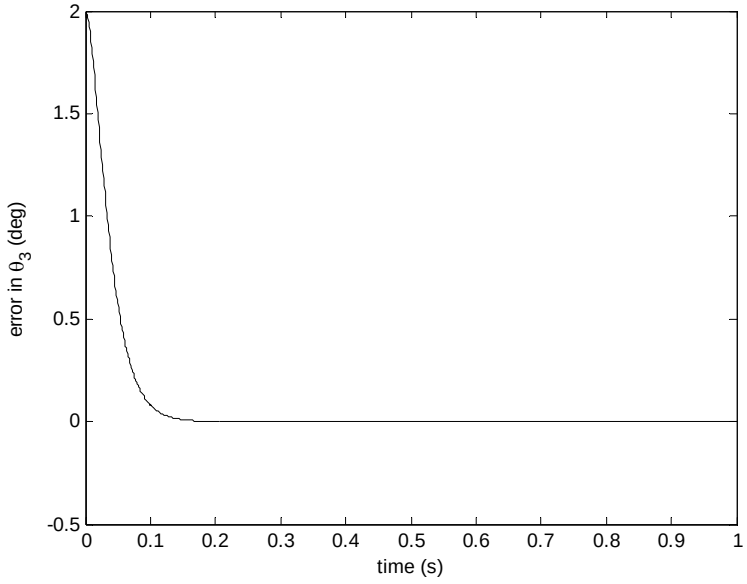

Figure 21 2nd Scenario – error in θ_3

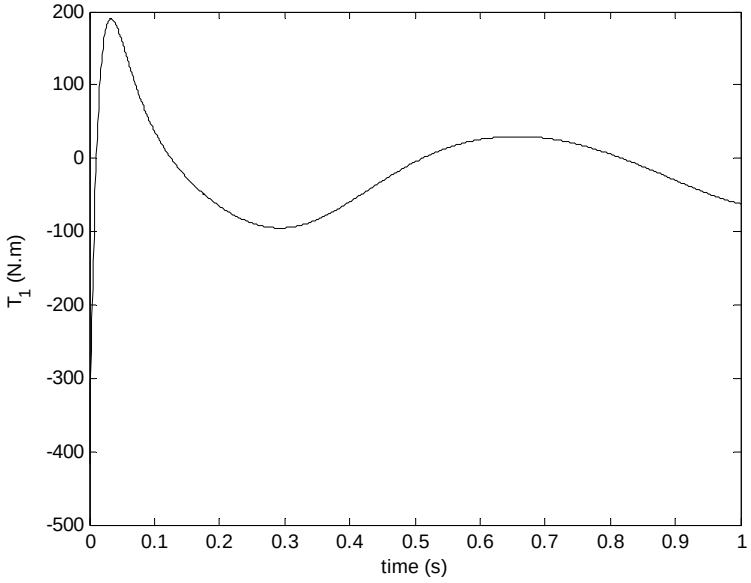

Figure 22 2nd Scenario – Motor torque T_1

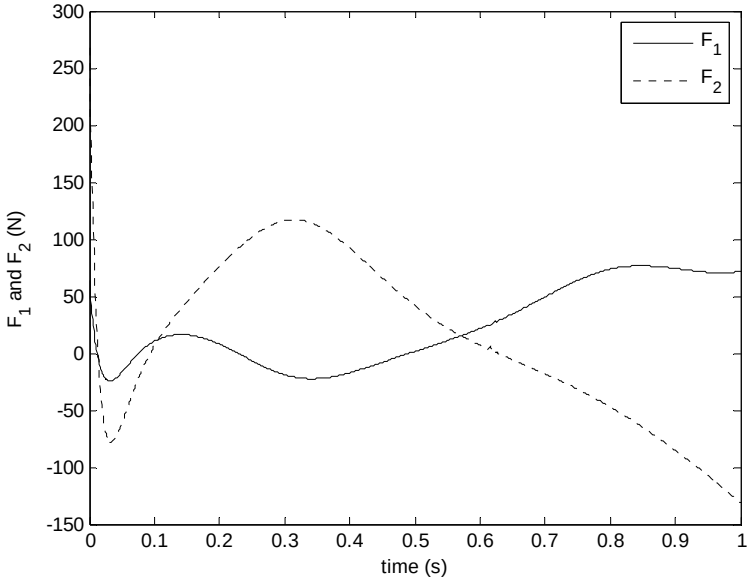

Figure 23 2nd Scenario – Actuator forces F_1 and F_2

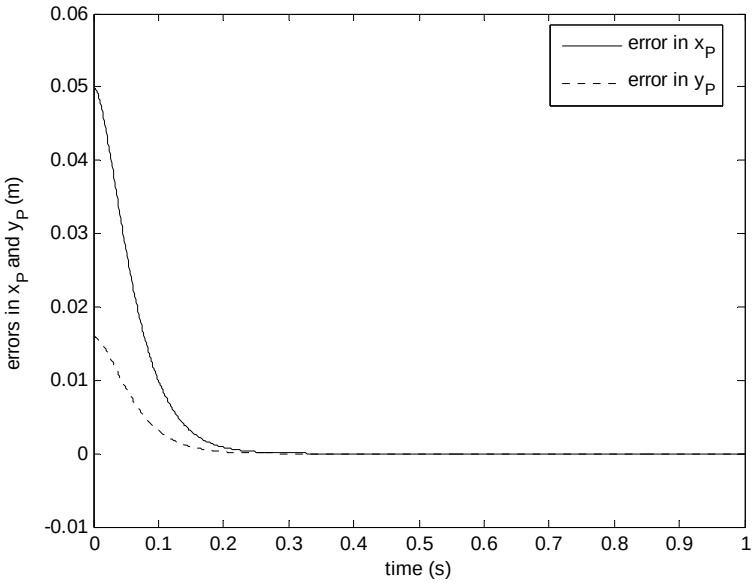

Figure 24 3rd Scenario – errors in x_P and y_P

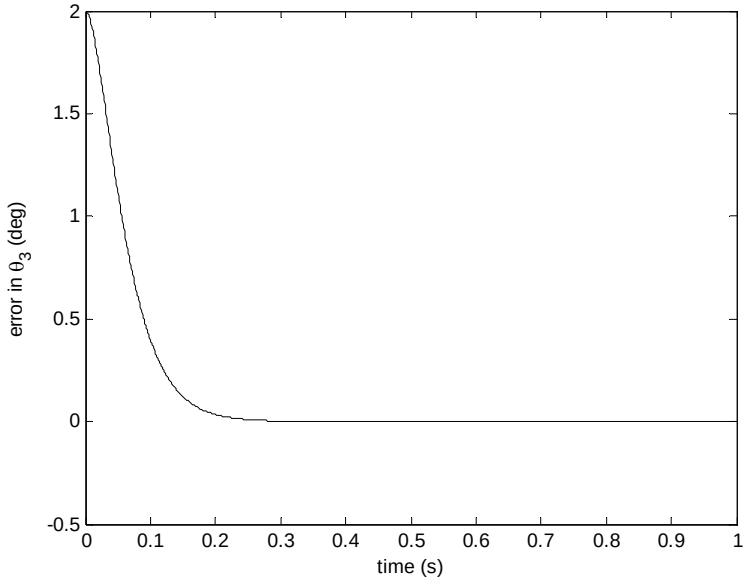

Figure 25 3rd Scenario – error in θ_3

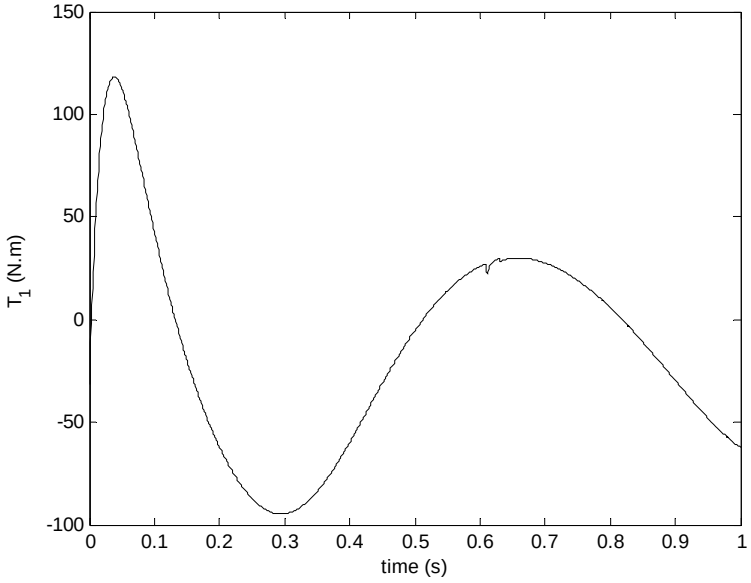

Figure 26 3rd Scenario – Motor torque T_1

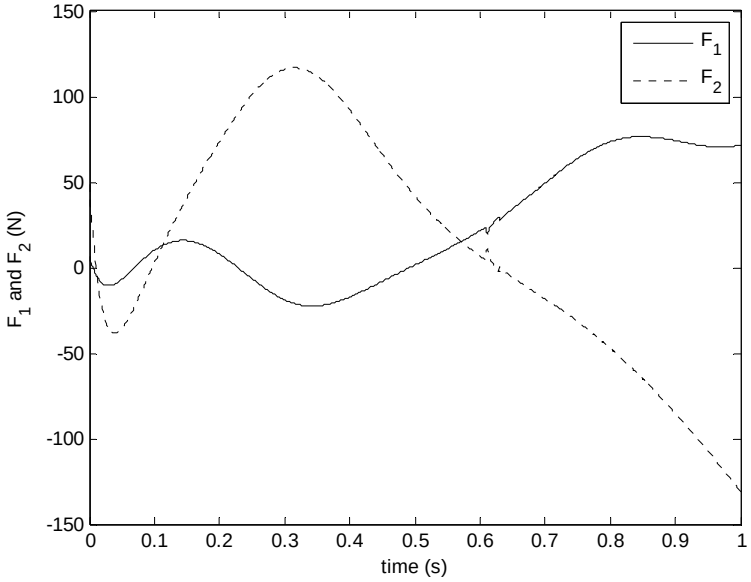

Figure 27 3rd Scenario – Actuator forces F_1 and F_2

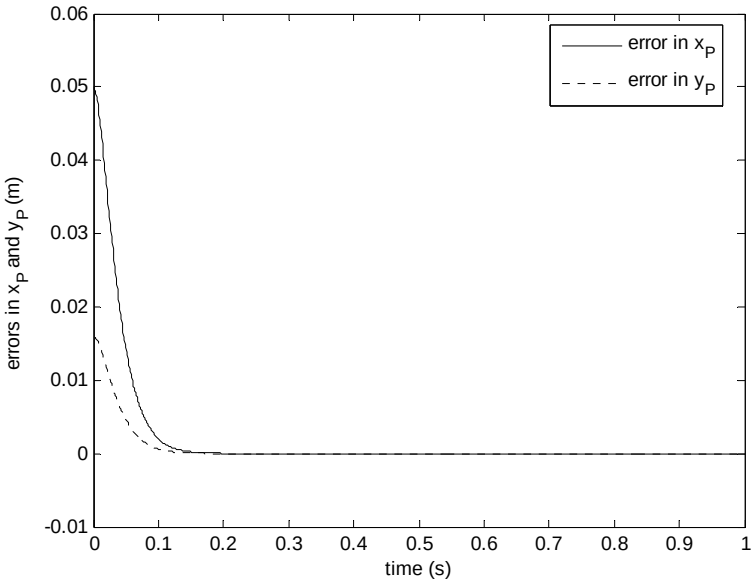

Figure 28 4th Scenario – errors in x_P and y_P

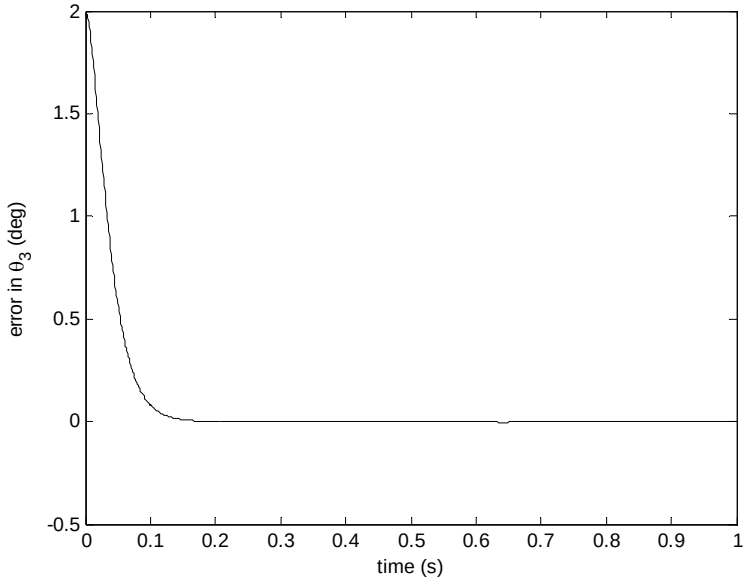

Figure 29 4th Scenario – error in θ_3

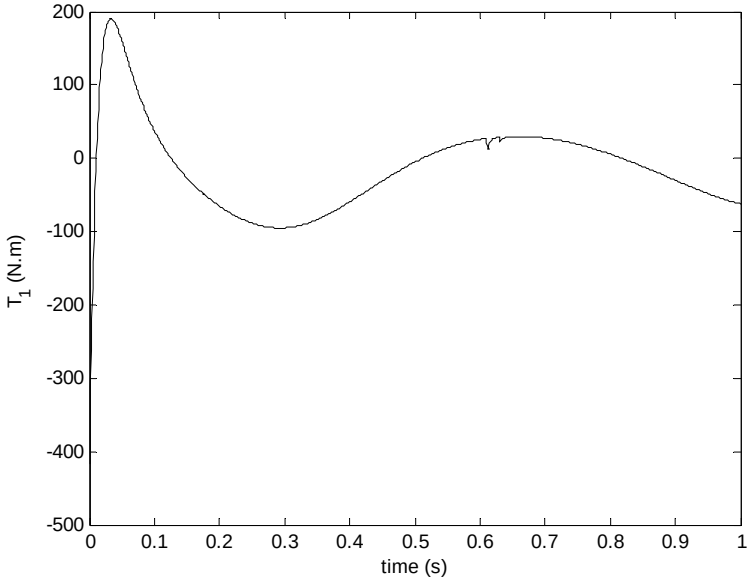

Figure 30 4th Scenario – Motor torque T_1

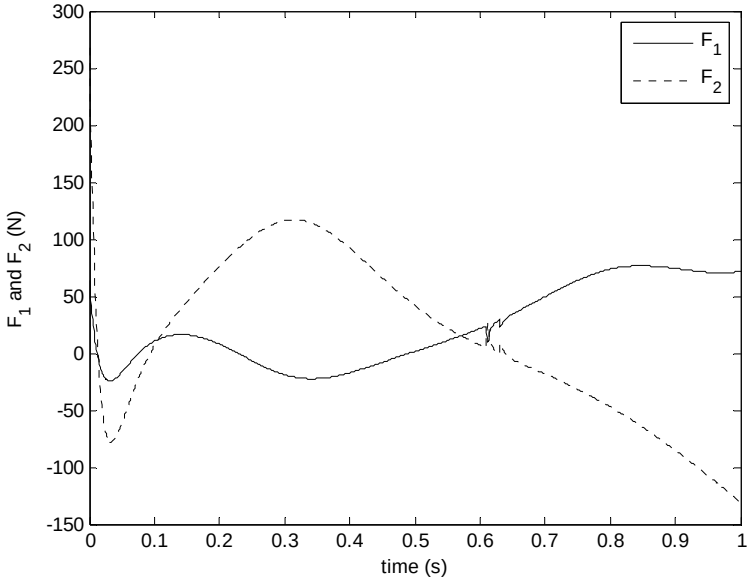

Figure 31 4th Scenario – Actuator forces F_1 and F_2

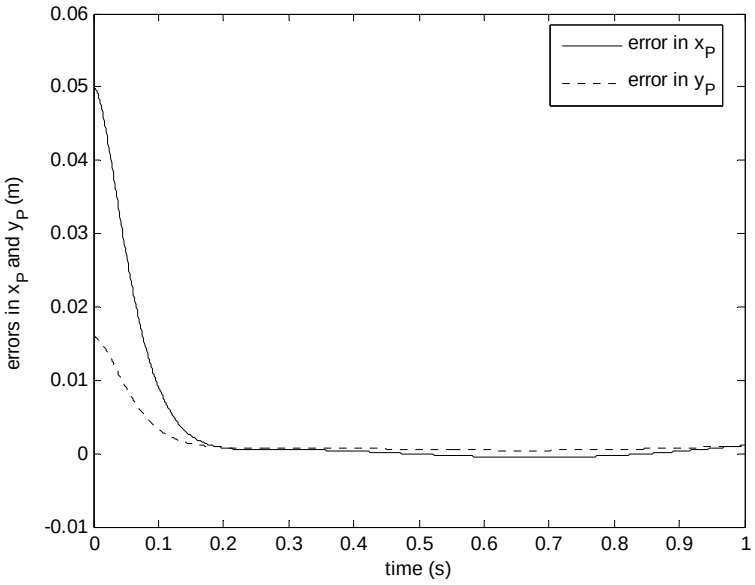

Figure 32 5th Scenario – errors in x_P and y_P

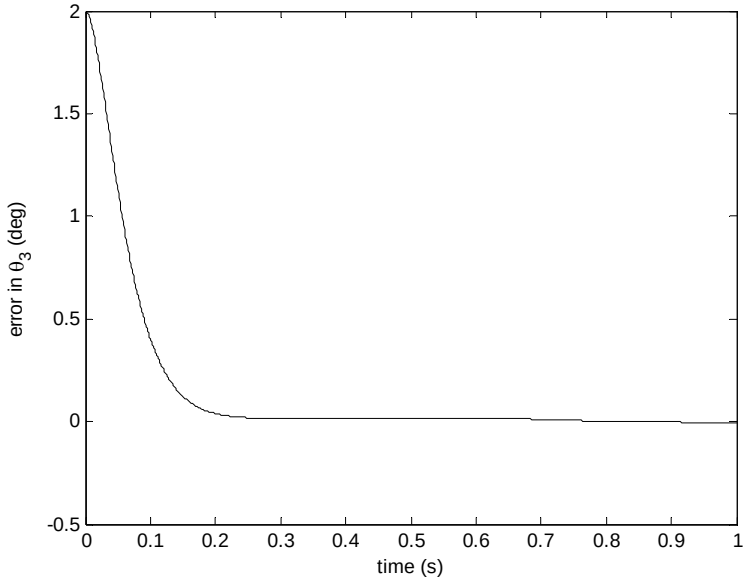

Figure 33 5th Scenario – error in θ_3

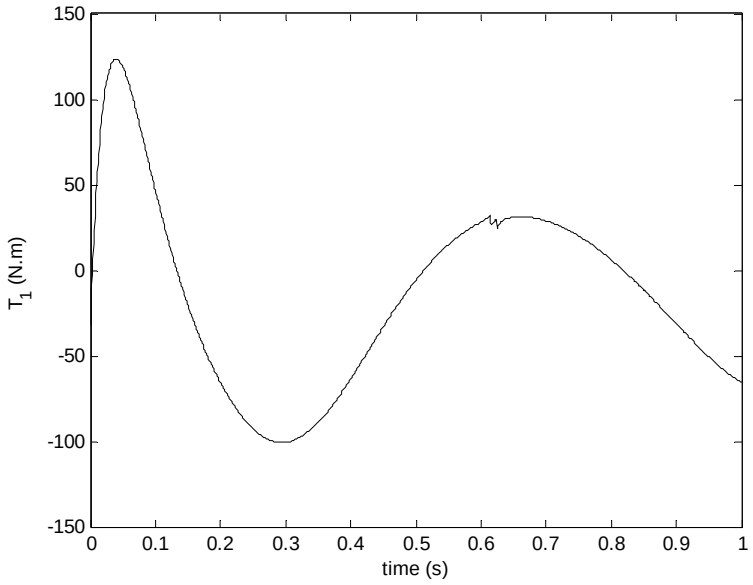

Figure 34 5th Scenario – Motor torque T_1

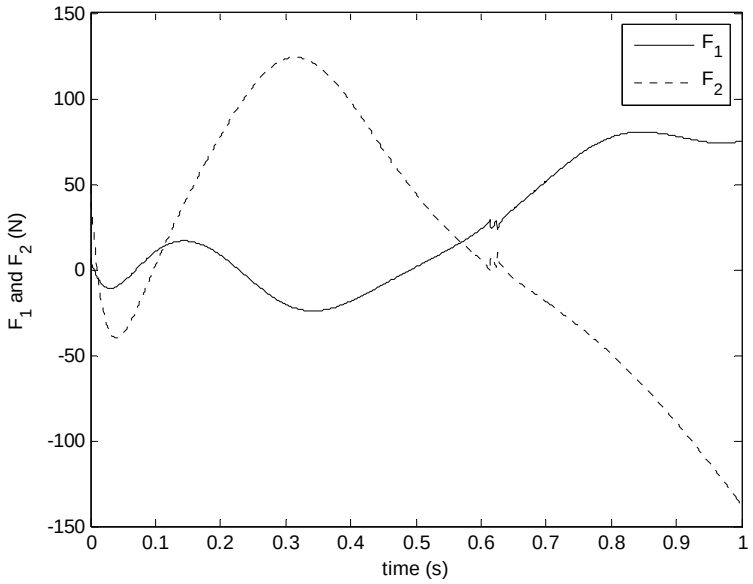

Figure 35 5th Scenario – Actuator forces F_1 and F_2

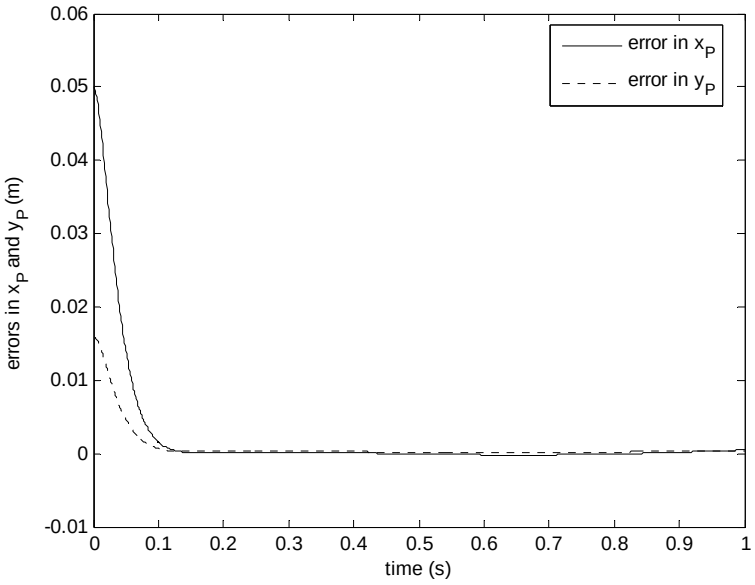

Figure 36 6th Scenario – errors in x_P and y_P

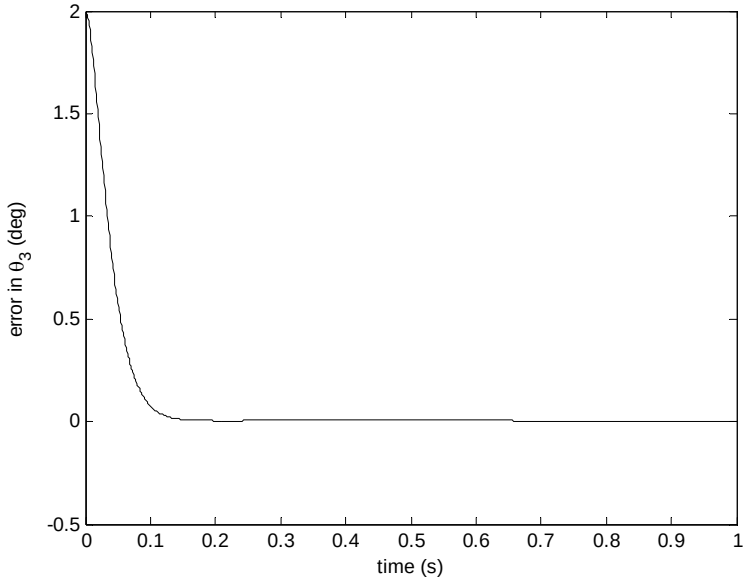

Figure 37 6th Scenario – error in θ_3

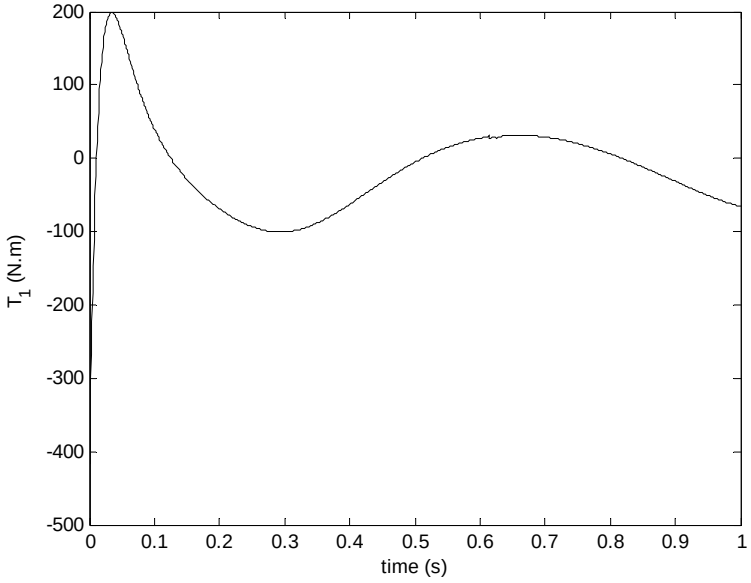

Figure 38 6th Scenario – Motor torque T_1

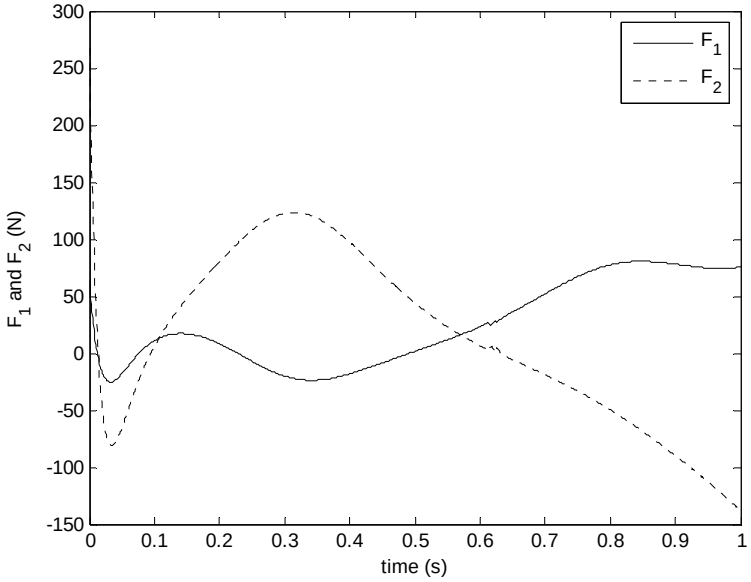

Figure 39 6th Scenario – Actuator forces F_1 and F_2

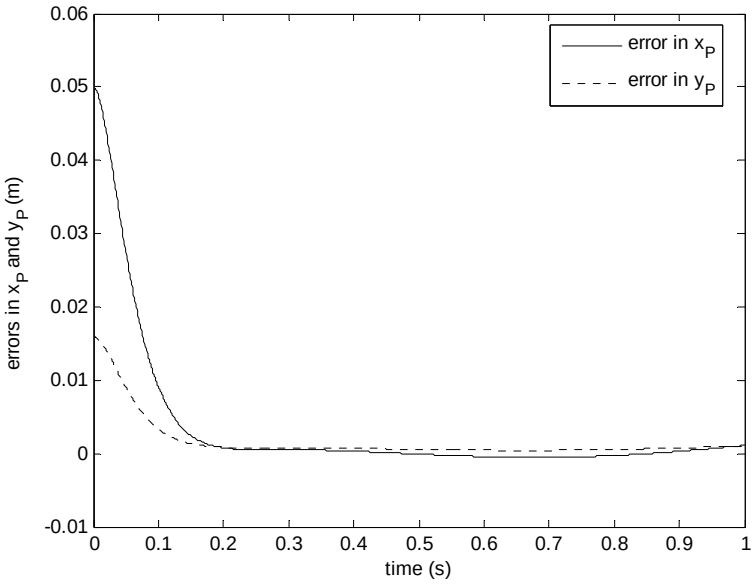

Figure 40 7th Scenario – errors in x_P and y_P

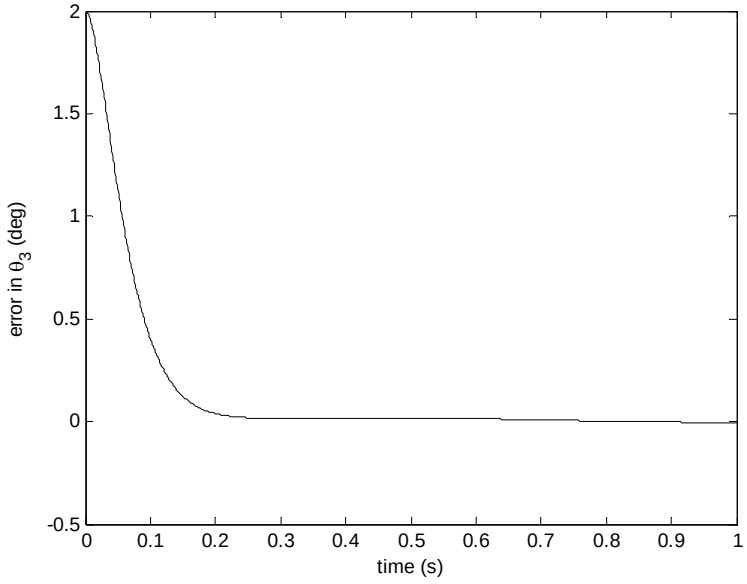

Figure 41 7th Scenario – error in θ_3

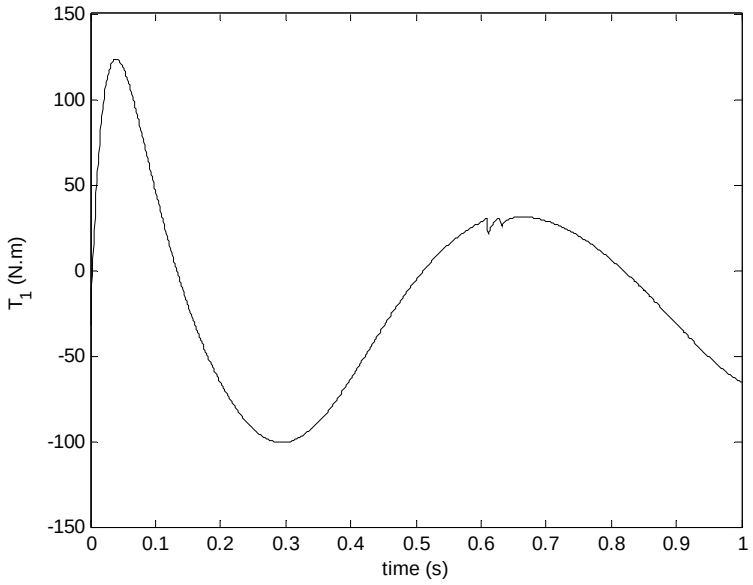

Figure 42 7th Scenario – Motor torque T_1

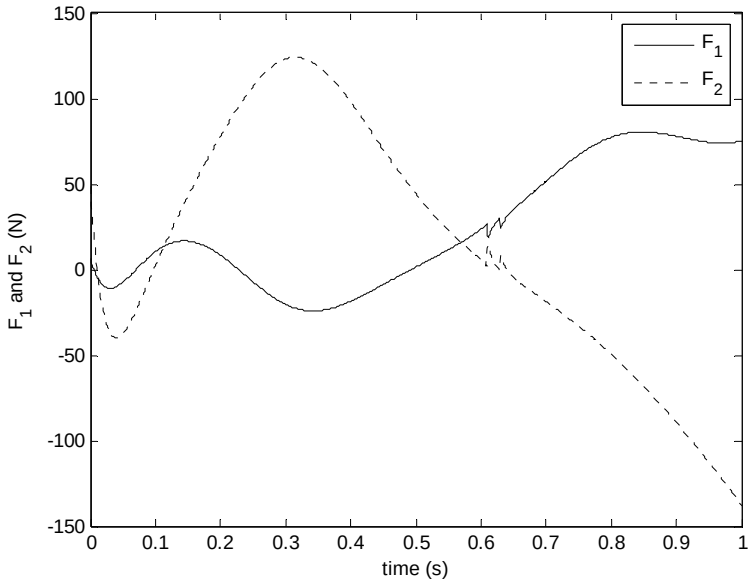

Figure 43 7th Scenario – Actuator forces F_1 and F_2

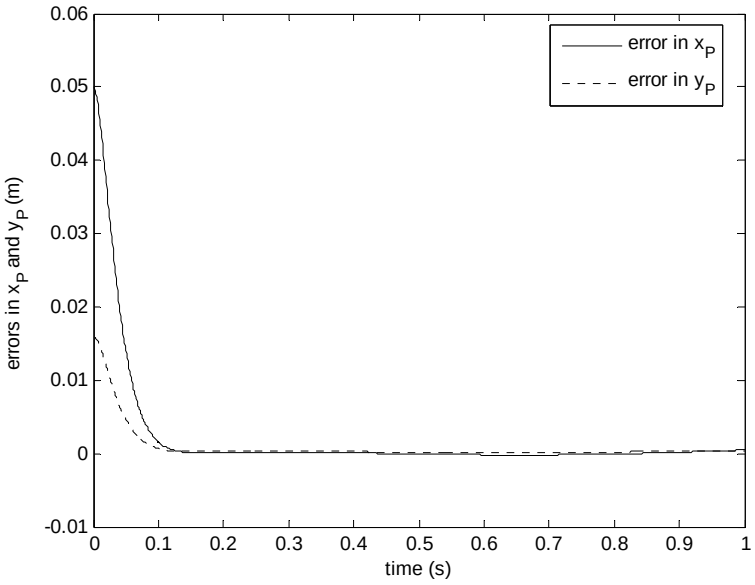

Figure 44 8th Scenario – errors in x_P and y_P

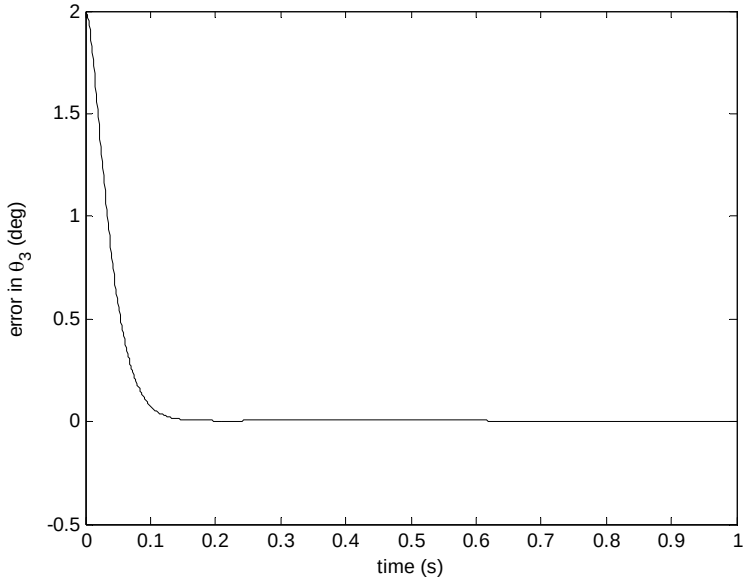

Figure 45 8th Scenario – error in θ_3

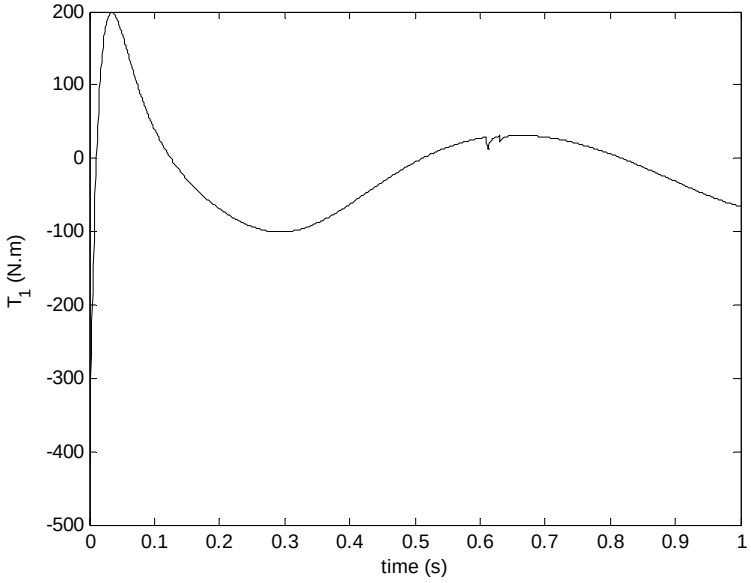

Figure 46 8th Scenario – Motor torque T_1

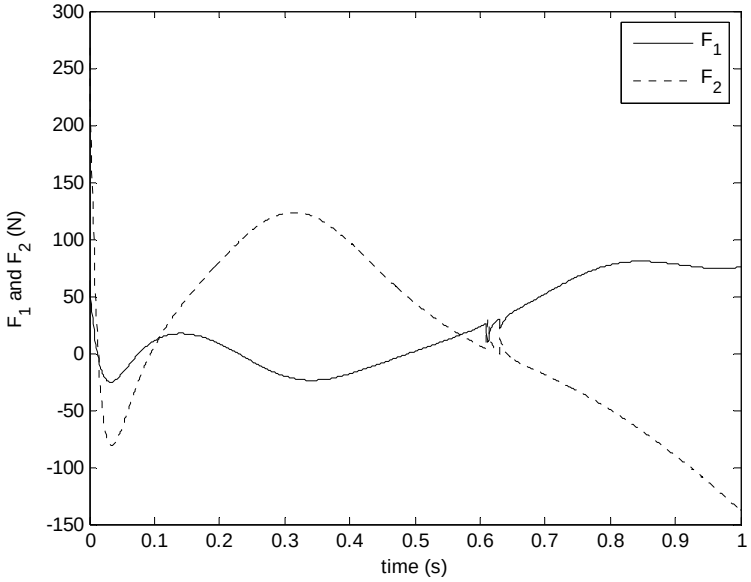

Figure 47 8th Scenario – Actuator forces F_1 and F_2

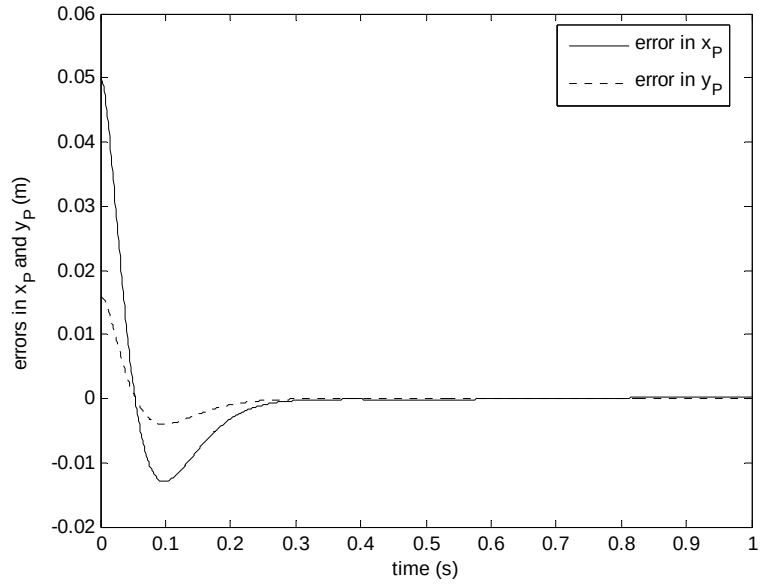

Figure 48 9th Scenario – errors in x_P and y_P

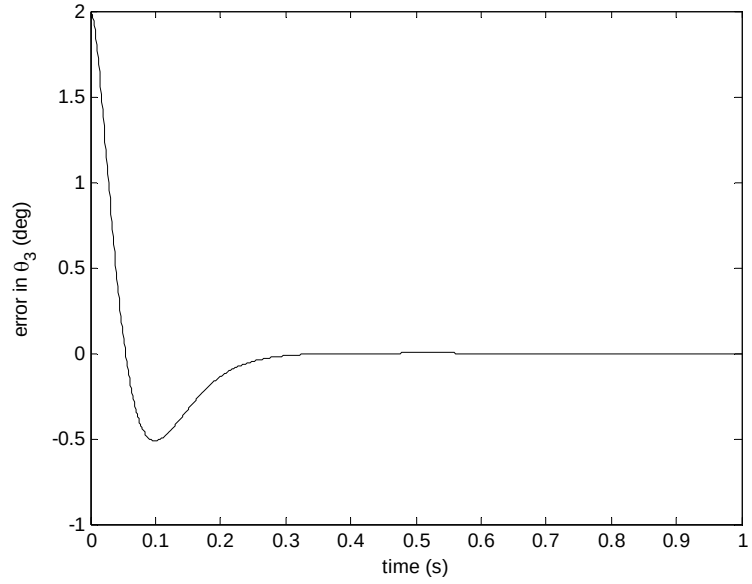

Figure 49 9th Scenario – error in θ_3

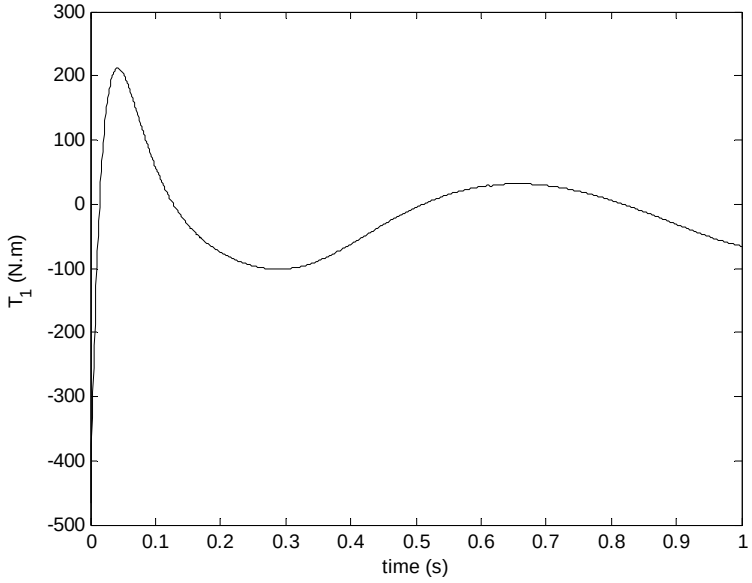

Figure 50 9th Scenario – Motor torque T_1

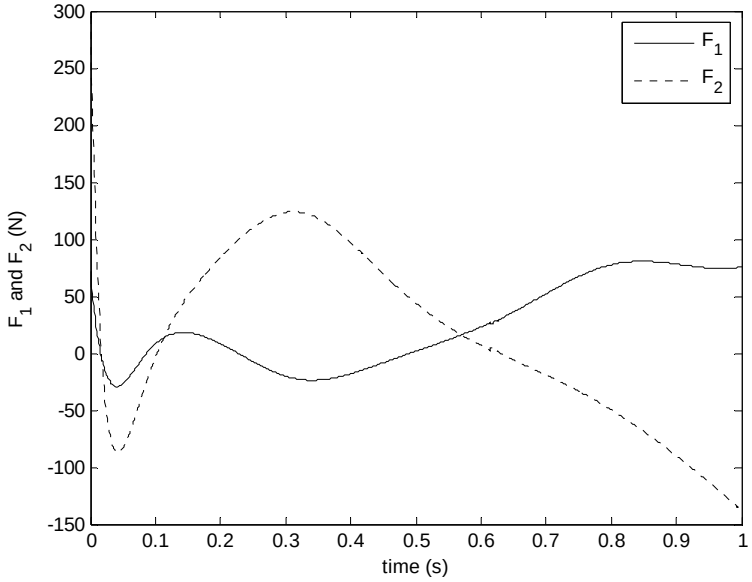

Figure 51 9th Scenario – Actuator forces F_1 and F_2

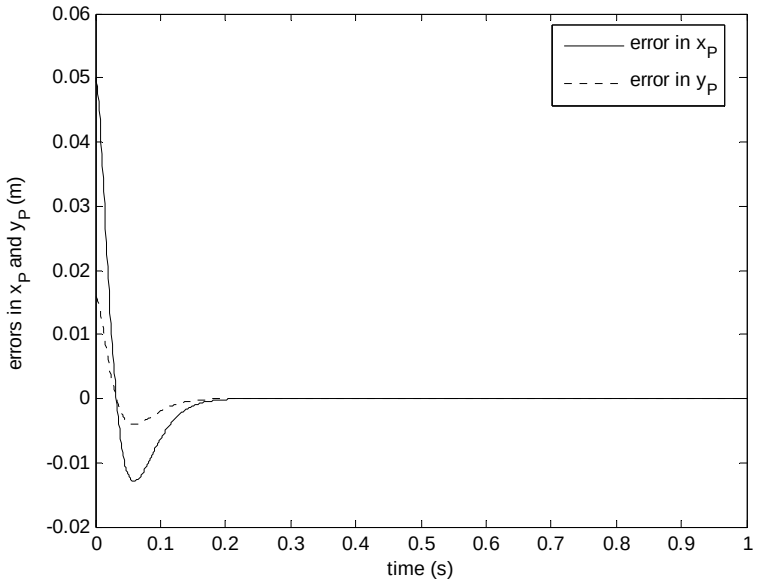

Figure 52 10th Scenario – errors in x_P and y_P

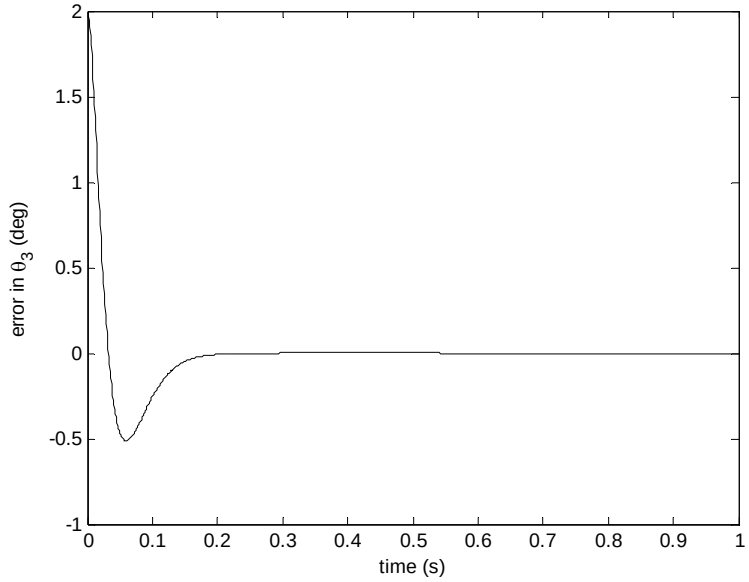

Figure 53 10th Scenario – error in θ_3

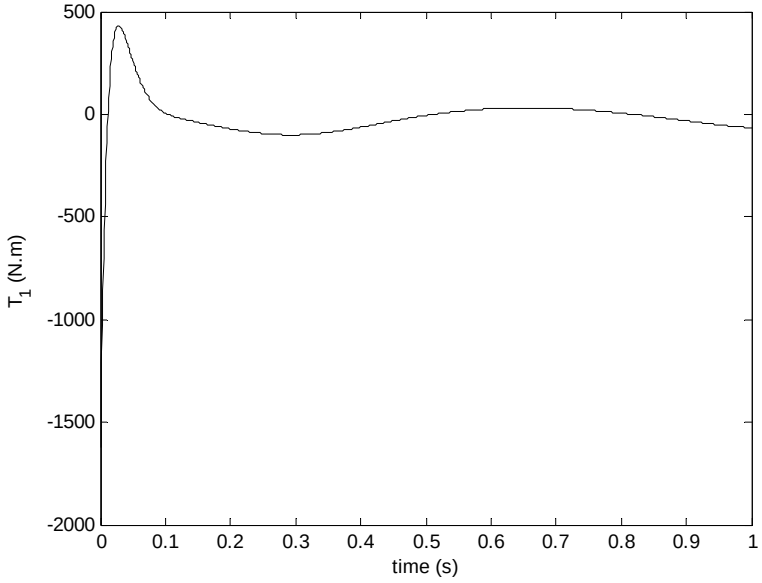

Figure 54 10th Scenario – Motor torque T_1

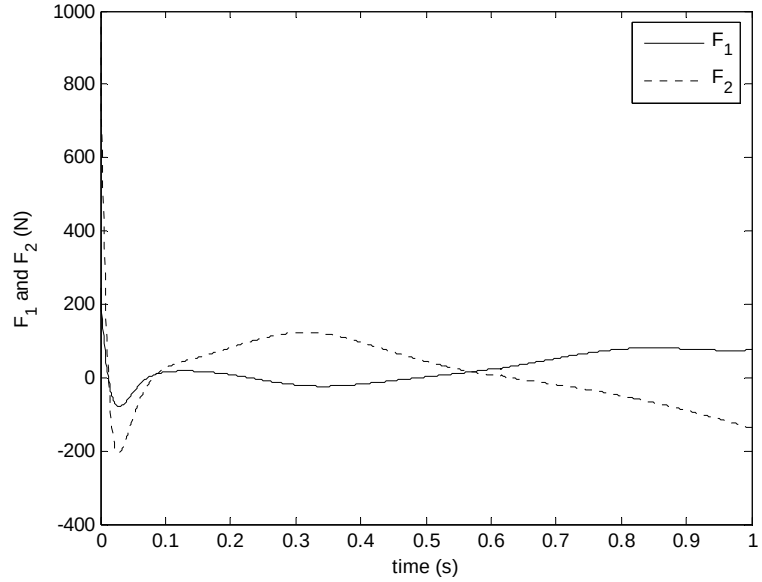

Figure 55 10th Scenario – Actuator forces F_1 and F_2

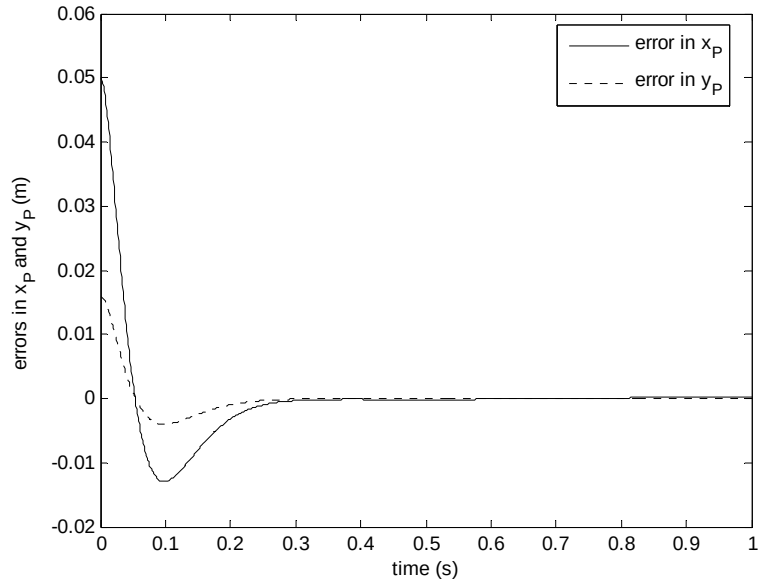

Figure 56 11th Scenario – errors in x_P and y_P

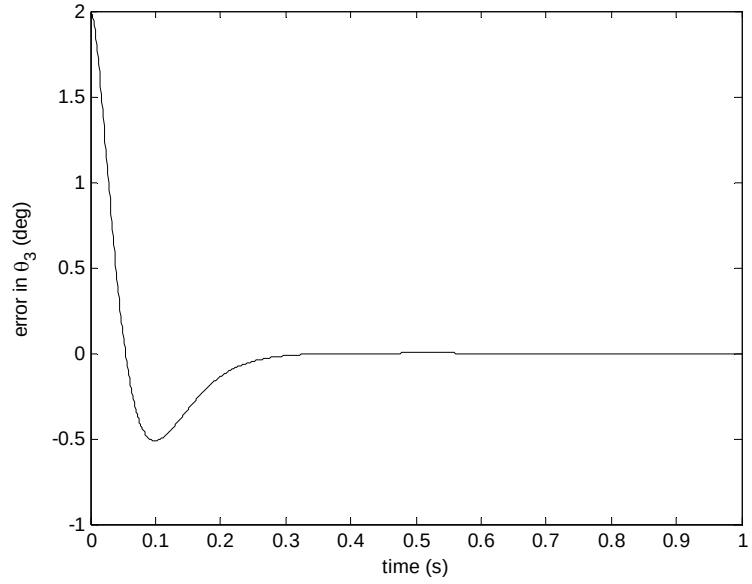

Figure 57 11th Scenario – error in θ_3

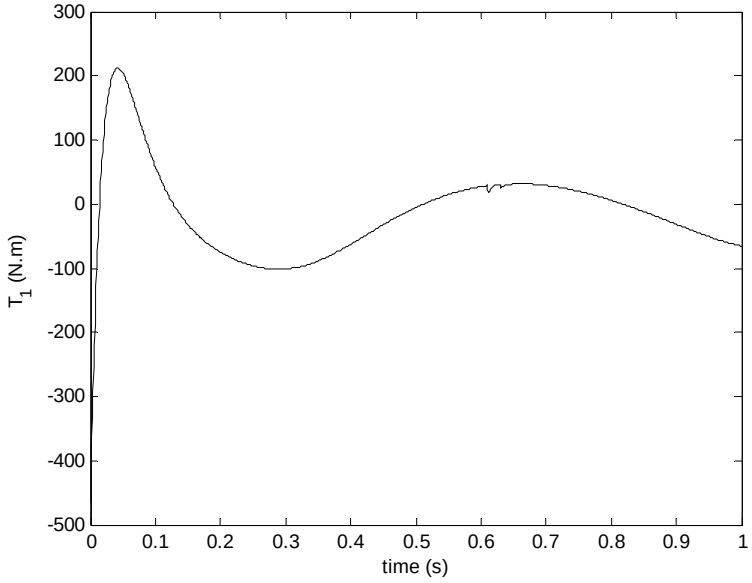

Figure 58 11th Scenario – Motor torque T_1

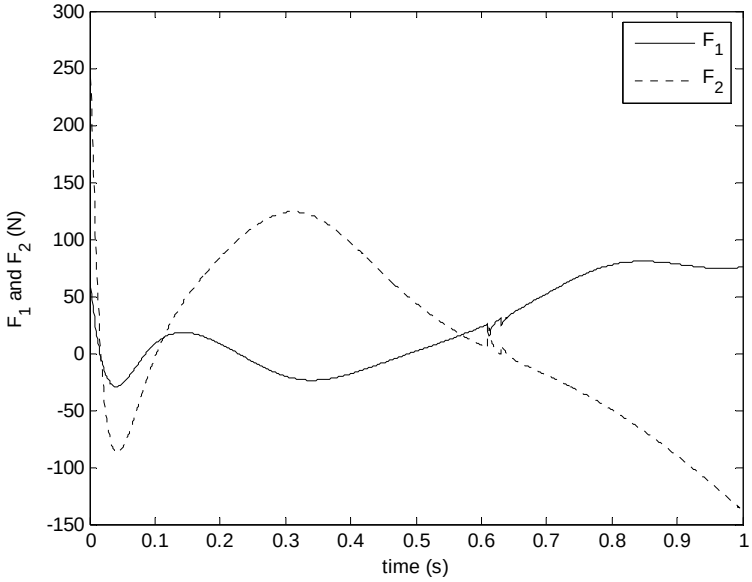

Figure 59 11th Scenario – Actuator forces F_1 and F_2

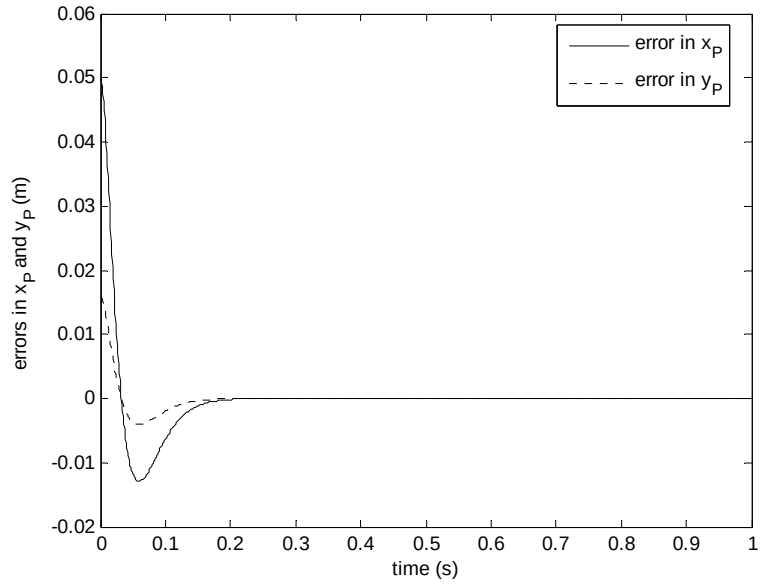

Figure 60 12th Scenario – errors in x_P and y_P

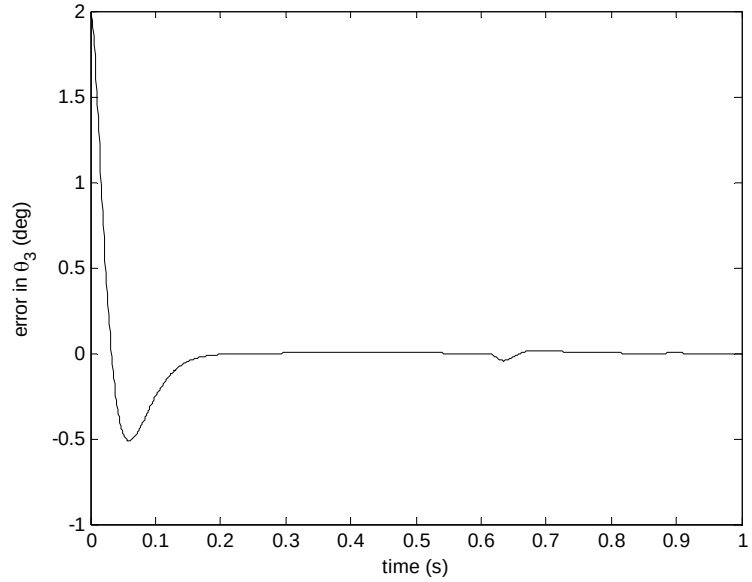

Figure 61 12th Scenario – error in θ_3

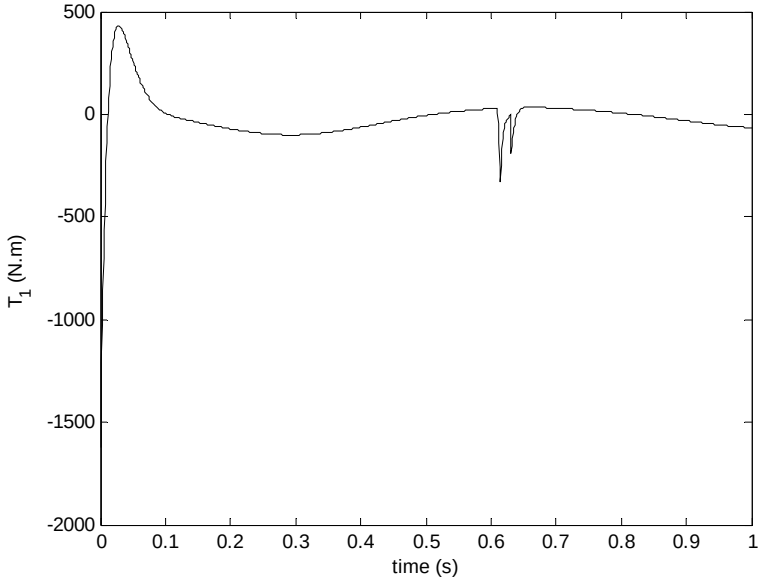

Figure 62 12th Scenario – Motor torque T_1

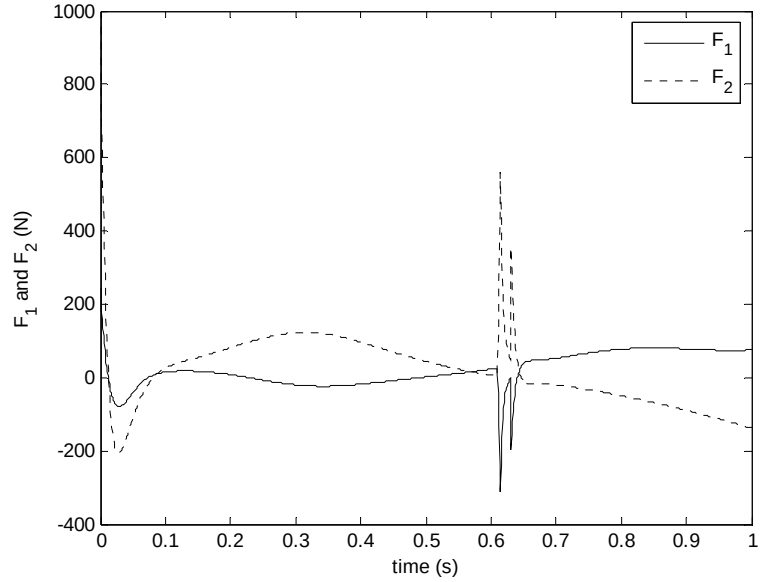

Figure 63 12th Scenario – Actuator forces F_1 and F_2

Table 2 Steady-state errors before the neighborhood of the singularity

Scenarios	error in x_P (mm)	error in y_P (mm)	error in θ_3 (deg)
1	0,0000	0,0000	0,0000
2	0,0000	0,0000	0,0000
3	0,0000	0,0000	0,0000
4	0,0000	0,0000	0,0000
5	-0,4538	0,4414	0,0157
6	-0,1862	0,1519	0,0055
7	-0,4432	0,4445	0,0158
8	-0,1836	0,1525	0,0056
9	-0,0928	-0,0301	-0,0004
10	-0,0139	-0,0039	-0,0002
11	-0,0965	-0,0317	-0,0003
12	-0,0149	-0,0043	-0,0002

Table 3 Maximum errors in the neighborhood of the singularity

Scenarios	error in x_P (mm)	error in y_P (mm)	error in θ_3 (deg)
1	-0,0001	-0,0001	0,0000
2	-0,0001	-0,0001	0,0000
3	-0,0016	-0,0019	-0,0008
4	-0,0050	-0,0059	-0,0026
5	-0,4734	0,4408	0,0157
6	-0,1912	0,1518	0,0055
7	-0,4853	0,4438	0,0158
8	-0,1985	0,1524	0,0055
9	-0,0921	-0,0298	-0,0006
10	-0,0137	-0,0038	-0,0003
11	-0,0958	-0,0314	-0,0027
12	-0,0859	-0,0931	-0,0392

Table 4 Maximum errors after the neighborhood of the singularity

Scenarios	error in x_P (mm)	error in y_P (mm)	error in θ_3 (deg)
1	-0,0002	-0,0002	-0,0001
2	-0,0002	-0,0002	-0,0001
3	-0,0026	-0,0031	-0,0013
4	-0,0062	-0,0075	-0,0032
5	1,1108	1,0543	0,0152
6	0,4820	0,4086	0,0051
7	1,1108	1,0543	0,0131
8	0,4820	0,4086	0,0024
9	0,2755	0,0972	-0,0033
10	0,0626	0,0223	-0,0008
11	0,2755	0,0972	-0,0035
12	-0,0947	-0,1053	-0,0446

Table 5 Steady-state errors after the neighborhood of the singularity

Scenarios	error in x_P (mm)	error in y_P (mm)	error in θ_3 (deg)
1	0,0000	0,0000	0,0000
2	0,0000	0,0000	0,0000
3	0,0000	0,0000	0,0000
4	0,0000	0,0000	0,0000
5	1,1108	1,0543	-0,0039
6	0,4820	0,4086	-0,0015
7	1,1108	1,0543	-0,0039
8	0,4820	0,4086	-0,0015
9	0,2755	0,0972	-0,0004
10	0,0626	0,0223	-0,0001
11	0,2755	0,0972	-0,0004
12	0,0626	0,0223	-0,0001

Table 6 Maximum control torque and forces

Scenarios	T_1 (N.m)	F_1 (N)	F_2 (N)
1	118,33	76,56	-131,04
2	-417,39	76,56	268,40
3	118,33	76,56	-131,04
4	-417,39	76,56	268,40
5	123,56	80,46	-137,75
6	-417,39	80,54	268,40
7	123,56	80,46	-137,75
8	-417,39	80,54	268,40
9	-465,61	80,58	295,89
10	-1622,80	244,97	955,59
11	-465,61	80,58	295,89
12	-1622,80	-312,50	955,59

Table 7 Jumps in the control torque and forces at the onset of the neighborhood of the singularity

Scenarios	T_1 (N.m)	F_1 (N)	F_2 (N)
1	-1,03	-0,83	1,50
2	-1,08	-0,88	1,58
3	-3,76	-3,34	5,66
4	-6,99	-6,31	10,56
5	-4,67	-4,23	7,09
6	-2,59	-2,28	3,89
7	-7,06	-6,36	10,67
8	-8,73	-7,90	13,22
9	-1,67	-1,43	2,48
10	-1,37	-1,15	2,03
11	-6,88	-6,20	10,40
12	-20,64	-18,86	31,34

Table 8 Jumps in the control torque and forces at the exit of the neighborhood of the singularity

Scenarios	T_1 (N.m)	F_1 (N)	F_2 (N)
1	-0,59	-0,41	0,81
2	-0,71	-0,53	1,00
3	-1,95	-1,79	2,98
4	-6,41	-6,32	10,10
5	-5,27	-5,03	8,18
6	-2,61	-2,41	4,00
7	-5,61	-5,47	8,79
8	-8,15	-8,09	12,88
9	-1,37	-1,17	2,03
10	-1,53	-1,33	2,29
11	-5,45	-5,34	8,56
12	-192,27	-195,14	306,88

Table 9 Control torque and forces at the singularity

Scenarios	T_1 (N.m)	F_1 (N)	F_2 (N)
1	28,12	26,17	1,91
2	28,07	26,12	1,99
3	27,96	26,02	2,15
4	26,59	24,70	4,29
5	28,35	26,25	4,05
6	28,65	26,60	3,52
7	28,03	25,95	4,54
8	27,01	25,02	6,08
9	29,25	27,19	2,58
10	29,08	27,05	2,82
11	27,92	25,91	4,65
12	-67,06	-65,52	152,39

CHAPTER 5

CONCLUSIONS

İder [21, 22] formerly showed that if the trajectory is planned as it makes the dynamic equations consistent at drive singularities, the parallel manipulator can pass through those singular positions while the actuator forces remain stable. Moreover, he modified the dynamic equations by using higher order derivative information to be utilized in the neighborhood of the singularities so that the control forces that cannot influence the end-effector accelerations affect the end-effector jerks instantaneously in singular directions.

In this thesis, a switching inverse dynamics control law is proposed for trajectory tracking control of parallel manipulators in the presence of drive singularities. For this purpose, a conventional inverse dynamics controller is used outside the neighborhood of drive singularities and this control law is modified to be switched inside the neighborhood to prevent actuator forces from becoming unboundedly large using the results of [21, 22]. A 2-RPR parallel manipulator with two legs is considered as a case study and several

numerical simulations are carried out using the developed SIMULINK® model. In all of the simulations performed, the manipulator is initially assumed to be mispositioned.

As it is shown in the first two simulations carried out with an arbitrary inconsistent trajectory using the conventional inverse dynamics controller and assuming no modeling error, the prescribed motion of the parallel manipulator should be chosen such that the consistency of the dynamic equations is satisfied at the drive singularity. Otherwise an inconsistent trajectory cannot be performed by the manipulator since the actuators would unavoidably saturate as the drive singularity is approached and unacceptably large task violations would be encountered.

Once the trajectory is chosen to be consistent, to test the performance of the proposed controller, it is applied to the manipulator under different scenarios. In the first four scenarios, it is assumed that there is no modeling error and the command accelerations are generated by a PD controller of which gains are chosen to be in binomial form. In the second four, the closed loop system is simulated introducing 5 % modeling error while the previous PD controller of which gains are chosen to be in binomial form remains unchanged. In the last four scenarios, a PID controller is decided to be used to see the effects of integral control action on the closed loop response in the presence of the same modeling error with the second four scenarios. The controller gains are again selected to be in binomial form.

In all these scenarios, good tracking performance is obtained while the motor torque and the actuator forces at the drive singularity are always within the saturation limits which can be assumed to be higher than the maximum torque and force values attained outside the neighborhood of the drive singularity. In the scenarios where modeling error is present, the errors in the end-effector states at the onset of the neighborhood of the singularity and towards the end of the task after the neighborhood of the singularity is passed

take almost constant values so that steady-state can be assumed to be reached whereas in the absence of modeling error steady state is fully reached at both the onset of the neighborhood and the end of the task. Furthermore, in all scenarios, steady state errors at the onset of the neighborhood of the singularity are negligible so that the actual trajectory manages to track the desired trajectory which is planned to be consistent until the neighborhood of the singularity is reached. This fact verifies the assumption made in Section 3.2 to be able to use the inverse dynamics algorithm of İder [21, 22] in the presence of drive singularities as a base for the proposed control law.

A careful examining of these scenarios reveals that the errors in the end-effector states do not change dramatically but an increase in the jumps in the control torque and forces at the onset and exit of the neighborhood of the singularity is observed when the size of the neighborhood of the singularity is increased. This is due to the fact that the errors in the approximate dynamics neglecting the terms involving the first time derivatives of the Lagrange multipliers are greater in larger neighborhoods. Such jumps yield a jerky motion which should be avoided by a proper selection of ε.

Another conclusion that can be drawn from these simulation results is that increasing the positive constant ω_0 would decrease the errors in the end-effector states to the expense of an increase in both the maximum control torque and forces and the jumps in the control torque and forces at the onset and exit of the neighborhood of the singularity. The former may be dangerous since the required maxima may fall beyond the saturation limits of the actuators being used in a real application while the reason why the latter should be avoided is explained earlier.

As a final remark, adding an integral control action results in better tracking performance and smaller jumps in the control torque and forces at the onset and exit of the neighborhood compared to PD controller in the presence of modeling error while the maximum torque and forces dramatically increase;

that may be an undesirable situation as explained formerly. However, despite the advantages, adding an integral control makes the system relatively less stable. This fact may lead situations, as 12th scenario, where the control torque and forces dramatically increase especially in the neighborhood of the singularity since in larger neighborhoods the errors in the approximate dynamics are greater as mentioned previously and the effect of these errors on the control torque and forces is further magnified with larger ω_0.

As an extension of this thesis, a study on the trajectory tracking control of parallel manipulators with flexible joints in the presence of drive singularities is strongly recommended for future work.

REFERENCES

1. Merlet, J.-P. (1999) 'Parallel robots: open problems', In *Proceedings of the 9th International Symposium of Robotics Research*, 9-12 October, Snowbird, Utah, 27-32

2. Gao, F., Li, W., Zhao, X., Jin, Z. and Zhao, H. (2002) 'New kinematic structures for 2-, 3-, 4-, and 5-DOF parallel manipulator designs', *Mechanism and Machine Theory*, 37:11, 1395-1411

3. Gunawardana, R. and Ghorbel, F. (1997) 'PD control of closed-chain mechanical systems: an experimental study', In *Proceedings of the 5th IFAC Symposium on Robot Control SYROCO'97*, 3-5 September, Nantes, 1, 79-84

4. Merlet, J.-P. (1987) 'Parallel manipulators, part I: theory, design, kinematics, dynamics and control', Technical Report no. 646, INRIA, France

5. Dasgupta, B. and Mruthyunjaya, T. S. (2000) 'The Stewart platform manipulator: a review', *Mechanism and Machine Theory*, 35 :1, 15-40

6. Gosselin, C. and Angles, J. (1990) 'Singularity analysis of closed loop kinematic chains', *IEEE Transactions on Robotics and Automation*, 6:3, 281-290

7. Daniali, H. R. M., Zsombor-Murray, P. J. and Angeles, J. (1995) 'Singularity analysis of planar parallel manipulators', *Mechanism and Machine Theory*, 30:5, 665-678

8. Sefrioui, J. and Gosselin, C. M. (1995) 'On the quadratic nature of the singularity curves of planar three-degree-of-freedom parallel manipulators', *Mechanism and Machine Theory*, 30:4, 533-551

9. St-Onge, B. M. and Gosselin, C. M. (2000) 'Singularity analysis and representation of the general Gough–Stewart platform', *The International Journal of Robotics Research,* 19:3, 271-288

10. Merlet, J.-P. (1989) 'Singular configurations of parallel manipulators and Grassman geometry', *The International Journal of Robotics Research*, 8:5, 45-56

11. Collins, C. L. and Long, G. L. (1995) 'The singularity analysis of an in-parallel hand controller for force-reflected teleoperation', *IEEE Transactions on Robotics and Automation*, 11:5, 661-669

12. Basu, D. and Ghosal, A. (1997) 'Singularity analysis of platform-type multi-loop spatial mechanisms', *Mechanism and Machine Theory*, 32:3, 375-389

13. Alici, G. (2000) 'Determination of singularity contours for five-bar planar parallel manipulators', *Robotica*, 18, 569-575

14. Ji, Z. (2003) 'Study of planar three-degree-of-freedom 2-RRR parallel manipulators', *Mechanism and Machine Theory*, 38:5, 409-416

15. DiGregorio, R. (2001) 'Analytic formulation of the 6–3 fully-parallel manipulator's singularity determination', Robotica, 19, 663-667

16. Kong, X. and Gosselin, C. M. (2001) 'Forward displacement analysis of third-class analytic 3-RPR planar parallel manipulators', *Mechanism and Machine Theory*, 36:9, 1009-1018

17. Choudhury, P., and Ghosal, A. (2000) 'Singularity and controllability analysis of parallel manipulators and closed-loop mechanisms', *Mechanism and Machine Theory*, 35:10, 1455-1479

18. Özgören, M. K. (2001) 'Motion control of constrained systems considering their actuation-related singular configurations', *Proceedings of the Institution of Mechanical Engineers Part I: Journal of Systems and Control Engineering*, 215:2, 113-124

19. Jui, C. K. K. and Sun, Q. (2005) 'Path tracking of parallel manipulators in the presence of force singularity', *ASME Journal of Dynamic Systems, Measurement, and Control*, 127:4, 550-563

20. İder, S. K. (2005) 'Inverse dynamics of parallel manipulators in the presence of drive singularities', *Mechanism and Machine Theory*, 40:1, 33-44

21. İder, S. K. (2004) 'Singularity robust inverse dynamics of 2-RPR planar parallel manipulators', *Proceedings of the Institution of Mechanical Engineers, Part C: Journal of Mechanical Engineering Science*, 218:7, 721-730

22. İder, S. K. and Amirouche, F. M. (1989) 'Numerical stability of the constraints near singular positions in the dynamics of multibody systems', *Computers and Structures*, 33:1, 129-137

23. İder, S. K. (1995) 'Inverse dynamics of redundant manipulators using a minimum number of control forces', *Journal of Robotic Systems*, 12:8, 569-579

24. Greenberg, M. D. (1998) *Advanced Engineering Mathematics* (2nd edn/ international edn), Prentice-Hall, Upper Saddle River, New Jersey